LBL-13994
Preprint

Lawrence Berkeley Laboratory
UNIVERSITY OF CALIFORNIA

RECEIVED
LAWRENCE
BERKELEY LABORATORY
LIBRARY AND
DOCUMENTS SECTION

Submitted as a chapter in HEAVY ION NUCLEAR SCIENCE (Vols. I and II -- NUCLEAR SCIENCE), Ed. D. Allan Bromley, Plenum Publishing Corp, New York, NY

TRANSURANIUM NUCLEI

G. T. Seaborg and W.D. Loveland

February 1982

TWO-WEEK LOAN COPY

This is a Library Circulating Copy which may be borrowed for two weeks. For a personal retention copy, call Tech. Info. Division, Ext. 6782

NUCLEAR SCIENCE DIVISION

LBL-13994 c.2

Prepared for the U.S. Department of Energy under Contract W-7405-ENG-48

DISCLAIMER

This document was prepared as an account of work sponsored by the United States Government. While this document is believed to contain correct information, neither the United States Government nor any agency thereof, nor the Regents of the University of California, nor any of their employees, makes any warranty, express or implied, or assumes any legal responsibility for the accuracy, completeness, or usefulness of any information, apparatus, product, or process disclosed, or represents that its use would not infringe privately owned rights. Reference herein to any specific commercial product, process, or service by its trade name, trademark, manufacturer, or otherwise, does not necessarily constitute or imply its endorsement, recommendation, or favoring by the United States Government or any agency thereof, or the Regents of the University of California. The views and opinions of authors expressed herein do not necessarily state or reflect those of the United States Government or any agency thereof or the Regents of the University of California.

Submitted as a chapter in HEAVY ION NUCLEAR SCIENCE (Volumes I and II -- NUCLEAR SCIENCE) edited by D. Allan Bromley, which is to be published by Plenum Publishing Corporation, New York, New York.

Transuranium Nuclei

by

G. T. Seaborg

Nuclear Science Division

Lawrence Berkeley Laboratory

University of California

Berkeley, CA 94720

and

W. D. Loveland

Radiation Center

Oregon State University

Corvallis, OR 97331

This work was supported by the Director, Office of Energy Research, Division of Nuclear Physics of the Office of High Energy and Nuclear Physics of the U. S. Department of Energy under Contract W-7405-ENG-48.
This manuscript was printed from originals provided by the authors.

Table of Contents

		Page
1.	INTRODUCTION	
	1.1 General	1
	1.2 History of Discovery	2
	1.3 General References	5
2.	NUCLEAR PROPERTIES OF THE TRANSURANIUM ELEMENTS	7
	2.1 Nuclear Masses and Fission Barriers	7
	2.2 Spontaneously Fissioning Isomers	11
	2.3 Density of Levels Above the Fission Barrier	13
	2.4 Effect of Angular Momentum Upon Fission Barriers	14
	2.5 Decay Properties of the Transuranium Nuclei	16
	2.6 Ground State Spontaneous Fission Systematics	17
	2.7 Fission Fragment Energy and Yield Distribution	19
3.	CHEMICAL AND PHYSICAL PROPERTIES OF THE TRANSURANIUM ELEMENTS	22
	3.1 General Properties	22
	3.2 Chromatography of the Transuranium Elements	23
	3.3 Use of Transuranium Targets in Heavy Ion Reaction Studies	24
	3.4 Health and Safety Aspects of Transuranium Element Use	26
4.	IDENTIFICATION OF TRANSURANIUM REACTION PRODUCTS	27
	4.1 General Considerations	27
	4.2 Chemical Methods	27
	4.3 The Helium Jet/Drums, Tapes, and Wheels	28
	4.4 Magnetic Spectrometers, Velocity Filters	30
	4.5 Time of Flight (TOF), Decay in Flight (DIF) and Blocking Techniques	31

5. SYNTHESIS OF TRANSURANIUM ELEMENTS 33

5.1 General Considerations 33

5.2 Deexcitation of Primary Reaction Products 34

5.3 Deep Inelastic Transfer Reactions 37

5.4 "Transfer" Reactions 41

5.5 Complete Fusion Reactions 45

6. FUTURE DIRECTIONS 49

6.1 New Technical Developments 49

6.2 Deep Inelastic Transfer and Incomplete Fusion Reactions 50

6.3 Cold Fusion Reactions 50

6.4 Secondary Beams 51

6.5 Summary 52

1. INTRODUCTION

1.1 General

Over forty years ago, the first transuranium elements, neptunium and plutonium, were synthesized and identified (Mc 40, Se 46), i.e. "discovered". The intervening years have witnessed the discovery of 13 more transuranium elements so that this group now consists of 15 known elements ranging from neptunium (element number 93) to the unnamed element with atomic number 107. All of these elements are man-made in that they do not exist in appreciable quantities in nature. Therefore these elements represent a 15 percent expansion of mankind's heritage of the building blocks of nature.

A list of these elements, their atomic numbers and their chemical symbols is shown in Table 1. The first eleven of these elements (Z=93-103) are termed "actinide elements" in that their electronic configurations involve the filling of the 5f atomic orbitals and thus they bear a general chemical similarity to actinium (Z=89). The remaining four elements, (104, 105, 106, 107) bear or should bear chemical similarities to their periodic table homologs hafnium, tantalum, tungsten and rhenium. Figure 1 shows a modern periodic table with these elements in their proper positions.

While the elements 93-101 were synthesized first in nuclear reactions involving light ions, the remaining elements were synthesized first in nuclear reactions involving heavy ions and these reactions continue to be the primary way of producing many of these nuclei. Many heavy ion reactions involving medium or high A targets will produce significant amounts of these nuclides. Thus it is appropriate that these elements be discussed in a treatise on heavy ion nuclear science.

In Section 1 of this discussion, we review the history of the discovery of these elements along with making some introductory remarks. In Section 2 , we discuss the nuclear properties of these elements as they relate to heavy

ion reactions while in Section 3, we discuss their relevant chemical properties. Section 4 is devoted to a discussion of the techniques of identifying these nuclei as reaction products while Section 5 includes a discussion of use of different types of heavy ion reactions to make these nuclei. Finally, in Section 6, we discuss future directions for research in this field.

While nuclear fission is one of the dominant decay modes of excited transuranium nuclei, we leave the general discussion of heavy ion induced fission to the chapter by Y. T. Oganessian (Og 82). In a similar vein, the discussion of the exciting field of superheavy elements is to be found in the chapter by Flerov (Fl 82).

1.2 History of Discovery

The history of the discovery of these elements is a fascinating story that has been told in a variety of ways and places (Se 67, Se 78, Se 79, Se 80). The reader is particularly advised to note one of the most interesting and charming of these accounts, the first-hand narrative of Ghiorso concerning the discovery of mendelevium (Gh 72). The story of the discovery of elements 93-103 is relatively non-controversial and is summarized in Table 2. From examining accounts of these discoveries, one concludes, there is a continuous gradation in complexity and difficulty of synthesis as the atomic number increases. The identification of mendelevium and higher Z elements was made on a one-atom-at-a-time basis, using methods outlined in Section 4. In all of the element discovery experiments, <u>it was crucial to the claim of discovery that the Z of the reaction product be cleanly identified using chemical or physical techniques. This criterion continues to be applied today to claims of discovery of new elements</u> (Ha 76).

There is considerable controversy, frequently punctuated by acerbic comments, over the discovery of elements 104, 105 and 106. In 1964, Flerov and

coworkers (Fl 64) bombarded ^{242}Pu with ^{22}Ne ions from the Dubna cyclotron and reported finding a radionuclide which decayed by spontaneous fission with $t_{\frac{1}{2}}$ = 0.3 sec. This nuclide was assigned to be ^{260}104 on the basis of nuclear reaction systematics and the name kurchatovium (Ku) was suggested for this new element. Subsequently, these authors suggested that the half-life was 0.1 sec (Og 70) and most recently (Dr 76) 80 ms. In 1966, Zvara et al.(Zv 66) reported a chemical identification of these radionuclides based upon the volatility of their chlorides. However, if the half-life of the ^{260}104 nuclide was 0.08 sec it seems improbable that it could have survived passage through the apparatus of Zvara, et al. which involved a 1.2 sec transit time for the volatile chlorides (Zv 71). Ghiorso and co-workers at Berkeley reported (Gh 69) what now seems to be the first definitive production (involving establishment of the atomic number) of an isotope of element 104. They produced α-particle emitting ^{257}104 and ^{259}104 by bombarding ^{249}Cf with ^{12}C and ^{13}C ions. They were able to establish the Z of the α-emitting nuclides by collecting their recoiling alpha-decay products, ^{253}No and ^{255}No, and identifying the No alpha-decay. They suggested the name rutherfordium (Rf) for this element.

A controversy continues concerning whether or not the 80 ms isotope of element 104 really exists. The most dramatic evidence of the difficulty of reconciling this dispute is shown in Figure 2 where the spontaneous fission decay curves for the reaction of ^{249}Bk + 82 MeV ^{15}N (to produce the ^{260}104 isotope) as measured at Dubna and Berkeley are shown (Ni 81, Dr 77). While there is some possibility that the Berkeley data includes an unresolved 80 ms component, the magnitude of such a component is estimated to be negligibly small. Perhaps the matter can be summarized by saying that it appears clear that the first correct identification of the atomic number (and thus the discovery) of element 104 was done by Ghiorso et al. (an identification later confirmed by Bemis, et al. (Be 73).

A similar controversy exists over the discovery of element 105. In 1968, Flerov and co-workers at Dubna (Fl 68, Fl 68b) reported the production and identification of two α-emitting isotopes of element 105 produced in the reaction of ^{22}Ne with ^{243}Am. The identification of the atomic number of the isotopes was based upon comparing the measured α-decay energies to α-decay systematics and apparently (Fl 68), measuring the time correlated α-decays of the daughter Lr nuclei. The half-lives were estimated to be >0.015 and <3s sec respectively for the 9.7 and 9.4 MeV α-emitting isotopes, tentatively identified as ^{260}105 and ^{261}105. This group suggested the name nielsbohrium (Ns) for this element.

In 1970, Ghiorso and co-workers at Berkeley (Gh 70) conclusively identifield the formation of 1.6 sec ^{260}105 in the bombardment of ^{249}Cf with ^{15}N. This identification was based upon seeing the time correlation between the 9.06, 9.10 and 9.14 Mev α-particles emitted by ^{260}105 and known α-groups from the 30 second ^{256}Lr daughter. Detailed comparison of their α-spectra with those measured at Dubna does not show any evidence for the significant production of either 9.4 or 9.7 MeV α-particles. Thus Ghiorso et al. suggested the name hahnium (Ha) for this element. In 1970 Flerov et al. (Fl 70) did observe a spontaneous fission activity with $t_{\frac{1}{2}}$ = 1.8 ± 0.6 sec in the ^{243}Am + ^{22}Ne reaction which was assigned to Z = 105, A = 261 based upon analysis of excitation functions. Studies of the chemistry of element 105 were also made and it was found that the chloride of 105 is less volatile than niobium chloride but more volatile than hafnium chloride, in agreement with expectations (Zv 70). Further α-recoil milking and time correlation measurements by Ghiorso et al. (Gh 71) have led to the identification of 1.8 sec ^{261}105 and 40 sec ^{262}105 which decay by emitting α-particles of energy 8.93 and 8.45 MeV, respectively.

Simultaneous experiments in Dubna and Berkeley in 1974 have led to competing claims for the discovery of element 106. Ghiorso et al. (Gh 74) produced a nuclide identified as 0.9 sec $^{263}106$ by following its decay to the known $^{259}104$ which in turn decays to the known ^{255}No. Oganessian et al. (Og 74) at Dubna reported the observation of a spontaneous fission activity with a half-life of 4-10 ms which was produced by bombarding $^{207,208}Pb$ with ^{54}Cr. Based upon nuclear reaction systematics, this activity was assigned to $^{259}106$. Neither group has suggested a name for element 106.

In 1976, Oganesyan et al. (Og 76) reported the observation of a 2 ms spontaneous fission activity produced in the ^{209}Bi (^{54}Cr, 2n) reaction which they assigned to $^{261}107$. In 1981, Münzenberg et al. (Mu 81) identified an α-activity produced in the ^{209}Bi (^{54}Cr,n) reaction which had a mass of 262 and underwent alpha decay ($t_{\frac{1}{2}} = 4.7^{+2.3}_{-1.6}$ ms) to produce a daughter $^{258}105$ whose alpha-decay was also measured.

The IUPAC Commission on Nomenclature of Inorganic Chemistry has recommended that temporary names be assigned to new transuranium elements until their names have been assigned in the traditional manner by their discoverers (Fe 75). They advocate using the "ium" ending preceded by the following roots: nil = 0, un = 1, bi = 2, tri = 3, quad = 4, pent = 5, hex = 6, sept = 7, oct = 8, and enn = 9. The corresponding chemical symbols would have three letters. Some examples from this system are: 108, Unniloctium (Uno); 112, Ununbium (Unb); 118, Ununoctium (Uuo); 140, Unquadnilium (Uqn); 200, Binilnilium (Bnn); 500, Pentnilnilium (Pnn). This system seems unnecessarily cumbersome and we shall designate the new elements simply by using their atomic numbers.

1.3 General References

There are a number of books, review articles, etc. that deal with the properties of the transuranium nuclei. Seaborg has written several of them (Se 58,

Se 63, Se 68, Se 78). Of these, the very simple paperback (Se 63) and the more comprehensive reprint collection (Se 78) are especially recommended. Another very highly recommended general reference is the monograph by Goldanskii and Polikanov (Go 73). The chemistry of the transuranium nuclei is discussed in a number of articles, books, etc. such as the monographs by Katz and Seaborg (Se 54, Ka 57) and Keller (Ke 71), the reviews of Cunningham (Cu 64), Peppard (Pe 71), Keller and Seaborg (Ke 77), etc. An interesting review of the nuclear properties of these elements is to be found in the book by Gorbacher _et al_. (Go 80).

2. NUCLEAR PROPERTIES OF THE TRANSURANIUM ELEMENTS

2.1 Nuclear Masses and Fission Barriers

While it is beyond the scope of this article to review all the information known about the nuclear structure of the transuranium nuclei (see for example, the older work by Hyde, Perlman, and Seaborg (Hy 64) and the theoretical paper of Rasmussen (Ra 75)), it is important to discuss certain of these properties which are relevant to transuranium nuclide production and identification in heavy ion reactions. Without a detailed knowledge of these properties, it is impossible to correctly interpret the results from many heavy ion reactions involving transuranium nuclei. The first relevant aspect of their nuclear structure is macroscopic in nature, namely, the masses and fission barrier heights for these nuclei. The masses, α-decay energies and β-decay energies for most transuranic nuclides near stability (with $A \lesssim 250$) have been measured and are tabulated in standard references (Wa 77). Very few values of these quantities are known experimentally for the neutron-deficient species with $A \lesssim 250$ but reasonably accurate values of these quantities can be obtained using nuclear systematics (Wa 77). The values of the masses for the neutron-rich species and for the heaviest transuranium nuclei must be estimated using modern theoretical calculations of these quantities.

While occasional success is met in predicting these macroscopic properties of the heavy elements using a simple semiempirical least squares fit to known data with prudent extrapolation to unknown nuclei (Wi 64), the general approach in recent years is to use the so-called Strutinsky method (St 67) to calculate nuclear masses and fission barriers. In this method, one uses microscopic shell effects estimated by the shell model predicted deviations from a uniform single

particle level density as a correction to predictions made by a liquid droplet model. More specifically, the total energy of the nucleus E is taken as the sum of a liquid droplet model energy E_{LDM} and the shell (δS) and pairing (δP) corrections to this energy, i.e.,

$$E = E_{LDM} + \sum_{p,n} (\delta S + \delta P) \qquad (1)$$

The liquid droplet model energies are calculated using the best droplet model parameters (My 77) while the shell and pairing corrections are calculated as the difference between these energies as calculated for a realistic nuclear model with non-uniform level spacings, etc., and a "uniform" distribution. For the shell correction energy we have

$$\delta S = S - \tilde{S} \qquad (2)$$

where the shell energy for a realistic nuclear model is given as

$$S = \sum_{\nu} 2\varepsilon_{\nu} N_{\nu} \qquad (3)$$

where ε_{ν}, N_{ν} are the energies and occupation numbers of the νth level in a realistic shell model. The "uniform" distribution energy is simply calculated as

$$\tilde{S} = 2 \int_{-\infty}^{\lambda} \varepsilon \tilde{g}(\varepsilon) d\varepsilon \qquad (4)$$

where $\tilde{g}(\varepsilon)$ is uniform level density and λ the chemical potential corresponding to this distribution. The "uniform" level density is calculated by "smearing out" the realistic distribution, i.e.,

$$g(\varepsilon) = (\pi\gamma)^{-\frac{1}{2}} \sum_{\nu} \exp[(\varepsilon-\varepsilon_{\nu})^2/\gamma^2] \qquad (5)$$

where γ is a smearing parameter. The pairing energy corrections can be calculated in a similar manner using BCS theory.

The significance of these shell corrections is that they tend to lower the ground state mass of the spherical nucleus with near-magic or magic numbers of neutrons and protons and lower the ground state mass of mid shell nuclei at some finite deformation ($\sim$0.3). They introduce local minima in variation of the nuclear energy with deformation (i.e., minima in the fission barriers). These effects can be understood as corresponding to minima in the nuclear level density at the ground state deformation and at larger deformations where the ratio of the nuclear semi-major axis to the semi-minor axis is a ratio of simple whole numbers. Figure 3 shows a schematic view of the effect of these corrections upon the liquid drop fission barrier for a typical heavy nucleus. As one can see from examining Figure 3, the realistic calculated fission barriers are enhanced relative to the liquid droplet model barriers due primarily to a lowering of the ground state mass.

Due to the appearance of a secondary minimum, the fission barrier becomes double humped for many nuclei. Nuclei can be trapped in this secondary minimum and will experience considerable hindrance of their γ-ray decay back to the ground state and considerable enhancement of their decay by spontaneous fission. Such nuclei are called fission isomers and they were first observed (Po 62) in 1962. In addition, experimental results (Br 68) showing sub-barrier resonances in fission probability distributions and intermediate structure (Mi 68, Fu 68) in neutron induced fission can be explained in terms of the double-humped fission barrier.

Since the initial development of the calculational method by Strutinsky, there have been many calculations and measurements made of the ground state masses, deformations, and fission barriers of the heavy nuclei. These measurements and calculations have been the subject of an encyclopedic review article by Bjørnholm and Lynn (Bj 80) and the subject of several papers in a recent conference (P1). In general the calculations are able to reproduce the values of

the ground state masses of known nuclei to ±1 MeV (Bj 80, Br 80, Mö 80).

The situation with respect to the fission barriers is more complex. There is now ample experimental and theoretical evidence (Br 81) that the lowest energy path in the fission process corresponds to having the nucleus, initially in an axially symmetric and mass symmetric shape, pass over the first maximum in the fission barrier with an axially asymmetric, but mass symmetric shape, and then pass over the second maximum in the barrier with an axially symmetric, mass asymmetric shape. The fission barriers for the lighter nuclei (Ra,Th) may actually involve a triple-humped fission barrier (Mö 74) in which the second or outer maximum in the barrier is split in two. The suggestion has also been made (Br 81) that for nuclei with N=154 the first or inner maximum is split in two.

Both Back and Britt (Br 81) and Bjørnholm and Lynn (Bj 80) have independently surveyed all of the available data on fission barriers and have attempted to derive a self-consistent set of barrier systematics. Representing the fission barrier as shown schematically in Figure 3, the combined barrier systematics are given in Table 3 and Figure 4. The compilation of Back and Britt (Br 81) and Bjørnholm and Lynn (Bj 80) disagree slightly in the actual numerical values of the barrier heights E_A and E_B because of different numerical assumptions when calculating fission barrier penetrabilities. By convention, the shape of one maximum of a fission barrier near its top is taken to be that of an inverted harmonic oscillator potential (a parabola) and the transmission coefficient is given by the Hill-Wheeler formula (Hi 53)

$$T = \{1 + \exp[2\pi(E_{barrier} - E)/\hbar\omega]\}^{-1} \qquad (6)$$

where $\hbar\omega$ is the barrier "curvature" (spacing between the levels in a regular harmonic oscillator potential). Large values of $\hbar\omega$ imply tall, thin barriers with high penetrability; low values of $\hbar\omega$ imply short, fat barriers with low penetrability. In their compilation, Back and Britt allowed $\hbar\omega$ to vary freely for both the inner and outer barrier while Bjørnholm and Lynn constrained $\hbar\omega$

as follows: e-e nuclei, $\hbar\omega_A$ = 1.04 MeV, $\hbar\omega_B$ = 0.6 MeV; odd A nuclei, $\hbar\omega_A$ = 0.8 MeV, $\hbar\omega_B$ = 0.52 MeV; o-o nuclei, $\hbar\omega_A$ = 0.65 MeV, $\hbar\omega_B$ = 0.45 MeV. When these differences are taken into account, the derived values of the barrier parameters are in good agreement, In general, these experimental barrier heights should be accurate to 0.3 MeV.

Upon surveying the data in Figure 4, one can observe the general trend that the inner barrier height, E_A, is roughly constant (at ∿6 MeV) over a wide range of nuclei while the outer barrier height, E_B, decreases steadily from about 6 MeV in the Th isotopes to about 4 MeV in the Cm isotopes. In Figure 5 we show a comparison between experimental (Br 81) and theoretical (Mö 80b) values for these fission barrier heights. The calculations agree with the experimental barrier heights for the first and second barrier heights within ± 1 MeV which is the estimated limit (Br 80) of the accuracy of this method of calculation. There is less accuracy in predicting the height of the second minimum, particularly for heavy actinides, as that is a more stringent test of the single particle potentials involved.

2.2 Spontaneously Fissioning Isomers

As previously mentioned, the first spontaneously fissioning isomer was discovered in 1962 by Polikanov (Po 62). During the late 1960's and early 1970's, a considerable number of different isomers were found and characterized. A systematics of the isomer half-lives was developed. Recently, a good deal of attention has been given to investigating the nuclear spectroscopy of these unusual nuclear states. From these investigations which are summarized in a recent book about nuclear fission (Va 73) and recent reviews (Va 77, Me 80), a reasonably complete description of this phenomenon has emerged. The central feature of this description, as mentioned earlier, is the fact that spontaneously

fissioning isomers are stationary states in the second minimum in the fission barrier.

A list of the known spontaneously fissioning isomers and their half-lives is given in Table 4 and illustrated in Figure 6. As seen in Figure 6, these isomers ranging from U to Bk form an island about a point of maximum stability. Gamma ray decay limits the stability of isomers with lower Z and N than those in the island while spontaneous fission limits the formation of nuclei with higher Z and N. As discussed in References (Bj 80) and (Me 80), the isomer half-lives show a strong dependence upon neutron number and a strong odd-even effect. Metag (Me 75) has made a phenomenological analysis of these effects by fitting the spontaneous fission half-lives of the isomers with the equation

$$t_{1/2}^{SF} = (\ln 2)(4 \times 10^{-21})\{1 + \exp \frac{2\pi}{\hbar\omega} [ax + b\,(N - No)^2 + d + S]\} \tag{7}$$

with

$$\hbar\omega = \hbar\omega_o \begin{cases} 1/\delta & \text{odd-odd} \\ 1 & \text{odd-even} \\ \delta & \text{even-even} \end{cases} \quad \text{and} \quad S = \begin{matrix} 2S_o \\ S_o \\ 0 \end{matrix} \begin{cases} \text{odd-odd} \\ \text{odd-even} \\ \text{even-even} \end{cases} \tag{8}$$

where the fissility parameter x was assumed to be

$$x = \frac{Z^2/A}{2(\frac{a_s}{a_c})\{1 - [k\,(N - Z)^2/A^2]\}} \tag{9}$$

with k = 1.87, a_s = 17.64 MeV, a_c = 0.72 MeV and No = 146. Least squares fitting gave

$$\frac{a}{\hbar\omega_o} = -49.4 \pm 5.2 \tag{10}$$

$$\frac{b}{\hbar\omega_o} = -(3.9 \pm 0.4) \times 10^{-2} \tag{11}$$

$$\frac{d}{\hbar\omega_o} = 46.0 \pm 4.4 \tag{12}$$

$$\frac{S_o}{\hbar\omega_o} = 0.43 \pm 0.26 \tag{13}$$

$$\delta = 1.16 \pm 0.08 \tag{14}$$

The quality of the fits to the half-lives is shown in Figure 7 and is sufficiently good to allow use of the above relations to predict $t_{1/2}$ for unknown isomers.

Spontaneously fissioning isomers have become of interest to nuclear spectroscopists because of their large deformation and special symmetry (Bj 80). The first major development in isomer spectroscopy was the measurement of the rotational transitions for the ground state band and for the band built on the spontaneously fissioning isomeric state of ^{240}Pu by Specht et al. (Sp 72) They found the moment of inertia for the isomeric state to be more than twice as large as the moment of inertia for the ground state band providing unequivocal evidence for the large deformation of the isomeric state. Confirming this measurement and providing additional information as to the exact deformation of the isomeric state has been the measurement of the electric quadrupole moment of the isomeric state. Habs et al. (Ha 77) measured the lifetimes of the E2 rotational transitions for the 8 μsec isomer of ^{239}Pu using an elegant version of the charge plunger technique; Metag and Sletten (Me 77) used the anisotropy of the delayed fission fragments from the 37 psec isomer of ^{236}Pu while Bemis et al. (Be 79) used an optical technique for ^{240}Am to establish the relevant quadrupole moments. The measurements all indicate that these isomeric states have quadrupole moments typical of prolate ellipsoids with a ratio of axes of 2:1.

2.3 Density of Levels Above the Fission Barrier

In calculations of the survival probability of transuranium nuclei formed in heavy ion reactions, one must evaluate the density of nuclear states at the fission barrier. The probability of fission, P_f, is given as

$$P_f = \frac{N_f}{N_f + N_n + N_\gamma + N_{ch.p.}} \qquad (15)$$

where N_i is the effective number of open channels for the $i^{\underline{th}}$ reaction channel ($= 2\pi\Gamma/D$). When evaluating N_f, one must evaluate ρ_f, the level density at the fission barrier. Bjørnholm, Bohr, and Mottelson have pointed out (Bj 74) that the symmetry of the nucleus is an important consideration in such calculations. For a spherically symmetric nucleus, one gets the familiar Fermi gas expression for the nuclear level density, ρ

$$\rho_f\,(E,J) = \frac{1}{24\sqrt{2}} \cdot \frac{(2J+1)}{a_f^{1/4} E^{5/4} \sigma^3} \exp\left(2\sqrt{aE} - \frac{J(J+1)}{2\sigma^2}\right) \qquad (16)$$

where E is the nuclear excitation energy, J its total angular momentum, σ the spin cutoff parameter and a is the level density parameter. If the nucleus is deformed with an axis of symmetry, the corresponding expression becomes

$$\rho_f\,(E,J) \simeq \frac{1}{24\sqrt{2}} \cdot \frac{(2J+1)}{a_f^{1/4}\, E^{5/4}\, \sigma_{\parallel}} \exp\left(2\sqrt{aE} - \frac{J(J+1)}{2\sigma_{\perp}^2}\right) \qquad (17)$$

where $\sigma_{\parallel}$ and $\sigma_{\perp}$ are the spin cutoff parameters calculated using the moments of inertia parallel and perpendicular to the nuclear symmetry axis. If the developed nucleus has no rotational symmetry, one must use the expression

$$\rho_f\,(E,J) \simeq (2J+1)\,\frac{\sqrt{\pi}}{12}\,\frac{(2J\ 1)}{a_f^{1/4} E^{5/4}} \cdot \exp\left[2\sqrt{aE} - \frac{J(J+1)}{2\sigma^2}\right] \qquad (18)$$

If, in any of the above cases, the nucleus does not have reflection symmetry (i.e., is mass asymmetric), then the level density is further increased by a factor of 2. The practical effect of these developments is to enhance the probability of fission for nuclei with shapes of low symmetry.

2.4 Effect of Angular Momentum Upon Fission Barriers

In heavy ion reactions, one is often dealing with the fission of a system having large angular momentum. In general, we expect that effects of in-

creasing angular momentum will be to make the nucleus more fissionable, either by increasing the level density at the top of the fission barrier or by a centrifigal stretching of the nucleus along the fission direction. A macroscopic description of these phenomena has been presented in the work of Cohen, Plasil, and Swiatecki (Co 74) who investigated the equilibrium configurations of rotating liquid drops and predicted the limiting angular momenta for fission. Figure 8, taken from (Co 74) shows the angular momentum I for which the fission barrier vanishes ($B_f = 0$). The other curve in Figure 8 shows the angular momentum I necessary to make the fission barrier equal 8 MeV, a typical neutron binding energy. Thus, this curve represents the maximum amount of angular momentum a compound nucleus can have and still survive the risk of fission in the de-excitation process. For angular momenta below the limiting angular momentum, the fission barrier is diminished by an amount that can be estimated from calculations of Plasil and Swiatecki (Pl 73). The calculation procedure is described in the textbook of Vandenbosch and Huizenga (Va 73).

A second effect is the change in the shell corrections to the liquid droplet barriers at high angular momentum. This subject has been discussed in recent papers of Åberg et al. (Åb 80) and Faber et al. (Fa 80). For low excitation energies, the inclusion of shell corrections to the liquid droplet model causes the fission barrier of strongly deformed nuclei to disappear at a much higher spin value than is the case for the pure liquid droplet model. Figure 9 shows the behavior of a typical shell corrected actinide fission barrier, B_f, as a function of angular momentum. One sees that the fission barrier does not vanish until $I > 100\ \hbar$ while the rotating liquid drop model predictions shown in Figure 8 would indicate that $B_f = 0$ at $\ell \sim 80\ \hbar$. Furthermore, as shown in Figure 10, the angular momentum at which $B_f = B_n$ is significantly raised when one includes shell corrections to the rotating liquid drop model,

although there is a precipitous drop in high spin fission barriers around Z=90.

Unfortunately, when one imparts high angular momentum to a nucleus, one usually increases the excitation energy significantly. As pointed out by Faber et al. (Fa 80) this has the effect of causing the shell effects to decrease. For temperatures T $\simeq$ 0.5-1.0 MeV, the shell effects become negligibly small and one returns to the basic rotating liquid drop considerations.

2.5 Decay Properties of the Transuranium Nuclei

Quite often, in attempting to identify transuranium nuclei produced in heavy ion reactions, one uses the radioactive decay properties of these nuclei as signatures for their presence. Tables 5-17, taken from the Table of Isotopes (Le 78), summarize what is known about the decay properties of the transuranium nuclei. In this tabulation, we include only those radionuclides whose properties, etc., are given reliability class "C" or better by the authors of (Le 78). (There is only one class "D" transuranium nucleus, ^{246}Es.) This was done because less reliable information (class "E" or worse) and its use is actually detrimental in identifying transuranium nuclides produced in heavy ion reactions, especially when the reaction mechanism(s) involved are complex or partially unknown.

One of the most important uses of the decay properties of the known transuranium nuclei is the prediction of the decay properties of unknown nuclei. Figures 11 and 12 show semi-empirical correlations of α-decay half-lives and energies for the known nuclei and predictions (Mö 80a) for unknown transuranium nuclei. The α-decay information shown in these figures was taken from a recent compilation of α-decay energies (Lo 81). Figures 13 and 14 show similar information for β-decay energetics (Wa 77).

As one can see from examining Figure 11, there is discontinuity in the α-decay energy at N = 152-154, indicating the special stability associated with these neutron numbers similar to the well known discontinuity at N = 126. Due

to simple electrostatics, the α-decay energy increases with increasing Z, decreasing N. The Möller-Nix mass formula used to estimate the α-decay energies for unknown nuclei in Figure 11 is generally accurate to 0.3 MeV for most transuranium nuclei, with a tendency to overestimate the magnitude of Qα.

In Figure 12, we have plotted $t_{\frac{1}{2}}$ for α-decay for e-e nuclides. The dependence of $t_{\frac{1}{2}}$ upon α-energy shown in Figure 12 for known nuclei is reasonably well described by the Taagepera-Nurmia equation (Ta 61)

$$\log_{10} t_{\frac{1}{2}} (y) = 1.61 \, (Z \, E_{\alpha}^{-1/2} - Z^{2/3}) - 28.9 \qquad (19)$$

The half-lives of odd A and o-o nuclei are appreciably longer. One can estimate the $t_{\frac{1}{2}}$ for an odd-even isotope using the adjacent even element (with Z greater by one unit) while estimates for even-odd nuclei may be made by using α-decay energies reduced by about 0.2-0.3 MeV. Both corrections should be applied for odd-odd nuclides. If one uses the Möller-Nix mass equation (Mö 80) to estimate Qα and the Taagepera-Nurmia equation to calculate $t^{\alpha}_{\frac{1}{2}}$ for possible e-e isotopes of elements 104-108, one finds that the calculated values of $t^{\alpha}_{\frac{1}{2}}$ all exceed 10^{-6} sec. Thus α-decay is not expected to restrict the possibility of discovering new elements and/or isotopes in this region. The β-decay energetics shown in Figures 13 and 14 show considerable odd-even effects due to the influence of nuclear pairing.

2.6 Ground State Spontaneous Fission Systematics

One of the most important modes of decay of the transuranium nuclei is spontaneous fission (from the nuclear ground state). The values of ground state spontaneous fission half-lives for actinide nuclei (with reliability classification "C" or better according to Le 78) are given in Table 18. In Figure 15, we show the dependence of the spontaneous fission half-life upon neutron number N for e-e transuranium nuclei. In examining the data of

Table 18 and Figure 15, one sees a general decrease in spontaneous fission half-life with increasing Z^2/A as expected in a simple liquid drop model treatment of fission, and a tendency of odd A and o-o nuclei to have abnormally long half-lives. This latter effect is presumably due to increased fission barriers for these odd nuclei due to single particle effects (Va 73). However, one also observes a tendency for the heavier isotopes of each element to show reduced spontaneous fission lifetimes, particularly when N>152, presumably related to the apparent shell closure in this region. If this last effect persisted for heavier elements, it would seriously limit the range of new isotopes and elements that could be synthesized and studied.

However, there is some evidence to indicate that for higher neutron numbers, there is no catastrophic decrease in spontaneous fission half-lives. Figure 16 shows theoretical predictions for the spontaneous fission half-lives of e-e transuranium nuclei by Randrup et al. (Ra 76) along with a large number of experimental measurements (with some being of reliability class E or worse). The prediction by Randrup et al. is that the precipitous decrease in spontaneous fission lifetimes with increasing neutron number washes out for element 104 or higher, a prediction in agreement with the class F data for $t_{\frac{1}{2}}^{SF}$ for Z = 104.

Another approach which suggests a similar answer is that of Swiatecki (Sw 55) who has shown that there is a correlation between deviations of the spontaneous fission $t_{\frac{1}{2}}$ from a smooth dependence on Z^2/A with the deviations δm of the ground state mass from a smooth liquid drop model mass surface. We have therefore plotted (in Figure 17) [log $t_{\frac{1}{2}}^{SF}$(expt'l) + $5\delta m$] vs the fissility parameter x. The fissility parameter x was calculated using the prescription of Krappe et al. (Kr 79) with parameters determined by Moller and Nix (Möller 80). The values of δm were taken from (Möller 80). As one can see there is a very good linear correlation between the "corrected" half-lives and the fissility parameter in the general form

$$\log t_{\frac{1}{2}}^{SF}\ (yr) + 5\,\delta m = a + b\,x \qquad (20)$$

where a = 300.7 ± 4.1 and b = -402.8±5.4. Use of this equation would predict $t_{\frac{1}{2}}^{SF}$ for $^{260}104$ to be 18 ms, a value not inconsistent with work at Berkeley (Ni 81). More importantly, a very large (and perhaps unjustified) extrapolation using this formula would predict $t_{\frac{1}{2}}^{SF}$ for $^{266}108$ to be ∿20 ms. (The Randrup et al. (Ra 76) prediction is ∿ 3 μs). If one remembers the large spontaneous fission hindrance factors associated with odd A nuclei, it becomes possible to think of synthesizing new isotopes and elements with high Z but the small yields, detection and identification of these species will challenge the experimentalist.

2.7 Fission Fragment Energy and Yield Distributions

The subject of the distribution of fragment kinetic energies and yields in nuclear fission is complex and well-studied (Va 73). We shall comment only on those distributions as they are used to identify reaction products in heavy ion reactions. To a first approximation, one can understand that the kinetic energies of the fragments produced in the fission process are the result of the Coulomb repulsion between the fragments following scission. Thus one might expect that the total kinetic energy release (TKE) in fission might vary as $Z^2/A^{1/3}$ of the fissioning system and that a measurement of fission fragment kinetic energies could serve as a rough identification of the (Z,A) of the fissioning system. Viola (Vi 66), in fact showed that a fairly large amount of data on fission TKE could be summarized in a semi-empirical equation of the form

$$\text{TKE (MeV)} = 0.1071\,\frac{Z^2}{A^{1/3}} + 22.2 \qquad (21)$$

or more recently (Wa 81)

$$\text{TKE (MeV)} = 0.1166\ Z^2/A^{1/3} + 9.0 \qquad (22)$$

where Z,A refer to the atomic and mass numbers, respectively, of the fissioning system. Unik et al. (Un 74) refined this approach for the nuclei with $230 \leq A \leq 256$ arriving at a correlation equation of the form

$$TKE = 0.13323 \frac{Z^2}{A^{1/3}} - 11.64 \qquad (23)$$

Most TKE data (for A<250) can be described by one of these equations. In the region of the heavy fermium isotopes (^{258}Fm, ^{259}Fm) one sees (Hu 80, Ho 80) a very high value of the fragment TKE (∿230 - 240 MeV) as compared to predictions of the aforementioned semi-empirical systematics (TKE = 190-200 MeV). This has been explained by Wilkins, Steinberg and Chasman (Wi 76), among others, as the consequence of deformed shell effects upon the scission point configuration. In this case of the heavy Fm isotopes, both fragments have A near the magic Z=50, N=82 configuration with the result of a small total deformation at scission and a high total kinetic energy release.

The variation of the fission fragment mass distributions with the Z,A, excitation energy and angular momentum of the fissioning system is complex and is indicated schematically in Figure 18 taken from the review article (Ho 74) of Hoffman and Hoffman. Low Z systems ($Z \leq 84$) fission symmetrically at all excitation energies at which fission is energetically possible with the fragment mass distributions broadening with increasing excitation energy E^* and angular momentum J. Intermediate mass systems ($84 < Z < 90$) fission asymmetrically at low excitation energies, show equal amounts of symmetric and asymmetric fission at intermediate excitation energies, and fission symmetrically at the highest excitation energies. Typical actinide elements ($90 \leq Z < 100$) fission asymmetrically at low energies with the amount of symmetric fission increasing with excitation energy until $E^* \sim 50$ MeV, at which

time symmetric fission dominates. At higher energies and angular momenta, the symmetric distributions broaden considerably. The heaviest elements ($Z \geq 100$) show asymmetric fission in the light mass isotopes at low energies with the fission becoming symmetric about $A \sim 258$ and broadening considerably with increasing excitation energy and angular momentum.

3. CHEMICAL AND PHYSICAL PROPERTIES OF THE TRANSURANIUM ELEMENTS

3.1 General Properties

The chemical and physical properties of the transuranium elements, especially the actinides, have been extensively studied (see section 1.3 for general references). There are several specialized monographs which deal with the specific properties of individual elements and their chemical compounds (Br 68b, Cl 79, Co 65, Fi 67, Hi 60, My 74, Na 80, Pe 60, Sc 76, Sp 76). Keller and Seaborg (Ke 77) discuss the limited but fascinating information about the chemistry of the transactinides. While it is beyond the scope of this review article to comment upon these properties in detail, the nuclear scientist studying the heavy ion induced nuclear reactions of the transuranium elements will usually need to know certain basic information to prepare and handle targets, identify reaction products, etc.

The fourteen actinide elements (Th-Lr) form a second rare earth series involving the filling of the 5f electronic orbitals, although due to the similar energies of the 6d, 7s, and 5f electronic orbitals, the 5f orbitals fill differently than the 4f orbitals. (For example, the ground state electron configuration of the gaseous atom thorium contains no 5f electrons). The elements uranium, neptunium and plutonium show multiple oxidation states in solution (with the most common oxidation states being +6, +5, and +4, respectively) while the elements Am-Lr commonly exhibit +3 oxidation states in solution (with the exception of nobelium whose most common oxidation state is +2). Because of this behavior of Am-Lr, their chemical properties (and to some extent, their physical properties) are closely analogous to the corresponding members of the lanthanide elements. One can

often simulate the behavior of these elements in test experiments by using the corresponding lanthanide elements, thereby avoiding many problems associated with the handling of the highly radioactive actinides. Elements with $Z \geq 104$ should have chemical and physical properties similar to their periodic table homologs.

The transuranium elements known at this point, $Z \leq 107$, are metals, dissolving in mineral acid (albeit slowly in strongly oxidizing media such as HNO_3 due to the formation of passivating oxide films upon the metal). The solution chemistry of the elements is complex, with extensive hydrolysis occurring.

3.2 Chromatography of the transuranium elements

To purify these elements prior to preparing targets or to collect transuranium reaction products, chemical separations of these elements from one another or from lower Z elements are often carried out. In general, chemical separations of the actinides are usually done using chromatographic techniques (see Se 63 for a simple discussion of these techniques). The lower actinides (such as uranium, neptunium and plutonium) in their higher oxidation states are often separated using anion exchange chromatography (Ne 64) while the higher actinides (in the +3 oxidation state) are usually separated using cation exchange chromatography. The first solvent extraction separations involved extraction of uranyl nitrate by diethyl ether, while succeeding generations of procedures employed other more polar molecules such as methyl isobutyl ketone ("hexone"), or electron donor, coordination species such as tributyl phosphate or finally alkyl phosphoric acids, such as HDEHP, (bis (2-ethyl hexyl) - phosphoric acid) as extracting agents. The most ideal single elution agent for the cation exchange separation of the higher tripositive actinides is α-hydroxy isobutyric acid (2-methyl lactic acid) first utilized by Choppin *et al*. (Ch 56) to separate americium and curium.

In recent years, separations of the higher actinides have utilized extraction chromatography. This method combines the techniques of ion exchange chromatography and solvent extraction. The extractant is made part of the stationary phase in the chromatographic separation, usually by coating the surface of plastic beads with the liquid extractant. A dilute acid (such as HDEHP) or chelating agent is made the mobile phase. Very good separations of the higher actinides are achieved, particularly when this technique is combined with the use of high performance liquid chromatography (HPLC) (Ho 69, Mo 68).

3.3 Use of Transuranium Targets in Heavy Ion Reaction Studies.

When studying heavy ion reactions involving transuranium nuclides as targets, the availability of target materials becomes an important question. Information concerning the availability in the United States of transuranium nuclei as targets for heavy ion reaction studies is summarized in Table 19. The information summarized in Table 19 represents a summary of the efforts of the Transuranium Processing Plant associated with the HFIR at the Oak Ridge National Laboratory (Bi 81). One should also note that while large quantities of ^{239}Pu are available, it is classified as a Special Nuclear Material because of its use in weaponry and very strict complicated regulations govern the possession and use of this nuclide.

The preparation of actinide targets is similar to that used for lower Z materials except that the target material is radioactive. Frequently used target preparation techniques are electrospraying, electromagnetic isotope separation, electrodeposition and vacuum deposition (Pa 68). Because these elements are alpha particle emitters, and because of the large

quality factors associated with exposure to alpha-particle emitters, the maximum permissible body burdens, atmospheric concentrations, etc. of these nuclei are very small (generally < 0.1 μg or 10^{-12} μci/ml, see section 3.4). This means that target preparation should take place within hoods or glove boxes and evaporators, electroplating cells, etc. used for the preparation of a specific actinide target should not be used for other targets until they have been thoroughly decontaminated. Once prepared, actinide targets should be stored in dry, inert atmosphere sealed containers which are periodically monitored. The high specific activities of the higher actinides may limit the amount of target material that can be used without incurring significant radiation stability problems.

When actinide targets are used in very intense heavy ion beams as in attempts to make new elements or radionuclides, special attention must be given to the problem of the radiation stability of the target. For example, early attempts to make superheavy elements using the $^{238}U + ^{248}Cm$ reaction were generally inconclusive (Sc 81) due to the premature failure of the ^{248}Cm targets after only $\sim 10^{15}$ ^{238}U ions had passed through the target. (This problem was solved later by new methods of target mounting and cooling (Hu 82, Lo 80)). Molitoris and Nitschke (Mo 81) have studied the properties of thin metal films as targets or backing materials. They found helium to be the best cooling gas and molybdenum or tantalum the most durable target backing material. Gäggeler et al. (Gä 79) have reported that coating the targets with an 0.03 mg/cm^2 carbon film will improve radiative cooling and Marx et al. (Ma 79) find that a rotating target wheel will enhance the thermal stability of the target.

Because of the intense radioactivity of many actinide targets, the low maximum permissible airborne concentrations of these materials and the possibility of target rupture, use of these targets in heavy ion

accelerators generally requires special techniques to isolate the targets from the main accelerator vacuum system. Moody et al. (Mo 81b) and Schädel et al. (Sc 81) describe typical actinide target handling systems in use at the heavy ion accelerators at Berkeley and Darmstadt, respectively.

3.4 Health and Safety Aspects of Transuranium Element Use

As discussed previously, the transuranium nuclei are alpha-particle emitters and many of them have high specific activities (Table 19) Table 20 shows a selection of data on the maximum permissible concentrations (MPCs) of some of these nuclei in the human body and in the atmosphere. (R1, R2). Because of the very low MPCs generally associated with some of these elements, the general strategy for safe use is containment by design. The biggest problem in their use is contamination control. One tries to avoid airborne activity, uses glove boxes for all procedures that could cause atmospheric release of material, continuously monitors (and informs personnel by alarm of) atmospheric activity in work areas, etc. A number of fine guides to the safe use of the transuranium nuclei exist. A highly recommended recent book by Stewart is among these (St 80). All use of these elements should be made in cooperation with and under the guidance of professional health and safety personnel.

4. IDENTIFICATION OF TRANSURANIUM REACTION PRODUCTS

4.1 General

In the study of heavy ion reactions resulting in transuranium reaction products, it is of paramount importance to be able to isolate and uniquely identify the products as to their Z, A and formation cross section. Indeed the claim to discovery of a new element must involve identification of Z (Ha 76) while the claim of discovery of a new nuclide must involve measurement (and/or deduction) of both Z and A. Nitschke (Ni 77) has classified the commonly used techniques of isolating transuranium reaction products by the $t_{\frac{1}{2}}$ of the products and the minimum detectable cross section. His classification scheme is shown in Figure 19. Some of the isolation techniques shown in Figure 19 such as chemistry, magnetic spectrometers, etc. can also serve as methods of establishing the Z and/or A of the species involved.

4.2 Chemical Methods

For reaction products with the longest half-lives, chemical separation techniques offer a convenient method of isolating individual reaction products and establishing their atomic numbers. These techniques offer the greatest sensitivity of all methods because of the large amounts of target material that can be used.

A typical example of the use of chemical techniques to study heavy ion reactions is the effort of Kratz, Herrmann and their coworkers at GSI (Sc 78, He 78) to study the production of trans-target actinides and possible superheavy elements formed in the reaction of ^{238}U with ^{238}U. The chemical problems involved in these studies are formidable. Because

of the large cross sections for deep inelastic scattering and the high fissionabilities of the transuranium nuclei, the sought after actinide (Fm, Md) production cross sections are $\sim 10^7$ less than those of interferring Ra, Ac and Th activities. The separation scheme used is illustrated in Figure 20 and involved the use of four linked chromatographic columns, three of which involved HPLC techniques. A chemical yield of 80-90% with a separation factor of $>10^7$ was achieved. Similar chromatographic techniques were used by Unik et al. (Un 72) to study actinide production in proton-irradiated U targets while a cation exchange procedure devised by Kratz, Liljenzin and Seaborg (Kr 74) has been widely used in heavy ion reaction studies at Berkeley.

4.3 The Helium Jet/Drums, Tapes and Wheels

For species with half-lives in the range from $0.1 \lesssim t_{\frac{1}{2}} \lesssim 10$ sec, the helium jet is a superior method of isolating reaction products, as witnessed by its use in the discovery of new elements (Gh 74). In this method, first developed by Ghiorso et al. (Gh 58), Friedman and Mohr (Fr 62) and Macfarlane and Griffoen (Ma 63), reaction products recoiling from the target are thermalized in $\sim$1 atm helium which exits the target chamber via a connection to a low pressure area, creating a "jet" or stream of helium (Be 74, Figure 21). The helium gas stream impinges upon a collection device such as a tape or wheel or drum which moves the activities to the detectors. The selectivity of the jet system may be improved by performing a gas phase chemical separation in the jet during transport of the stopped recoils (Ze 78).

Identification of the collected reaction products can be made with a variety of techniques. Perhaps the most important of these techniques is the "mother-daughter" or "double-recoil" method which establishes a genetic link between the unknown reaction product and known daughter and/or grand-

daughter activities. In this technique (see Figure 21), the revoil heavy atom produced by the alpha-decay of the collected initial reaction product strikes and imbeds itself in a "mother crystal" producing an electrical signal. The mother crystal is then moved in front of a "daughter crystal" which can detect the alpha-decay of the imbedded atom in the mother crystal. If the alpha-particle decay characteristics of the daughter nucleus are known, then a genetic link is established and the (Z, A) of the parent are established. This technique was used in the discovery of several elements (Gh 69, Gh 70, Gh 74, Es 71).

A newer technique of exceptional power to identify the Z of collected reaction products is the X-ray method (Di 71). In this technique one observes the coincidences between the alpha-particles emitted by the decay of the collected revoils and the K X-rays of the daughter nuclei (produced as a result of internal conversion decay in the daughter). The energies and relative intensities of the X-ray lines serve to identify the Z of the daughter nucleus. (Ca 69, Lu 71).

For species whose half-lives are in the range 1 ms $\lesssim t_{\frac{1}{2}} \lesssim$ 100 ms, the product collection device is placed in close proximity to the irradiated target and catches the recoils emerging from the target directly. In such systems, the heavy ion beam after passing through the target will strike the collection surface (drum, tape, etc.). Schematic diagrams of two such collection devices are shown in Figures 22 and 23 (Ni 80). Unfortunately, such devices offer little selectivity as to which reaction products are collected and it is difficult to detect the radioactive decay of the reaction products amidst a high alpha-particle background. Therefore these devices are used frequently to detect new spontaneously fissioning nuclides. Since spontaneous fission cannot, in general, be used to identify the Z and A of the fissioning system, experimenters frequently resort to arguments based upon nuclear reaction ener-

getics and systematics to identify the collected products. Such identifications are generally considered unreliable (Le 78) and make up the bulk of those identifications classified as E,F, and G by the Table of Isotopes compilers.

4.4 Magnetic Spectrometers, Velocity Filters

The principal problem with the isolation devices discussed previously (tapes, jets, etc.) is that the reaction product must be stopped and mechanically transported to radiation detectors before product identification can occur. This restricts their use to studies of nuclei whose $t_{\frac{1}{2}} \gtrsim 1$ ms. For detection and identification of species whose $t_{\frac{1}{2}} \gtrsim 1$ μs, one employs an instrument based upon magnetic and/or electrostatic deflation of target recoils. The most spectacularly successful of these devices in recent years is the velocity filter SHIP (Separator for Heavy Ion Reaction Products) based at the UNILAC at GSI. (Mü 79, Mü 81). A schematic diagram of this separator is shown in Figure 24. Evaporation residues produced in a nuclear reaction emerge from the target and pass through a thin carbon foil which has the effect of equilibrating the ionic charge distribution of the residues. The ions then pass through two filter stages consisting of electric deflectors, dipole magnets and a quadrupole triplet for focussing. The solid angle of acceptance of the separator is 2.7 msr with a separation time for the reaction products of ∿2 μs. Since complete fusion evaporation residues have very different velocities than target-like transfer and deep-inelastic products, the separator with its ±5% velocity range uniquely separates the evaporation residues from the other reaction products. Following separation, the residues pass through a large area time of flight detector and are stopped in an array of seven position-sensitive detectors. From their time of flight and their energy deposit in the position-sensitive detectors, a rough

estimate of their mass may be obtained. The final genetic identification of the residues is made by recording the correlations between position in the detector (average residue velocity) and subsequent decay signals (from α or spontaneous fission decay) or even signals from γ or X-ray detectors placed next to the position sensitive detector. This device has been used in the discovery of element 107 (Mü 81) and the identification of the new nuclides ^{247}Md, ^{243}Fm and ^{239}Cf (Mü 81c).

Separators like SHIP are quite expensive and represent major instrumentation projects. A less sophisticated spectrometer which costs considerably less and is capable of allowing one to measure the formation cross sections, recoil range distributions and angular distributions of short-lived ($t_{\frac{1}{2}} \gtrsim 1$ ms) alpha emitters formed in heavy ion reactions has been described by Dufour et al. (Du 81).

Another type of device used to isolate and identify transuranium nuclei is the mass separator, typified by the separator SASSY (Small Angle Separator System) in use at the Lawrence Berkeley Laboratory (Le 81). In this system, the heavy product recoils from a nuclear reaction enter a helium-filled (1 torr) magnetic spectrometer. The time of flight and energy of the recoil nuclei are measured, giving a rough determination of the product mass number. The recoil nuclei which are imbedded in the energy detectors are identified by their α-particle decay and the decay of their daughters.

4.5 Time of Flight (TOF), Decay in Flight (DIF) and Blocking Techniques

To detect species whose lifetimes are less than 1 μs, special techniques must be employed. They include time of flight (TOF) techniques which when combined with a measurement of the product energy will give information about the product mass number. For suitable mass resolution, the time of flight must be $\sim$10 ns. When searching for rare events, some selection process

(like SHIP) must be employed to reduce the "background" levels in the apparatus. The decay in flight technique (whose use is described in Gh 77) and the crystal blocking technique (Gi 74) ($10^{-18} \lesssim t_{\frac{1}{2}} \lesssim 10^{-14}$ sec) give very little information about the identity of a reaction product other than its existence and its approximate lifetime.

5. SYNTHESIS OF TRANSURANIUM ELEMENTS

5.1 General Considerations

As the masses of the newly synthesized transuranium nuclei have increased the emphasis has shifted from using light ion-induced reactions to using heavy ion-induced reactions as the mode of synthesis. Thus, as mentioned previously, elements 93-101 were synthesized first in reactions induced by neutrons, deuterons and helium ions while the remaining transuranium elemental syntheses involved the use of heavy ions such as ^{10}B, ^{11}B, ^{12}B, ^{13}C, ^{15}N, and ^{18}O. Recent developments in accelerator technology have made the use of heavy ion projectiles as massive as ^{238}U readily available. Attempts to synthesize element 107 have involved the use of ^{54}Cr projectiles (Og 76, Mü 81).

This availability of massive projectiles has dramatically altered the tools and strategies available to the practitioner of nuclear synthesis. In the past, new species were made by selecting the heaviest target nuclei possible and adding a few nucleons to them. In addition to this approach, one can now think of adding massive numbers of nucleons to lighter heavy elements (as done in the ^{209}Bi (^{54}Cr,n) $^{262}107$ reaction (Mü 81)) or even studying the products of "inverse" reactions such as ^{238}U + ^{48}Ca where ^{238}U is the projectile. A helpful guide in considering these questions is the recently published table of reaction parameters by Wilcke et al. (Wi 80).

Heavy ion reactions that involve transuranium nuclei as products do have a very serious complication which hinders one's understanding of them and thus separates them from other heavy ion reactions. This complication is the fact that many of the reaction products will have excitation energies E^* in excess of typical transuranium fission barriers ($B_f \lesssim 6$ MeV) and furthermore, may have large angular momentum, J. Thus, the initial product

distribution following the heavy ion reaction is greatly altered by fission. While many non-transuranium heavy ion reaction products undergo multiple particle emission and even moderate amounts of fission, the typical transuranium product survival probabilities of 10^{-10} - 10^{-5} make the study of these reactions especially difficult. The occurrence of the fission process obscures the physics of the heavy ion reaction and may be described as a "veil of tears". What is even more pernicious about the fission deexcitation of transuranium reaction products than the obvious decrease in production cross section for the surviving species, is the fact that because of the high average E^* and J, these reaction products frequently arise from the non-representative low E^*, low J tails of the E^* and J distributions (He 78). Frequently the general shape of these low E^* and J distribution tails, and their relationship to the average values of E* and J is poorly known. Thus, in general, studies of the transuranium products formed by heavy ion reactions will be most useful in understanding the survival of excited, fissionable nuclei and perhaps, less useful, in understanding primary reaction processes.

The scientist who wishes to predict the outcome of a given reaction producing a transuranium product will be faced with a difficult chore. In some cases, she will be forced to predict the second or higher moments of the initial product distributions to estimate the final product yields. In any case, the proper calculation of the survival probability of the initial reaction products may require careful consideration of the fission barriers, nuclear shapes and symmetries, shell effects, masses, and how they vary with energy, angular momentum and deformation.

5.2 De-excitation of Primary Reaction Products

Following the initial reaction between the heavy ion projectile and the target nucleus, one is left, in general, with many excited product nuclei which will de-excite. When the product nuclei are transuranium nuclei, the high coulomb barrier against charged particle emission will generally cause the

probability of charged particle emission (even in systems with high J) to not be significant when compared to neutron emission, γ-ray emission or fission (whose probability is enhanced by increasing angular momentum). Thus, it is usually sufficient when considering the de-excitation of transuranium reaction products to only consider neutron emission and fission. Vandenbosch and Huizenga (Va 73) present a simple, frequently used form for the ratio of the fission width, Γ_f, to the neutron emission width, Γ_n, namely

$$\frac{\Gamma_f}{\Gamma_n} = \frac{4A^{2/3} a_f (E-B_n)}{K_o a_n [2a_f^{1/2}(E-E_f)^{1/2}-1]} \exp [2a_n(E-B_n)^{1/2} - 2a_f (E-E_f)^{1/2}] \quad (24)$$

where A is the nuclear mass number, a_f, a_n are the level density parameters at the fission saddle point and ground state deformation, respectively; E, B_n, E_f are the nuclear excitation energy, neutron binding energy and fission barrier height, respectively. The quantity K_o is given by the equation

$$K_o^2 = \frac{TI_{eff}}{h^2} \quad (25)$$

where T is the nuclear temperature and I_{eff}, the effective moment of inertia. The effects of a finite nuclear angular momentum can be treated by replacing the fission barrier height, E_f, and the neutron binding energy, B_n, by

$$E_f^{effective} = E_f^r + E_H + R_{sph} \quad (26)$$

$$B_n^{effective} = E_H + R_{sph} + B_n \quad (27)$$

where

$$R_{sph} = \frac{h^2}{2I_{sph}} J(J+1) \quad (28)$$

and the quantities E_H and E_f^r are calculated from the rotating liquid drop model (Pl 73). Unfortunately, this simple calculational framework neglects

a number of important quantities (discussed in Section 2) which are known to dramatically affect the fission probability. They include the double-humped fission barrier and its penetration, the role of nuclear symmetry in affecting the density of states at the fission barrier, the effect of angular momentum upon the shell effects which govern the ground state fission barrier heights, the "washing out" of the shell effects with increasing excitation energy, etc. A more sophisticated framework that considers some of these effects has been used by some (Ba 74, Ga 76, Gr 76). Moretto (Mo 72) has calculated fission barrier heights, level densities as well as fission and neutron decay widths using microscopic models for a number of superheavy nuclei and $^{296}108$. Valuable as they are, such calculations are generally done neglecting angular momentum effects, collective enhancements of level densities, etc. Beckerman and Blann (Be 77, Be 77b, Be 78) have analyzed the fission probability including angular momentum effects for a number of medium A compound nuclei, but their treatment neglects many of the microscopic effects that are important for the actinides. In summary, there has been no completely correct treatment to date of the de-excitation of highly excited, high J species. What is more serious perhaps, is that we have no universally accepted ideas about the importance of many of the aforementioned effects (collective enhancements, angular momentum dependence of shell effects, etc.) although Reisdorf (Re 81) has made some interesting advances.

In view of this inability to approach the de-excitation of excited transuranium nuclei on sound theoretical grounds, many have reverted to the older semi-empirical approach of Sikkeland and co-workers. (Si 68, Si 68b). Sikkeland *et al*. created a simple crude framework for treating compound nuclear reactions using the Jackson model (Ja 56) and an energy-

independent Γ_n/Γ_f. The values of Γ_n/Γ_f were determined by fitting an extensive amount of data on survival probabilities in actinide nuclei. This approach has been enshrined in a widely used computer program (Al 74). It is not clear, however, that the systematics involved are useful in treating de-excitation of nuclei with high angular momentum.

5.3 Deep Inelastic Transfer Reactions

For heavy targets and heavy ions with $A \lesssim 40$, it has been observed that the complete fusion cross section is a very important part of the reaction cross section. By extrapolation, people felt that this situation would continue with projectiles as heavy as krypton. Thus, the reaction of ^{209}Bi with ^{84}Kr was thought to be a possible avenue for producing transuranium nuclei. However, it was discovered in the course of this attempt to make new transuranium nuclei, that the complete fusion cross section was negligibly small and that a new type of reaction, deep inelastic scattering, was occurring. (Ha 74). At first, this failure of heavy nuclei to fuse due to the fact that the Coulomb repulsive forces between the nuclei exceed the nuclear dissipative forces leading to fusion and the inability of the nuclei to interpenetrate inside the fission saddle point (Le 76), was thought to be a serious hindrance to efforts to synthesize new transuranium elements. However, many pioneering workers realized that this new reaction with its characteristic extensive exchange of nucleons between projectile and target nuclei during the reaction could lead to significant production of trans-target species. (The reaction product mass distributions are bimodal with centroids near the target and projectile masses (Sc 77)). Thus, deep inelastic transfer reactions involving U or heavier targets would be expected to lead to the production of transuranium nuclei.

Wolf et al. (Wo 77) measured the yields of Am, Cm, Cf, Es, and Fm nuclei produced in the interaction of 7.2 MeV/u ^{40}Ar and ^{84}Kr, and 8.3 MeV/u

^{136}Xe with thick ^{238}U targets. Using a semi-empirical diffusion model to calculate the primary fragment distributions (from the initial deep inelastic transfer reaction) and semi-empirical values of Γ_f/Γ_n, these workers were able to fit the Cf and Es isotopic distributions from the ^{84}Kr + ^{238}U and ^{136}Xe + ^{238}U reactions. Interestingly enough, they also predicted a peak cross section for producing element 106 from the ^{253}Es + ^{136}Xe reaction to be $\sim 10^{-32}$ cm^2 and the cross section for producing element 110 in the same reaction to be $\sim 10^{-36}$ cm^2 This work was extended to the ^{48}Ca + ^{238}U reaction by Baisden and Seaborg (Ba 78) and ultimately to the ^{208}Pb + ^{238}U reaction by Lund et al. (Lu 81).

The most significant use and understanding of deep inelastic transfer reactions to produce transuranium nuclei has been in the studies of the ^{238}U + ^{238}U reaction at the Unilac at GSI. The first realization of the unusual potential of this reaction for transuranium nuclide synthesis was in the work of Hildenbrand, Freiesleben and co-workers (Hi 77, Fr 79) who found, from reconstructed primary Z and Q value distributions, more particle transfer at a given energy loss than in other systems, i.e., the diffusion process seems to proceed colder in this system. Cold transfer is, of course, just what is needed to make the fragile transuranium species. Radiochemical studies by Schädel et al. (Sc 78b) confirmed the coldness of the reaction and its implications. (A somewhat expanded version of these studies has been reported by Gäggeler et al. (Gä 81)). In Figure 25, we show the product yields as a function of Z and A for the reaction of 1785 MeV ^{238}U ions with thick ^{238}U targets (Sc 78b). The distribution of target-like fragments from the deep inelastic reaction can be seen to peak at Z=91 rather than Z=85 (as found in the Xe + U reaction (Ot 76) or Z=79 (as found in the Kr + U reaction (Kr 74b)). Thus, the "goldfinger" (as this feature was dubbed in Kr 74b) had become the

"protactinium finger". This upward shift of Z of the peak of the survivor distribution and its broadening are further indications of the colder diffusion occurring in this system. Reconstruction of the primary target-like fragment distribution led to an estimation of the production cross section of Z=70 fragments in this reaction of $10^{-28}cm^2$ which, by symmetry, must also be the estimate of the primary fragment yield of the superheavy element 114 in this reaction.

The yields of the heavy actinides were measured (see Figure 26) and were found to show similar variations with Z and A as observed in the yields of the same species formed in the Xe + U reaction. The yields of the transuranium nuclei in the U + U reaction are much greater than those observed in the Xe + U reaction.

Herrmann (He 78) has pointed out that if one compares the Po and Fm product distributions (see Figure 27) from this reaction (both have $|Z-92|=8$), one observes that the center of the Fm distribution is $\sim$3.7 A units from the most probable primary fragment mass number A_p but the center of the Po distribution is $\sim$9.4 A units from A_p Thus, one concludes that the Fm yields result from the low excitation tails of the primary fragment distributions. The fact that the transuranium element distributions have the same general shape in the U + U and Xe + U reactions and the fact that the centroids and widths of the distributions change little with projectile energy (Kr 80) can be understood in terms of the fact that despite changes in the primary distributions with projectile Z,A and E, only those few nuclei in the low E^*, low J tails of the primary distributions will survive the grim reaper, fission. The principal advantage of the U + U reaction is that because of the generally broader primary product distributions, the number of nuclei in the tails of the distributions increases enormously.

Freiesleben et al. (Fr 79) and Schädel et al. (Sc 78b) have attempted using very simple phenomenological models and semi-empirical estimates of Γ_f/Γ_n to predict the yields of the transuranium nuclei in these reactions. The general shapes and centroids of the isotopic distributions are well reproduced in the calculations, but the calculated yields are 1-2 orders of magnitude higher than the measured yields. If instead of partitioning the total available excitation energy according to the primary fragment masses (i.e., the assumption of equal temperatures in the fragments), one assumes the heavy primary fragment has all the excitation energy (because of a "cold, magic" complementary fragment) better agreement between the calculation and data is obtained. Presumably, considerations of other effects (such as angular momentum) that increase Γ_f/Γ_n would lead to the same outcome.

A somewhat more fundamental approach to treating the initial deep inelastic transfer reaction has been taken by Nörenberg and collaborators (Ay 76, Ay 76b, Wo 78, Wo 78b, Sc 78c, Ay 78, Ri 79, Wo 77b, Ri 79b) as well as several others such as Moretto (Mo 75). In particular, in the work of Riedel and Nörenberg (Ri 79b), they use a semi-phenomenological classical diffusion model and apply it to predicting the primary fragment yields in the reaction of ^{238}U with a thick ^{238}U target (the thick target assumption necessitates accounting for a continuously varying projectile energy in the target). Their approach includes the use of semi-empirical drift and diffusion coefficients and Q_{gg} energetics. Comparison of the calculated primary product distributions with the measured final transuranium nuclide distributions indicates the necessity of assuming that the final product distributions only arise from the low energy tails of the initial distributions. Their work also indicated that large gains in the transuranium product yields would be obtained with heavier projectiles and

targets.

Gäggeler et al. (Gä 81) and Schädel et al. (Sc 81) have recently reported the results of attempts to produce transuranium nuclei in the reaction of 7.4 MeV/u ^{238}U with ^{248}Cm. Their results are shown in Figure 28 along with the results of other investigations of deep inelastic transfer reactions with ^{248}Cm targets. The shapes and centroids of the isotopic distributions are similar in all cases but the magnitudes of the yields are the greatest in the U + Cm reaction. For example, the ^{238}U + ^{248}Cm reaction gives $\sim 10^4$ times more Cf, and 10^3 times more Fm than the ^{238}U + ^{238}U reaction. This presumably demonstrates the large amplification factors that occur due to changes in processes in which the tails of the distributions are relevant. Gäggeler et al. (Gä 81) extrapolate these results to predict a 10^2 fold enhancement in the Md and No yields in the ^{238}U + ^{254}Es reaction and a $\sim 10^3$ fold enhancement in the Lr yields.

5.4 "Transfer" Reactions

Low energy (<10 MeV/u) heavy ion reactions may be classified by impact parameter. The most peripheral collisions lead to elastic scattering or the exchange of a small number of nucleons between the target and projectile nuclei, quasielastic scattering. (The typical product yields from this latter reaction are illustrated in Figure 25). The most central collisions lead to complete fusion of the projectile and target nuclei. Deep inelastic transfer reactions involving a strong dissipation of the initial kinetic energy and orbital angular momentum into internal energy and spin of the colliding nuclei along with mass and energy transfer between projectile and target appear to occur for a range of impact parameters beginning with the maximum impact parameter that leads to complete fusion and extending outward. In recent years, there has been increased interest in direct heavy ion reactions generally in-

volving the light heavy ions (C-Ne) in which only a portion of the incident projectile is captured by the target nucleus. Such direct reactions called "incomplete fusion" (Wi 80b) or "massive transfer" (Zo 78) are thought to occur at impact parameters greater than those involved in deep inelastic transfer reactions but less than the quasielastic transfer processes. In these reactions, the uncaptured piece of the projectile moves forward with near-beam velocity.

In heavy ion reactions induced by the lighter heavy ions leading to transuranium products, one generally observes a number of reactions collectively referred to as "transfer reactions" involving the addition of a few to several nucleons to the target nucleus (for example, Ar 71, Ha 74b, De 80, Ho 81, Le 81b) The classification of the mechanism(s) operating in these reactions is very difficult because up to now only single particle inclusive measurements, usually just involving product yields, are available. Furthermore, the appropriate measurements of the correlations between projectile-like and target-like fragments that would allow the distinction between direct processes (such as incomplete fusion) and deep inelastic transfer are probably not feasible at present. The yields of the transuranium survivors of such reactions are so low (typically 10-100 μb) as to preclude detailed multi-particle coincidence measurements involving detection of the survivor nuclei and any associated lighter particles.

With that gloomy note as a backdrop, let us examine some of what we know about these reactions and try to see why they have captured the interest of many.

One of the first and more careful studies of these heavy ion "transfer" reactions involving production of transuranium nuclei was by Hahn _et al_. (Ha 74b). This remains one of the few studies in which kinematic measurements

were attempted. Hahn et al. studied the excitation functions, recoil range distributions and angular distributions of the heavy transuranium recoil products. In particular, they studied the characteristics of the production of ^{244}Cf and ^{245}Cf via the transfer reactions ^{239}Pu (^{12}C, α2n) and ^{239}Pu (^{12}C α3n) and via the complete fusion reactions ^{238}U (^{12}C, 5n) and ^{238}U(^{12}C, 6n). As expected, the complete fusion reaction products are strongly forward focussed with their angular distribution peaked at 0° and show Gaussian range distributions with mean ranges that increase with increasing projectile energy and whose values agree with the assumption of complete fusion. The same ^{244,245}Cf products when produced in the transfer reaction show angular distributions which peak near the grazing angle and show asymmetric range distributions whose mean value decreases with increasing projectile energy. The yields of ^{244,245}Cf are much larger in the transfer reactions compared to the complete fusion reactions. The yields of the transfer products are described by Hahn et al. with modest success using a modification (Si 72) of the semi-empirical Sikkeland systematics of product yields in heavy element fusion reactions (Si 68, Si 68b). These calculations indicate that the reason for the higher product yields in the transfer reaction is the relatively cold residual nucleus produced in this reaction compared to the complete fusion reaction.

Demin et al. (De 80) used multi-nucleon transfer reactions to produce ^{246}Cf, ^{251,253}Es, ^{250,254}Fm, and ^{256}Md from ^{249}Cf using ^{22}Ne projectiles while Hoffman et al. (Ho 81) believe they have identified ^{259}Fm as being produced in the reaction of ^{248}Cm with ^{18}O. Perhaps the most significant of the recent "transfer" reaction studies as far as creating interest in these reactions as useful tools for transuranium nuclide synthesis is the work of Lee et al. (Le 81b) Lee et al. measured the yields of heavy actinides formed in the interaction of near barrier energy ^{16}O, ^{18}O, ^{20}Ne and ^{22}Ne with ^{248}Cm. Typical product yield distri-

butions are shown in Figure 29. Interestingly enough, when one compares the yields of products in Figure 29 with those seen in deep inelastic transfer reactions of much heavier projectile ions interacting with ^{248}Cm (Figure 28b), one sees similar values for the cross sections, and a similar range of species being produced. One also observes a shift in the centroids of the isotopic distributions of two A units when the projectile A increases by two units. This latter observation may be consistent with the known dependence of both deep inelastic transfer reactions (Ar 71) and incomplete fusion reactions (Wi 80b) upon the ground state mass surface ("Q_{gg} systematics"). This Q_{gg} dependence as pointed out (Bo 71) is a result of the existence of a partial statistical equilibrium of a strongly interacting nuclear system. Because of the partial equilibrium, the density of final states which in turn is proportional to Q_{gg} plays an important role. However, one must sound a note of caution. The observed product yields are most certainly not the typical primary reaction product yields. The observed products are the survivors after-excitation of the primary products. That de-excitation process may, in fact, be complex for if these products are truly incomplete fusion products, the angular momenta of the primary products will lie within some ℓ window whose mean value is not low. This high ℓ of the residual nucleus will, of course, increase the probability of fission. Regardless of the reaction mechanism involved, it seems clear that a proper estimation of the final product yields in such reactions may be as complex as the problems encountered in making such estimates for deep inelastic transfer reactions.

Regardless of the actual mechanism(s) operating in the reactions studied by Lee _et al_., it is interesting to consider the use of "incomplete fusion" or " massive transfer" reactions for transuranium nuclide synthesis. The "massive transfer" process, first recognized by Inamura _et al_. (In 77) and

Zolnowski et al. (Zo 78), is the subject of a recent review by Sugihara (Su 81). Massive transfer is a heavy ion reaction in which a relatively large part of the projectile is transferred to the target nucleus in a peripheral or near peripheral reaction. According to a model for these reactions formulated by Udagawa and Tamura (Ud 80), the projectile breaks up elastically in the nuclear field with the breakup probability having a maximum for the grazing trajectory. The massive projectile fragment then fuses with the target nucleus (with an appropriate ℓ_{crit} for the target-projectile fragment system), generally transferring significant angular momentum to it. However, since projectile spectator fragment carries away a large amount of the available energy as kinetic energy, the excitation energy of target + absorbed fragment system is reduced, producing cold nuclei near the yeast line. It is also possible, at least formally, to use such transfer reactions as a source of exotic projectiles. For example, ^{22}Ne could give rise to ^{21}F capture, ^{18}O could give rise to ^{17}N capture, etc.

This discussion of "transfer" reactions should not conclude without noting the possibility that many of the experimental data discussed here are consistent with the idea of a deep inelastic transfer reaction. Nitschke (Ni 80), in particular, argues that the similarities in excitation functions and isotopic distributions between deep inelastic transfer reactions (Figure 28b) and so called "transfer" reactions (Figure 29) indicates that the reaction mechanism(s) involved are one and the same.

5.5 Complete Fusion Reactions

The classical method of preparing transuranium nuclei has been through the use of the complete fusion reaction. A typical example is the synthesis of element 106 by Ghiorso et al. (Gh 74) who bombarded ^{249}Cf with 95 MeV ^{18}O and observed the ^{249}Cf (^{18}O, 4n) ^{263}106 reaction with a cross section of $\sim$0.3nb.

The $^{263}106$ atoms ($t_{\frac{1}{2}}$ = 0.9 ± 0.2 sec) were identified by observing the decay sequence $^{263}106 \xrightarrow{\alpha} {}^{259}Rf \xrightarrow{\alpha} {}^{255}No \xrightarrow{\alpha}$. The $^{263}106$ atoms were isolated using a helium jet and deposited on the rim of a wheel. The deposit was then rotated in front of a sequence of surface barrier detectors which detected the primary α-decay of $^{263}106$. These primary detectors were then moved to face another series of secondary detectors which detected the decay of the previously known daughter atoms implanted in the primary detectors recoil in the initial decay. The time correlated decay information was recorded using an on-line computer. A total of 14 time-correlated events was observed.

However, despite successes such as this, if one looks at the cross sections for complete fusion reactions such as the X (Heavy Ion, 4n) Y reaction, one sees a sharp decrease in the magnitude of these cross sections as the (Z,A) of the heavy ion projectile increase (Og 81, see Figure 30). If one takes as a further constraint, the limits on availability of target materials with Z > 98 (see Table 19), one forsees difficulties in synthesizing new transuranium nuclei with complete fusion reactions. A number of workers, particularly those in the Soviet Union, have pointed out that if one uses some heavy ion projectiles with $40 \leq A \leq 60$, one has the possibility of forming extremely "cold" compound nuclei whose survival probabilities might be high enough to compensate for the decreased complete fusion cross sections. This point is shown best in Figure 31 (Og 81) in which the minimum compound nuclear excitation energy is shown as a function of the projectile mass number for different target-projectile systems leading to the formation of the compound nuclei ^{242}Fm, ^{252}Rf and $^{266}108$.

A number of scattered experimental studies involving the magic Pb and Bi nuclei have shown that the possibility of such "cold fusion" reactions is, in fact, a reality. Flerov et al. (Fl 76) observed the pro-

duction of ^{252}No using the ^{206}Pb (^{48}Ca, 2n) reaction, while Nitschke et al. (Ni 79) found ^{254}No to be produced with a surprisingly large cross section of 3.4 ± 0.4 μb in the ^{208}Pb (^{48}Ca, 2n) reaction. In this same vein, Gäggeler et al. (Gä 79) observed the production of ^{244}Fm in the ^{206}Pb (^{40}Ar, 2n) reaction. "Cold fusion" energetics were combined with their fragmentation theory for ion-ion potentials by Magda et al. (Ma 80) to predict complete fusion cross sections for producing elements with Z=103, 105 and 107.

The principal development, however, that has pushed "cold fusion" reactions to the forefront in efforts to synthesize new transuranium nuclei was the work of Münzenberg et al. (Mü 81, Mü 81c) using the velocity filter SHIP at GSI. They have observed unambiguous evidence for the occurrence of the ^{207}Pb (^{50}Ti, 2n)^{255} Rf and ^{209}Bi (^{50}Ti, 2n) ^{257} Ha reactions at a bombarding energy of 4.85 MeV/u. Most interestingly at a ^{50}Ti energy of 235 MeV, they observed the ^{208}Pb (^{50}Ti,n) ^{257} Rf reaction. Since SHIP is a velocity separator, "transfer" and "deep inelastic" products are strongly suppressed since the products from these binary reactions cannot move with the velocity of the complete fusion evaporation residues. In addition, the separator accepts recoils only from a limited range of angles near 0°. Thus, the aforementioned reactions are quite probably cold complete fusion reactions.

The pièce de résistance of their efforts to date, however, is the use of cold fusion reactions to synthesize and, thus discover, element 107 (Mü 81). In this study ^{209}Bi was bombarded with 4.85 and 4.95 MeV/u ^{54}Cr and the ^{209}Bi (^{54}Cr, n) ^{262}107 reaction was observed. The identification of the ^{262}107 ($t_{\frac{1}{2}} = 4.7^{+2.3}_{-1.6}$ ms) was based upon the observation of a set of correlated alpha particle decays which end in the known ^{250}Fm decay shown in Figure 32. No complete decay chains were observed due to the small yield and the 50% efficiency of the detector system, but two partially complete chains ending

in ^{250}Fm were observed and one chain ending in ^{254}Lr was observed. The velocity of the ^{262}107 atoms was measured two different ways, by the velocity separator and by a time-of-flight measurement. The energy of the evaporation residue was measured and agreed with expectations for the cold fusion mechanism.

6. FUTURE DIRECTIONS

6.1 New Technical Developments

Having reviewed the highlights of current developments in the use of heavy ion reactions to synthesize transuranium nuclei, it is interesting to speculate what future developments might occur in this field. It is clear that future scientific progress in this area will be built on a foundation of new and better experimental techniques to study the very short half-life (ns $\lesssim t_{\frac{1}{2}} \lesssim$ s) species likely to be encountered in future work.

Of the isolation and identification techniques to be used in the future, only those capable of being used for the short half-lives discussed above are likely to find much use. Spectroscopic and chemical studies may be made using the newest chromatographic techniques to concentrate the longer lived species, but in general, chemical isolation and identification techniques will probably use the more modern physical chemical techniques. An example of these techniques is the use of lasers (Na 79) to do single atom detection as in the work of Bemis et al. (Be 79) to measure the optical isomer shift for the 1 ms spontaneously fissioning isomer ^{240}Am. The other traditional identification techniques involving genetic identification via observations of decay chains or direct measurement of product Z by X-ray or photoelectron detection appear to be quite applicable to short half-life species, especially with improvements in detector efficiency. Clearly the fast isolation techniques such as the magnetic spectrometers or velocity separators will have special importance especially if adapted to study transuranium nuclide production by a variety of different reaction mechanisms. For a number of the transuranium production methods of the future, new target technologies, similar to those currently used at the ISOLDE facility for p-nucleus reactions (Ra 79), to allow the use of high

intensity, high energy heavy ion beams will have to be developed. All of these marvelous developments will, of course, have to be made within whatever financial limitations future research faces.

6.2 Deep Inelastic Transfer and Incomplete Fusion Reactions

As indicated in Section 5.3, current research in the use of deep inelastic transfer reactions has progressed far enough to indicate (Gä 81) that deep inelastic transfer reactions involving heavier targets such as ^{249}Cf or ^{254}Es could lead to the production of more neutron rich actinides. This expectation has certainly been verified in the lighter nuclei produced from the projectile nucleus where the new neutron rich nuclides ^{37}Si, ^{40}P, ^{41}S and ^{42}S were made using deep inelastic reactions (Au 79). Viola et al. (Vi 80) have calculated that it should be possible to produce the new transuranium species ^{234}Cf, ^{236}Cf and ^{238}Cf with production cross sections of microbarns using the reaction of 464 MeV ^{56}Fe with ^{209}Bi.

In the case of incomplete fusion or other direct reactions, the possibility of producing "cold" reaction products with the use of existing projectile beams and targets is quite encouraging. Hoffman (Ho 81b) has speculated that in the ^{48}Ca + ^{248}Cm reaction one might be able to produce ^{288}112 or ^{291}113 in a relatively "cold" manner.

6.3 Cold Fusion Reactions

The success in synthesizing element 107 using cold fusion reactions has revived interest in the use of the ^{48}Ca and ^{248}Cm reaction to make superheavy elements. Efforts to use this reaction to synthesize superheavy elements have been reviewed previously (Se 79b). The thrust of the analysis presented in Se 79b was that if the ^{48}Ca and ^{248}Cm nuclei had fused, the failure to observe superheavy nuclei in this reaction meant that the fission barrier heights for these nuclei were $\lesssim$ 6 MeV (a conclusion suggested by some calculations (Ra 74).

It was recommended (Se 79b) that further attempts to synthesize superheavy nuclei using the ^{48}Ca + ^{248}Cm cold fusion reaction occur at bombarding energies closer to the interaction barrier (in that all experiments had been carried out at ∿20 MeV above the barrier). The fundamental difficulty with this suggestion was that it conflicted with the best theoretical calculations of the energy needed to cause the ^{48}Ca and ^{248}Cm nuclei to fuse. Nix and Sierk (Ni 77b) and Swiatecki (see, for example, (Sw 81) have calculated that when two nuclei fuse, there must be an "extra push" (in excess of the interaction barrier) given to them to assume a deformation inside the fission saddle point and truly fuse. The magnitude of the "extra push" for the ^{48}Ca + ^{248}Cm system is estimated to be ∿ 9 MeV

However, Schmidt et al. (Sc 81b) have used SHIP to measure the excitation functions for the production of the evaporation residues ^{209}Fr and ^{218}Th from the ^{86}Kr + ^{123}Sb and ^{124}Sn + ^{94}Zr reactions. In these symmetric systems, the "extra push" effect is expected to be maximum but no evidence was found for the existence of an "extra push". Thus, the authors of Sc 81b suggest the use of the ^{48}Ca + ^{248}Cm reaction to produce superheavy nuclei at 10 MeV below the barrier.

6.4 Secondary Beams

One new interesting idea for using heavy ion reactions to synthesize transuranium nuclei has been put forth by Dufour, Fleury and Bimbot (Du 81b). The basic idea is to use a heavy ion reaction to create an "exotic" secondary beam with which to do the actual synthesis reaction. The principal difficulty, as one recognizes, is that such processes involve the product of the probabilities of two events, the initial beam generation reaction and the synthesis reaction. However, as Dufour, Fleury and Bimbot show, there are

some particularly attractive secondary beam possibilities. For example, with the use of projectile fragmentation reactions in the intense 10^{12}part/sec 86 MeV/n heavy ion beams at the SC synchrocyclotron at CERN, one might expect to produce ^{16}C beams with an intensity of $\sim 10^{9}$ part/sec. The use of such neutron-rich secondary beams in complete fusion reactions might lead to the production of 10-100 atoms/hr of $^{260,261}No$. Similar studies with proton-rich secondary beams are estimated to produce 10^{1}-10^{2} atoms/hr of $^{237,238,239}Bk$.

6.5 Summary

Although over forty years have elapsed since the discovery of the first transuranium element, the study of these elements and their production in heavy ion reactions is still an active, important, and productive endeavor. Amongst the many significant scientific issues which research in this field helps to address are the behavior of nuclear matter under unusual conditions (such as the large deformations encountered in the spontaneously fissioning isomers), the fission stability of nuclei at high angular momentum, the development of nuclear hydrodynamics and the search for the illusive super-heavy elements. There are many new exciting developments in the use of heavy ions to synthesize new transuranium nuclei whose gross features have been barely sketched out. Years of exciting research lie ahead of us.

This work was supported by the Director, Office of Energy Research, Division of Nuclear Physics of the Office of High Energy and Nuclear Physics of the U. S. Department of Energy under Contract W-7405-ENG-48.

References

Åb 80 S. Åberg, S.E. Larson, P. Möller, S.G. Nilsson, G. Leander, and I. Ragnarsson, Physics and Chemistry of Fission, 1979, Vol. I, IAEA, Vienna, (1980) p. 303.

Al 74 J.R. Alonso in Genelin Handbuch der Anorganischen Chemie, Erganzungswerk, Springer, Berlin, 1974, Vol. 7b, Part A 1, II, p. 28.

Ar 71 A.G. Artukh, V.V. Avdeichikov, J. Ero, G.F. Gridnev, V.L. Mikheev, V.V. Volkov, and J. Wilczynski, Nucl. Phys. A160: 511 (1971).

Au 79 P. Auger, T.H. Chiang, J. Galin, B. Gatty, D. Guerreau, E. Nolte, J. Pouthas, X. Tarrago, and J. Girard, Z. Phys. A289: 255 (1979).

Ay 76 S. Ayik, B. Schürmann and W. Nörenberg, Z. Phys. A277: 299 (1976.

Ay 76b S. Ayik, B. Schürmann and W. Nörenberg, Z. Phys. A279: 145 (1976).

Ay 78 S. Ayik, G. Wolschin, and W. Nörenberg, Z. Phys. A286: 271 (1978).

Ba 74 B.B. Back, H.C. Britt, O. Hansen, B. Levoux, and J.D. Garrett, Phys. Rev. C10: 1948 (1974).

Ba 78 P.A. Baisden and G.T. Seaborg, Lawrence Berkeley Laboratory Report LBL-8151, June 1978, p. 35.

Be 73 C.E. Bemis, Jr., R.J. Silva, D.C. Hensley, O.L. Keller, Jr., J.R. Tarrant, L.D. Hunt, P.F. Dittner, R.L. Hahn, and C.D. Goodman, Phys. Rev. Lett. 31: 647 (1973).

Be 74 C.E. Bemis, in Proc. Int'l Conf. on Reactions Between Complex Nuclei, Vol. 2. (1974) p. 529.

Be 77 M. Beckerman and M. Blann, Phys. Rev. Lett. 38: 272 (1977).

Be 77b M. Beckerman and M. Blann, Phys. Lett. 68B: 31 (1977).

Be 78 M. Beckerman and M. Blann, Phys. Rev. C17: 1615 (1978).

Be 79 C.E. Bemis, J.R. Beene, J.P. Young, and S.D. Kramer, Phys. Rev. Lett. 43: 1854 (1979).

Bi 81 J.E. Bigelow, private communication, 1981.

Bj 74 S. Bjørnholm, A. Bohr and B.R. Mottelson, Physics and Chemistry of Fission, 1973, Vol. I, IAEA, Vienna (1974) p. 367.

Bj 80 S. Bjørnholm and J.E. Lynn, Rev. Mod. Phys. 52: 725 (1980).

Bo 71 J.P. Bondorf, F. Dickmann, D.H.E. Gross, and P.J. Siemens, J. Phys. (Paris), Colloq. 32: C6 (1971).

Br 68 H.C. Britt, F.A. Rickey, Jr., and W.S. Hall, Phys. Rev. 175: 1525 (1968).

Br 68b D.R. Brown, Halides of the Lanthanides and Actinides, Wiley, London 1968.

Br 80 M. Brack, Physics and Chemistry of Fission, 1979, Vol. I, IAEA, Vienna, (1980), p. 227.

Br 80b H.C. Britt, E. Cheifetz, D.C. Hoffman, J.B. Wilhelmy, R.J. Dupzyk, and R. Lougheed, Phys. Rev. C21: 761 (1980).

Br 81 H.C. Britt, Physics and Chemistry of Fission, 1979, Vol. I, IAEA, Vienna (1980) p. 31.

Ca 69 T.A. Carlson, C.W. Nestor, J.R., F.B. Malik and T.C. Tucker, Nucl. Phys. A135: 57 (1969).

Ch 56 G.R. Choppin, B.G. Harvey and S.G. Thompson, J. Inorg. Nucl. Chem. 3: 66 (1956).

Cl 79 J.M. Cleveland, The Chemistry of Plutonium, ANS, LaGrange Park (1979).

Co 65 G.H. Coleman, The Radiochemistry of Plutonium, NAS-NS-3058 (1965).

Co 74 S. Cohen, F. Plasil, and W.J. Swiatecki, Ann. Phys. 82: 557 (1974).

Cu 64 B.B. Cunningham, Ann. Rev. Nucl. Sci. 14: 323 (1964).

De 80 A.G. Demin, V.A. Druin, Y.V. Lobznov, R.N. Sagaidak, V.K. Utenkov and S. Hubener, Int'l Symp. on the Synthesis and Properties of New Elements, Dubna, 1980, Abstract D7-80-556, p. 60.

Di 71 P.F. Dittner, C.E. Bemis, Jr., D.C. Hensley, R.J. Silva, and C.D. Goodman, Phys. Rev. Lett. 26: 1037 (1971).

Dr 76 V.A. Druin, Y.S. Korotkin, Y.V. Lobanov, Y.V. Poluboyarinov, R.N. Sagaidak, G.M. Solov'eva, S.P. Tret'yakov and, Y.P. Kharitonov, Yad. Fiz. 24: 254 (1976).

Dr 77 V.A. Druin, B. Bochev, Y.P. Kharitonov, Y.S. Kovotkin, V.N. Kosyakov, Y.V. Lobanov, E.A. Minin, Y.V. Poluboyarinov, A.G. Rykov, R.N. Sagaidak, S.P. Tret'yakova, JINR Report E7-10499 (1977).

Du 81 J.P. Dufour, R. Del Moral, A. Fleury, F. Hubert, Y. Llabador, M.B. Manhourat, R. Bimbot, D. Gardes, and M.F. Rivet, Proc. of the Int'l Conf. on Nuclei far from Stability, Helsingør, Denmark, June, 1981.

Du 81b J.P. Dufour, A. Fleury and R. Bimbot, Phys. Rev. C23: 801 (1981).

Es 71 K. Eskola, P. Eskola, M. Nurmia and A. Ghiorso, Phys. Rev. C4: 632 (1971).

Fa 80 M.E. Faber, A. Faessler, and M. Ploszajczak, Physics and Chemistry of Fission, 1979, Vol. I, IAEA, Vienna (1980) p. 361.

Fe 75 W.C. Fernelius, K. Loening and R.M. Adams, J. Chem. Ed. 52: 583 (1975).

Fi 67 P.R. Fields and T. Moeller, Lanthanide/Actinide Chemistry, ACS, Washington (1967).

Fl 64 G.N. Flerov, Y.T. Oganessian, Y.V. Lobanov, V.I. Kuznetsov, V.A. Druin, V.P. Perelygin, K.A. Gavrilov, S.P. Tretyiakova, V.M. Plotko, At. Energ. (USSR), 17: 310 (1964) [Trans. Sov. At. Energ. 17: 1046 (1964)]; Phys. Lett. 13: 73 (1964.

Fl 68 G.N. Flerov, J. Phys. Soc. Japan Suppl. 24: 327 (1968).

Fl 68b G.N. Flerov, V.A. Druin, A.G. Demin, Y.V. Lobanov, N.K. Skobelev, G.N. Akapiev, B.V. Fefilov, I.V. Kolesov, K.A. Gavrilov, Y.P. Kharitonov, and L.P. Chelnokov, JINR Report JINR-P7-3808, 1968.

Fl 70 G.N. Flerov, Y.T. Oganessian, Y.V. Lobanov, Y.A. Lazarev, S.P. Tret'yakova, I.V Kolesov, and V.M. Plotko, Atom. Energ. 29: 243 (1979).

Fl 76 G.N. Flerov, Y.T. Oganessian, A.A. Pleve, N.V. Pronin and Y.P. Tretyakov, Nucl. Phys. A267: 359 (1976).

Fl 82 G.N. Flerov, "Superheavy Nuclei."

Fr 62 A.M. Friedman and W.C. Mohr, Nucl. Instru. Meth. 17: 78 (1962)

Fr 79 H. Freiesleben, K.D. Hildenbrand, F. Pühlhofer, W.F.W. Schneider, R. Bock, D.V. Harrach, and H.J. Specht, Z. Phys. A292: 171 (1979).

Fu 68 A. Fubini, J. Blons, A. Michaudon, and D. Paya, Phys. Rev. Lett. 20: 1373 (1968).

Ga 76 A. Gavron, H.C. Britt, E. Konecny, J. Weber and J.B. Wilhelmy, Phys. Rev. C13: 2374 (1976).

Gä 79 H. Gäggeler, A.S. Iljninov, G.S. Popeko, W. Seidel, G.M. Ter'Akopian, S.P. Tretyakova, Z. Phys. A289: 415 (1979).

Gä 81 H. Gäggeler, M. Schädel, W. Brüchle, J.V. Kratz, K. Summerer, G. Wirth, N. Trautmann, P. Peuser, G. Tittel, R. Stakeman, G. Herrmann, E.K. Hulet, R.W. Lougheed, J.M. Nitschke, R.L. Hahn, and R.L. Ferguson, Int'l. Conf. on Nuclei Far From Stability, Helsingør, Denmark, June, 1981.

Gh 58 A. Ghiorso, T. Sikkeland, J.R. Walton and G.T. Seaborg, Phys. Rev. Lett. 1: 18 (1958).

Gh 69 A. Ghiorso, M. Nurmia, J. Harris, K. Eskola, and P. Eskola, Phys. Rev. Lett. 22: 1317 (1969).

Gh 70 A. Ghiorso, M. Nurmia, K. Eskola, J. Harris, and P. Eskola, Phys. Rev. Lett. 24: 1498 (1970).

Gh 71 A. Ghiorso, M. Nurmia, K. Eskola, and P. Eskola, Phys. Rev. C4: 1980 (1971).

Gh 72 A. Ghiorso, in Adventures in Experimental Physics β (B. Maglich, ed.), World Science Education, Princeton (1972), p. 243.

Gh 74 A. Ghiorso, J.M. Nitschke, J.R. Alonso, C.T. Alonso, M. Nurmia, G.T. Seaborg, E.K. Hulet, and R.W. Lougheed, Phys. Rev. Lett. 33: 1490 (1974).

Gh 77 A. Ghiorso, J.M. Nitschke, M.J. Nurmia, R.E. Leber, L.P. Somerville and S. Yashita, Lawrence Berkeley Laboratory Report LBL-6575 (1977).

Gi 74 W.M. Gibson and N. Maruyama in Channeling, (D.V. Morgan, ed.) Wiley, New York (1974).

Go 73 V.I. Goldanskii and S.M. Polikanov, The Transuranium Elements Trans. by J.E.S. Bradley, Plenum, New York (1973).

Go 80 V.M. Gorbacher, Y.S. Zamyatnin, and A.A. Lbov, Nuclear Reactions in Heavy Elements, Pergamon, Oxford, (1980).

Gr 76 H.R. Groening and W. Loveland, Phys. Rev. C10: 697 (1976).

Ha 74 F. Hanappe, M. Lefort, C. Ngo, J. Peter and B. Tamain, Phys. Rev. Lett. 32: 738 (1974).

Ha 74b R.L. Hahn, P.F. Dittner, K.S. Toth and O.L. Keller, Phys. Rev. C10: 1889 (1974).

Ha 76 B.G. Harvey, G. Herrman, R.W. Hoff, D.C. Hoffman, E.K. Hyde, J.J. Katz, O.L. Keller, Jr., M. Lefort, and G.T. Seaborg, Science 193: 1271 (1976).

Ha 77 D. Habs, V. Metag, H.J. Specht, G. Ulfert, Phys. Rev. Lett. 38: 387 (1977).

He 78 G. Herrmann in Superheavy Elements, (M.A.K. Codhi, ed.) Pergamon, New York (1978) p. 24.

Hi 53 D.L. Hill and J.A. Wheeler, Phys. Rev. 89: 1102 (1953).

Hi 60 G.H. Higgins, The Radiochemistry of the Transuranium Elements, NAS-NS-3031 (1960).

Hi 77 K.D. Hildenbrand, H. Freiesleben, F. Pühlhofer, W.F.W. Schneider, R. Bock, D.v. Harrach, and H.J. Specht, Phys. Rev. Lett. 39: 1065 (1977).

Ho 69 E.P. Horwitz, C.A.A. Bloomquist, and D.J. Henderson, J. Inorg. Nucl. Chem. 31: 1149 (1969).

Ho 74 D.C. Hoffman and M.M. Hoffman, Ann. Rev. Nucl. Sci. 24: 151 (1974).

Ho 80 D.C. Hoffman, J.B. Wilhelmy, J. Weber, W.R. Daniels, E.K. Hulet, R.W. Lougheed, J.H. Landrum, J.F. Wild, and R.J. Dupzyk, Phys. Rev. C21: 972 (1980).

Ho 81 D.C. Hoffman, D. Lee, A. Ghiorso, M.J. Nurmia, K. Aleklett and M. Leino, Phys. Rev. C24: 495 (1981.

Ho 81b D.C. Hoffman, Los Alamos Scientific Laboratory Report LA-UR-81-2678.

Hu 77 E.K. Hulet, R.W. Lougheed, J.F. Wild, J.H. Landrum, P.C. Stevenson, A. Ghiorso, J.M. Nitschke, R.J. Otto, D.J. Morrissey, P.A. Baisden, B.F. Gavin, D. Lee, R.J. Silva, M.M. Fowler and G.T. Seaborg, Phys. Rev. Lett. 39: 385 (1977).

Hu 80 E.K. Hulet, R.W. Lougheed, J.H. Landrum, J.F. Wild, D.C. Hoffman, J. Weber, and J.B. Wilhelmy, Phys. Rev. C21: 966 (1980).

Hu 82 E.K. Hulet and R.W. Lougheed, Lawrence Livermore National Laboratory Report UCAR-10062-81/1, January, 1982.

Hy 64 E.K. Hyde, I. Perlman, and G.T. Seaborg, The Nuclear Properties of The Heavy Elements, Vol. I, II, III Prentice-Hall, Englewood Cliffs, (1964).

In 77 T. Inamura, M. Ishihara, T. Kukuda, T. Shimoda and K. Furuta, Phys. Lett. 68B: 51 (1977).

Ja 56 J.D. Jackson, Can. J. Phys. 34: 767 (1956).

Ka 57 J.J. Katz and G.T. Seaborg, The Chemistry of the Actinide Elements, Methuen, London (1957).

Ke 71 C. Keller, The Chemistry of the Transuranium Elements, Verlag Chemie, Weinheim (1971).

Ke 77 O.L. Keller, Jr. and G.T. Seaborg, Ann. Rev. Nucl. Sci. 27: 139 (1977).

Kr 74 J.V. Kratz, J.O. Liljenzin and G.T. Seaborg, Inorg. Nucl. Chem. Lett. 10: 951 (1974).

Kr 74b J.V. Kratz, A.E. Norris and G.T. Seaborg, Phys. Rev. Lett. 33: 502 (1974).

Kr 80 J.V. Kratz, International Conf. on Extreme States in Nuclear Systems, Dresdin, February, 1980.

Le 76 M. Lefort, J. de Physique, C5, (11), 5 (1976).

Le 78 C.M. Lederer and V.S. Shirley, Table of Isotopes, 7th Edition, Wiley, New York (1978).

Le 81 M. E. Leino, S. Yashita and A. Ghiorso, Phys. Rev. C24, 2370 (1981).

Le 81a D. Lee, H. von Gunten, B. Jacak, M. Nurmia, Y.F. Liu, C. Luo, G.T. Seaborg and D.C. Hoffman, Los Alamos Scientific Laboratory Report LA-UR-81-1193 Rev., September, 1981.

Lo 80 R.W. Lougheed, E.K. Hulet, J.M. Nitschke, R.L. Landingham and H Folger, Lawrence Livermore National Laboratory Report, UCRL-84604, January 1980.

Lo 81 W. Loveland, Oregon State University Report DOE/ER/70035-4, January, 1981.

Lu 71 C.C. Lu, F.B. Malik, and T.A. Carlson, Nucl. Phys. A175: 289 (1971).

Lu 81 T. Lund, D. Hirdes, H. Jungclas, D. Molzahn, P. Vater, R. Brandt, P. Lemmertz, R. Fass, H. Wollnik, and H. Gäggeler, Z. Phys. A303: 115 (1981).

Ma 63 R.D. MacFarlane and R.D. Griffoen, Nucl. Instru. 24: 461 (1963).

Ma 79 D. Marx, F. Nickel, G. Münzenberg, K. Güttner, H. Ewald, W. Faust, S. Hofmann, H.J. Schött, Nucl. Instr. Meth. 163: 15 (1979).

Ma 80 M.T. Magda, A. Sandalescu, D.G. Popescu and W. Greiner, J. Phys. G: Nucl. Phys. 6: 221 (1980).

Mc 40 E. McMillan and P.H. Abelson, Phys. Rev. 57: 1185 (1940).

Me 75 V. Metag, Nukleonika, 20: 789 (1975).

Me 77 V. Metag and G. Sletten, Nucl. Phys. A282: 77 (1977).

Me 80 V. Metag, Physics and Chemistry of Fission, 1979, Vol. I, IAEA, Vienna, (1980) p. 153.

Mi 68 E. Migneco and J.P. Theobald, Nucl. Phys. A112: 603 (1968).

Mo 68 F.L. Moore, Anal. Chem. 40: 2130 (1968).

Mo 72 L.G. Moretto, Nucl. Phys. A180: 337 (1972).

Mo 74 P. Möller and J.R. Nix, Physics and Chemistry of Fission, 1973 Vol. I, IAEA, Vienna, (1974) 103.

Mo 75 L.G. Moretto and J.S. Sventek, Phys. Lett. B58: 26 (1975).

Mö 80 P. Möller and J.R. Nix, Los Alamos Scientific Laboratory Report La-UR-80-1996, July, 1980.

Mö 80b P. Möller, Physics and Chemistry of Fission, 1979, Vol. I, Vienna, (1980) p. 283.

Mo 81 J.D. Molitoris and J.M. Nitschke, Lawrence Berkeley Laboratory Report LBL-9725, January, 1981.

Mo 81b K.J. Moody, M.J. Nurmia and G.T. Seaborg, Lawrence Berkeley Laboratory Report LBL-11588, March, 1981 p. 188.

Mü 79 G. Münzenberg, W. Faust, S. Hofmann, P. Armbruster, K. Güttner, and H. Ewald, Nucl. Instru. and Meth. 161: 65 (1979).

Mü 81 G. Münzenberg, S. Hofman, F.P. Hessberger, W. Reisdorf, K.H. Schmidt, J.H.R. Schneider, P. Armbruster, C.C. Sahm and B. Thuma, Z. Phys. A300: 107 (1981).

Mü 81b G. Münzenberg, W. Faust, F.P. Hessberger, S. Hofmann, W. Reisdorf, K.H. Schmidt, W.F.W. Schneider, H.J. Schött, P. Armbruster, B. Thuma, H. Ewald, and D. Vermeulen, Nucl. Instr. Meth. 186: 423 (1981).

Mü 81c G. Münzenberg, S. Hofmann, W. Faust, F.P. Hessberger, W. Reisdorf, K.H. Schmidt, T. Kitihara, P. Armbruster, K. Güttner, B. Thuma and D. Vermeulen, Z. Phys. A302: 7 (1981).

My 74 B.F. Myasoedov, L.I. Guseva, I.A. Lebedov, M.S. Milynkova, and M.K. Chmutova, Analytical Chemistry of Transplutonium Elements, Wiley, New York (1974).

Na 79 M.H. Nayfeh, Amer. Scientist, 67: 204 (1979).

Na 80 J.D. Navratil and W.W. Schulz, Actinide Separations, ACS, Washington (1980).

Ne 64 F. Nelson, D.C. Michelson and J.H. Holloway, J. Chromatography 14: 258 (1964).

Ni 77 J.M. Nitschke, in Superheavy Elements, M.A.K. Lodhi, ed., Pergamon, New York (1978) p. 42.

Ni 77b J.R. Nix and A.J. Sierk, Phys. Rev. C15: 2072 (1977).

Ni 79 J.M. Nitschke, R.E. Leber, M.J. Nurmia and A. Ghiorso, Nucl. Phys. A313: 236 (1979).

Ni 80 J.M. Nitschke, Lawrence Berkeley Laboratory Report LBL-11712, September, 1980.

Ni 81 J.M. Nitschke, M. Fowler, A. Ghiorso, R.E. Leber, M.E. Leino, M.J. Nurmia, L.P. Somerville, K.E. Williams, E.K. Hulet, J.H. Landrum, R.W. Lougheed, J.F. Wild, C.E. Bemis, Jr., R.J. Silva, and P. Eskola, Nucl. Phys. A352: 138 (1981).

Og 70 Y.T. Oganessian, Y.V. Lobanov, S.P. Trettyakova, Y.A. Lazarev, I.V. Kolesov, K.A. Gavrilov, V.M. Plotko, and Y.V. Poluboyarinov, At. Energ. (USSR) 28: 393 (1979) [Trans. Sov. At. Energ. 28: 502 (1970)].

Og 74 Y.T. Oganessian, Y.P. Tret'yakov, A S. Iljinov, A.G. Demin, A.A. Pleve, S.P. Tret'yakov, V.M. Plotko, M.P. Ivanov, N.A. Danilov, Y.S. Korotkin, and G.N. Flerov, JETP Lett. 20: 265 (1974).

Og 76 Y.T. Oganessian, A.G. Demin, N.A. Danilov, M.P. Ivanov, A.S. Iljinov N.N. Kolesnikov, B.N. Markov, V.M. Plotko, vanov, N.A. Danilov, Y.S. Korotkin, and G.N. Flerov, JETP Lett. 20: 265 (1976).

Og 81 Y.T. Oganessian, "Actinides 81", Asilomar, CA, Sept. 1981.

Og 82 Y.T. Oganessian, "Heavy Ions and Nuclear Fission."

Ot 76 R.J. Otto, M.M. Fowler, D. Lee, and G. T. Seaborg, Phys. Rev. Lett. 36: 135 (1976).

P 1 Physics and Chemistry of Fission, 1979, IAEA, Vienna, (1980).

Pa 68 W.C. Parker and H. Slätis in Alpha-Beta-and Gamma-Ray Spectroscopy, Vol. I. K. Siegbahn, ed. North-Holland, Amsterdam, (1968) p. 379.

Pe 60 R.A. Penneman and T.K. Keenan, The Radio Chemistry of Americum and Curium, NAS-NS-3006, (1960).

Pe 71 D.F. Peppard, Ann. Rev. Nucl. Sci. 21: 365 (1971).

Pl 73 F. Plasil and W.J. Swiatecki as quoted in Va 73, page 244.

Po 62 S.M. Polikanov, V.A. Druin, V.A. Karnaukov, V.L. Mikhaev, A.A. Pleve, N.K. Skobelev, V.G. Subbottin, G.M. Ter-Akopyan, and V.A. Fomichev, Sov. Phys. JETP 15: 1016 (1962).

R 1 Recommendations of the International Commission on Radiological Protection, ICRP Publ 2, Pergamon, London (1959.

R 2 Recommendations of the International Commission on Radiological Protection, ICRP Publ. 6, Pergamon, London (1964).

Ra 74 J. Randrup, S.E. Larsson, P. Möller, A. Sobiczewski, and A. Lukasiak, and Phys. Scr. 10A: 60 (1974).

Ra 75 J.O. Rasmussen, in Nuclear Spectroscopy and Reactions, Part D, (J. Cerny, ed.) Academic, New York (1975) p. 97.

Ra 76 J. Randrup, S.E. Larsson, P. Möller, S.G. Nilsson, K. Pomorski and A. Sobiczewski, Phys. Rev. C13: 229 (1976).

Ra 79 H.L. Ravn, Phys. Rep. 54: 201 (1979).

Re 81 W. Reisdorf, Z. Phys. A300: 227 (1981).

Ri 79 C. Riedel, G. Wolschin, and W. Nörenberg, Z. Phys. A290: 47 (1979).

Ri 79b C. Riedel and W. Nörenberg, Z. Phys. A290: 385 (1979).

Sc 76 W.W. Schulz, The Chemistry of Americium, ERDA, Washington (1976).

Sc 77 W.U. Schröder and J.R. Huizenga, Ann. Rev. Nucl. Sci. 27: 465 (1977).

Sc 78 M. Schädel, W. Bruchle, B. Haefner, J.V. Kratz, W. Schorstein, N. Trautmann, and G. Herrmann, Radiochimica Acta 25: 111 (1978).

Sc 78b M. Schädel, J.V. Kratz, H. Ahrens, W. Brüchle, G. Franz, H. Gäggeler, I. Warnecke, G. Wirth, G. Herrmann, N. Trautmann, and M. Weis, Phys. Rev. Lett. 41 469 (1978).

Sc 78c B. Schürmann, W. Nörenberg and M. Simbel, Z. Phys. A286: 263 (1978).

Sc 81 M. Schädel, W. Bruchle, H. Gäggeler, J.V. Kratz, K. Summerer, G. Wirth, G. Herrmann, R. Stakemann, N. Trautmann, J.M. Nitschke, E.K. Hulet, R.W. Lougheed, R.L. Hahn, and R.L. Ferguson, GSI Report GSI-81-2, March, 1981.

Sc 81b K.H. Schmidt, P. Armbruster, F.P. Hessberger, G. Münzenberg, W. Reisdorf, C.C. Sahm, D. Vermeulen, H.G. Clerc, J. Keller and H. Schulte, Z. Phys. A301: 21 (1981).

Se 46 G.T. Seaborg, E.M. McMillan, J.W. Kennedy and A.C. Wahl, Phys. Rev. 69: 366 (1946).

Se 54 G.T. Seaborg and J.J. Katz, The Actinide Elements, McGraw-Hill, New York (1954).

Se 58 G.T. Seaborg, The Transuranium Elements, Yale University Press, New Haven, (1958).

Se 63 G.T. Seaborg, Man-Made Transuranium Elements, Prentice-Hall, Englewood Cliffs (1963).

Se 67 G.T. Seaborg, Actinides Reviews, 1: 3 (1967).

Se 68 G.T. Seaborg, Ann. Rev. Nucl. Sci. 18: 53 (1968).

Se 78 G.T. Seaborg, Transuranium Elements Dowden, Hutchinson, and Ross, Inc. Stroudsburg (1978).

Se 79 G.T. Seaborg, Chemical Engineering News, 57, 46 (1979).

Se 79b G.T. Seaborg, W. Loveland and D. J. Morrissey, Science, 203: 711 (1979).

Se 80 G.T. Seaborg, American Scientist 68: 279 (1980).

Si 68 T. Sikkeland, A. Ghiorso and M. Nurmia, Phys. Rev. 172: 1232 (1968).

Si 68b T. Sikkeland, J. Maly and D.F. Lebeck, Phys. Rev. 169: 1000 (1968).

Si 72 T. Sikkeland, N.H. Shafir and N. Trautman, Phys. Lett. 42B: 201 (1972).

Sj 73 S. Bjornholm, A. Bohr, and B.R. Mottelson, Physics an Chemistry of Fission, 1973, Vol. I, IAEA, Vienna, (1974) p. 303.

Sp 72 H.J. Specht, J. Weber, E. Konecny, and D. Heunemann, Phys. Lett. 41B: 43 (1972).

Sp 76 V.I. Spitsyn and J.J. Katz, Chemistry of Transuranium Elements, Pergamon, Oxford (1976).

St 67 V.M. Strutinsky, Nucl. Phys. A95: 420 (1967).

St 80 D.C. Stewart, Handling Radioactivity,, Wiley, New York (1981).

Su 81 T.T. Sugihara, Phys. Scr. 24: 108 (1981).

Sw 55 W.J. Swiatecki, Phys. Rev. 100: 937 (1955).

Sw 81 W.J. Swiatecki, Phys. Scr. 24: 113 (1981).

Ta 61 R. Taagepera and M. Nurmia, Ann. Acad. Sci. Fennicae, Ser. A. Vi, No. 78 (1961) p. 1.

Ud 80 T. Udagawa and T. Tamura, Phys. Rev. Lett. 45: 1311 (1980).

Un 72 J.P. Unik, E.P. Horwitz, K.L. Wolf, I. Ahmad, S. Fried, D. Cohen, P.R. Fields, C.A.A. Bloomquist and D.J. Henderson, Nucl. Phys. A191: 233 (1972).

Un 74 J.P. Unik, J.E. Gindler, L.E. Glendenin, K.F. Flynn, A. Gorski, R.K. Sjoblom, Phys. and Chem. of Fission, 1973, Vol. II, IAEA, Vienna, (1974) p. 19.

Va 73 R. Vandenbosch and J.R. Huizenga, Nuclear Fission, Academic, New York (1973).

Va 77 R. Vandenbosch, Ann. Rev. Nucl. Sci. 27: 1 (1977).

Vi 66 V.E. Viola, Jr., Nucl. Data Sect. A1: 391 (1966).

Vi 80 V.E. Viola, Jr., A.C. Mignerey, H. Breuer, K.L. Wolf, B.G. Glagola, W.W. Wilcke, W.U. Schröder, J.R. Huizenga, D. Hilscher and J.R. Birkelund, Phys. Rev. C22: 122 (1980).

Wa 77 A.H. Wapstra and K. Bos, At. Data and Nucl. Data Tables 19: 177 (1977).

Wa 81 M. Walker, and V.E. Viola, Jr., private communication (1981).

Wi 64 J. Wing and J.D. Varley, Calculated Values of Wing-Fong's Nuclidic Mass Equation, Argonne National Laboratory Report ANL-6886, May, 1964.

Wi 76 B.D. Wilkins, E.P. Steinberg and R.R. Chasman: Phys. Rev. C14, 1832 (1976).

Wi 80 W.W. Wilcke, J.R. Birkelund, H.J. Wollersheim, A.D. Hoover, J.R. Huizenga, W.U. Schroeder, and L.E. Tubbs, At. Data and Nucl. Data Tables 25: 391 (1980).

Wi 80b J. Wilczynski, K. Siwek-Wilcznski, J. van Driel, S. Ganggrijp, D.C.J.M. Hageman, R.V.F. Janssens, J. Lukasiak, and R.H. Siemsson, Phys. Rev. Lett. 45: 606 (1980).

Wo 77 K.L. Wolf, J.P. Unik, E.P. Horwitz, C.A.A. Bloomquist, and W. Delphin, Bull. Am. Phys. Soc. 22: 67 (1977).

Wo 77b G. Wolschin, Nuklesnika, 22: 1165 (1977).

Wo 78 G. Wolschin and W. Nörenberg, Z. Phys. A284: 209 (1978).

Wo 78b G. Wolschin and W. Nörenberg, Phys. Rev. Lett. 41: 691 (1978).

Ze 78 M. Zendel, E. Stender, N. Trautmann, and G. Herrmann, Nucl. Instr. and Meth. 153: 149 (1978).

Zo 78 D. R. Zolnowski, H. Yamada, S.E. Cala, A.C. Kahler, and T.T. Sugihara, Phys. Rev. Lett 41: 92 (1978).

Zv 66 I. Zvara, Y.T. Chuburkov, R. Tsaletka, T.S. Zvarova, M.R. Shalaevskii, and B.V. Shilov, At. Energ. 21: 83 (1966) [Trans. Sov. At. Energ. 21: 709 (1966)].

Zv 70 I. Zvara, V.Z. Belov, Y.S. Korotkin, M.R. Shalaesky, V.A. Shchegolev, M. Yussonnuas and B.A. Zager, Dubna Report P12-5120 (1970).

Zv 71 I. Zvara, V.Z. Belov, L.P. Chelnokov, V.P. Domanov, M. Hussonois, Y.S. Korotkin, V.A. Shchelgev, and M.R. Shalayevsky, Inorg. Nucl. Chem. Lett 7: 1109 (1971).

TABLE 1

The Known Transuranium Elements

Element	Atomic Number	Chemical Symbol
Neptunium	93	Np
Plutonium	94	Pu
Americium	95	Am
Curium	96	Cm
Berkelium	97	Bk
Californium	98	Cr
Einsteinium	99	Es
Fermium	100	Fm
Mendelevium	101	Md
Nobelium	102	No
Lawrencium	103	Lr
Rutherfordium	104	Rf
Hahnium	105	Ha
-	106	
-	107	

TABLE 2

Summary of Actinide Element Synthesis

lement (symbol)	Z	Synthesis Reaction	Discoverers & Date of Discovery
eptunium (Np)	93	$^{238}U + n \rightarrow {}^{239}U + \gamma$ $^{239}U \xrightarrow{\beta} {}^{239}Np (t_{1/2} = 2.35d)$	E.M. McMillan & P.H. Abelson, 1940.
lutonium (Pu)	94	$^{238}U + {}^{2}H \rightarrow {}^{238}Np + 2n$ $^{238}Np \xrightarrow{\beta-} {}^{238}Pu (t_{1/2} = 86.4y)$	G.T. Seaborg, E.M. McMillan, J.W. Kennedy & A.C. Wahl, 1940-1941.
mericum (Am)	95	$^{239}Pu + n \rightarrow {}^{240}Pu + \gamma$ $^{240}Pu + n \rightarrow {}^{241}Pu + \gamma$ $^{241}Pu \xrightarrow{\beta} {}^{241}Am (t_{1/2} = 433y)$	G.T. Seaborg, R.A. James, L.O. Morgan and A. Ghiorso, 1944-45
urium (Cm)	96	$^{239}Pu + {}^{4}He \rightarrow {}^{242}Cm (t_{1/2}=162.5d) + n$	G.T. Seaborg, R.A. James A. Ghiorso, 1944
erkelium (Bk)	98	$^{241}Am + {}^{4}He \rightarrow {}^{243}Bk (t_{1/2} = 4.5h) + 2n$	S.G. Thompson, A. Ghiorso, G.T. Seaborg, 1949.
alifornium (Cf)	98	$^{242}Cm + {}^{4}He \rightarrow {}^{245}Cf (t_{1/2}=44m) + n$	S.G. Thompson, K. Street,Jr., A. Ghiorso, G.T. Seaborg, 1950
insteinium (Es)	99	"Mike" thermonuclear explosion	A. Ghiorso, S. G. Thompson, G. H. Higgins, G. T. Seaborg, M. H. Studier, P. R. Fields, S. M. Fried, H. Diamond, J. F. Mech, G. L. Pyle, J. R. Manning, C. I. Browne, H. L. Smith, and R. W. Spence, 1952

TABLE 2 (cont.)

Element (symbol)	Z	Synthesis Reaction	Discoverers & Date of Discovery
Fermium (Fm)	100	"Mike" thermonuclear explosion	A. Ghiorso, S. G. Thompson, G. H. Higgins, G. R. Seaborg, M. H. Studier, P. R. Fields, S. M. Fried, H. Diamond, J. F. Mech, G. L. Pyle, J. R. Huizenga, A. Hirsch, W. M. Manning, C. I. Browne, H. L. Smith, and R. W. Spence, 1953.
Mendelevium (Md)	101	$^{253}Es + {}^{4}He \rightarrow {}^{256}Md$ ($t_{\frac{1}{2}}$ = 75m) + n	A. Ghiorso, B. G. Harvey, G. R. Choppin, S. G. Thompson, and G. T. Seaborg, 1955.
Nobelium (No)	102	$^{246}Cm + {}^{12}C \rightarrow {}^{258}No + 4n$	A. Ghiorso, T. Sikkeland, J. R. Walton, and G. T. Seaborg, 1958.
Lawrencium (Lr)	103	$\left.\begin{matrix}^{250}Cf \\ ^{251}Cf \\ ^{252}Cf\end{matrix}\right\} + {}^{11}B \rightarrow {}^{258}Lr + \left\{\begin{matrix}3n \\ 4n \\ 5n\end{matrix}\right.$	A. Ghiorso, T. Sikkeland, A. E. Larsh, and R. M. Latimer, 1961.
		$\begin{matrix}^{250}Cf \\ ^{251}Cf \\ ^{252}Cf\end{matrix} + {}^{10}B \rightarrow {}^{258}Lr + \left\{\begin{matrix}2n \\ 3n \\ 4n\end{matrix}\right.$	

TABLE 3

Fission Barrier Systematics[a]

Isotope	E_A	E_{II} (Relative to ground state)	E_B
^{226}Ra	8.0 ± 0.5		8.5 ± 0.5
^{226}Ac	6.0 ± 0.6		7.7 ± 0.3
^{227}Th	5.9 ± 0.3		6.6 ± 0.3
^{228}Th	6.2 ± 0.3		6.5 ± 0.3
^{229}Th			6.5 ± 0.3
^{230}Th	6.1 ± 0.2		6.5 ± 0.3
^{231}Th	6.0 ± 0.1	<5.8	6.1 ± 0.3
^{232}Th	5.8 ± 0.2	<<4.5	6.2 ± 0.2
^{233}Th	6.3 ± 0.2	<6.2	6.3 ± 0.2
^{234}Th	6.1 ± 0.2		6.5 ± 0.2
^{231}Pa	5.9 ± 0.2		5.9 ± 0.3
^{232}Pa	6.1 ± 0.3	<5.7	6.2 ± 0.2
^{233}Pa	6.1 ± 0.3		6.1 ± 0.3
^{232}U	5.2 ± 0.2		5.1 ± 0.3
^{234}U	5.6 ± 0.2		5.5 ± 0.2
^{235}U	5.9 ± 0.2	2.5 ± 0.3	5.6 ± 0.2
^{236}U	5.6 ± 0.2	2.3 ± 0.2	5.5 ± 0.2
^{237}U	6.1 ± 0.2	2.5 ± 0.4	5.9 ± 0.2
^{238}U	5.7 ± 0.2	2.6 ± 0.01	5.7 ± 0.2
^{239}U	6.3 ± 0.2	1.9 ± 0.3	6.1 ± 0.2
^{240}U	5.7 ± 0.2		5.5 ± 0.2
^{234}Np	5.5 ± 0.2		5.1 ± 0.2
^{235}Np	5.5 ± 0.2		5.2 ± 0.2
^{236}Np	5.8 ± 0.2		5.6 ± 0.2
^{237}Np	5.7 ± 0.2	2.8 ± 0.3	5.4 ± 0.2
^{238}Np	6.1 ± 0.2	2.3 ± 0.3	6.0 ± 0.2
^{239}Np	5.9 ± 0.2		5.4 ± 0.2
^{232}Pu	5.3 ± 0.4		
^{234}Pu	5.8 ± 0.7		
^{235}Pu		2.6 ± 0.4	5.1 ± 0.4
^{236}Pu			4.5 ± 0.4
^{237}Pu		2.8 ± 0.2	

Fission Barrier Systematics[a]
(continued)

Isotope	E_A	E_{II} (Relative to ground state)	E_B
^{238}Pu	5.5 ± 0.2	2.7 ± 0.2	5.0 ± 0.2
^{239}Pu	6.2 ± 0.2	2.6 ± 0.2	5.5 ± 0.2
^{240}Pu	5.6 ± 0.2	2.4 ± 0.3	5.1 ± 0.2
^{241}Pu	6.1 ± 0.2	1.9 ± 0.3	5.4 ± 0.2
^{242}Pu	5.6 ± 0.2		5.1 ± 0.2
^{243}Pu	5.9 ± 0.2	1.7 ± 0.3	5.2 ± 0.2
^{244}Pu	5.4 ± 0.2		5.0 ± 0.2
^{245}Pu	5.6 ± 0.2		5.0 ± 0.2
^{237}Am		2.4 ± 0.2	
^{238}Am		2.6 ± 0.2	
^{239}Am	6.2 ± 0.3	2.4 ± 0.2	
^{240}Am	6.5 ± 0.2	3.0 ± 0.2	5.2 ± 0.3
^{241}Am	6.0 ± 0.2	2.2 ± 0.2	5.1 ± 0.3
^{242}Am	6.5 ± 0.2	2.9 ± 0.2	5.4 ± 0.3
^{243}Am	5.9 ± 0.2	2.3 ± 0.2	5.4 ± 0.3
^{244}Am	6.3 ± 0.2	2.8 ± 0.4	5.4 ± 0.3
^{245}Am	5.9 ± 0.2		5.2 ± 0.3
^{247}Am	5.5 ± 0.2		
^{241}Cm	6.3 ± 0.3	2.1 ± 0.3	4.3 ± 0.5
^{242}Cm	5.8 ± 0.4		4.0 ± 0.5
^{243}Cm	6.4 ± 0.3	1.9 ± 0.3	
^{244}Cm	5.8 ± 0.2		4.3 ± 0.3
^{245}Cm	6.2 ± 0.2	2.1 ± 0.3	
^{246}Cm	5.7 ± 0.2		4.2 ± 0.3
^{247}Cm	6.0 ± 0.2		
^{248}Cm	5.7 ± 0.2		
^{249}Cm	5.6 ± 0.2		
^{250}Cm	5.3 ± 0.2		
^{245}Bk	6.60[d]		
^{246}Bk	6.40[e]		
^{247}Bk	6.50[d]		
^{248}Bk	6.50[e]		
^{249}Bk	6.1 ± 0.2		
^{250}Bk	6.1 ± 0.2		4.1 ± 0.3

Fission Barrier Systematics[a]
(continued)

Isotope	E_A	E_{II} (Relative to ground state)	E_B
^{250}Cf	5.6 ± 0.3		
^{251}Cf	6.15[b]		
^{252}Cf	5.30[c]		4.80
^{253}Cf	5.4 ± 0.3		
^{250}Es	6.70[f]		
^{255}Es	5.40[g]		
^{256}Es	4.80[g]		
^{255}Fm	5.70[g]		

a. Unless otherwise indicated, the above values of the fission barrier parameters are taken from the compilation of Bjornholm and Lynn. For these parameters $h\omega$ values are as follows: e-e nuclei, $h\omega_A$ = 1.04 MeV, $h\omega_B$ = 0.6 MeV; odd-A nuclei, $h\omega_A$ = 0.8 Mev; $h\omega_B$ = 0.52 MeV; 0-0 nuclei, $h\omega_A$ = 0.65 MeV, $h\omega_B$ = 0.45 MeV.

b. From Br 81 $\hbar\omega_A = 0.75$.

c. From Br 81 $\hbar\omega_A = 1.10$.

d. From Br 81 $\hbar\omega_A = 0.85$.

e. From Br 81 $\hbar\omega_A = 0.45$.

f. From Br 81 $\hbar\omega_A = 0.40$.

g. From Br 80b

TABLE 4

Occurrence and Half-Life of Spontaneously Fissioning Isomers[a]

Nucleus	$t_{\frac{1}{2}}$	Nucleus	$t_{\frac{1}{2}}$
^{236}U	116 ± 7 ns	^{240}Am	0.91 ± 0.07 ms
^{238}U	195 ± 30 ns	^{241}Am	1.5 ± 0.6 μs
^{237}Np	45 ± 5 ns	^{242}Am	14.0 ± 0.2 ms
^{236}Pu	34 ± 8 ns	^{243}Am	5.2 ± 0.5 μs
	30 ± 12 ps	^{244}Am	1.0 ± 0.15 ms
^{237}Pu	110 ± 9 ns	^{245}Am	640 ± 60 ns
	1100 ± 80 ns	^{246}Am	73 ± 10 μs
^{238}Pu	0.5 ± 0.2 ns	^{240}Cm	10 ± 2 ps
	6.5 ± 1.5 ns		55 ± 5 ns[b]
^{234}Pu	8.1 ± 0.8 μs	^{241}Cm	15.3 ± 1.0 μs
^{240}Pu	3.8 ± 0.3 ns	^{242}Cm	180 ± 70 ns
^{241}Pu	23 ± 1 μs		40 ± 15 ps
^{242}Pu	3.5 ± 0.6 ns	^{243}Cm	42 ± 6 ns
	28 μs	^{244}Cm	>100 μs
^{243}Pu	58 ± 11 ns	^{245}Cm	13.2 ± 1.8 ns
^{244}Pu	380 ± 80 ps	^{242}Bk	600 ± 100 ns
^{245}Pu	90 ± 30 ns[b]		9.5 ± 2 ns
^{237}Am	5 ± 2 ns	^{244}Bk	820 ± 60 ns
^{239}Am	163 ± 12 ns	^{245}Bk	2 ± 1 ns

a) Unless otherwise noted, this table only includes isomers given a reliability classification of "C" or better in the Table of Isotopes. (Le 78). All $t_{\frac{1}{2}}$ values are from that publication.

b) Reference (Me 80)

Table 5

Decay Properties of the Neptunium Isotopes

Isotope	Half-Life	Mode of Disintegration	Source
^{229}Np	4.0 m	α $\geq$50%(6.89) EC $\leq$50%	$^{233}U(p,5n)$
^{230}Np	4.6 m	α >99%(6.66) EC $\leq$0.97%	$^{233}U(p,4n)$
^{231}Np	48.8 m	α >1%(6.28) EC <99%	$^{233}U(d,4n)$; $^{235}U(d,6n)$; $^{238}U(d,9n)$
^{232}Np	14.7 m	EC	$^{233}U(d,3n)$; $^{235}U(d,5n)$
^{233}Np	36.2 m	EC >99% α $\approx 10^{-3}$%(5.54)	$^{233}U(d,2n)$; $^{235}U(d,4n)$
^{234}Np	4.4 d	EC 99.95% β^+ 0.05%	$^{233}U(d,n)$; $^{235}U(d,3n)$; $^{235}U(p,2n)$
^{235}Np	396 d	EC >99% α 0.0016%(5.022, 5.004, 4.994, 4.922, plus others ranging from 5.105 to 4.81)	$^{235}U(d,2n)$; $^{233}U(\alpha,pn)$
^{236}Np	22.5 h	β^- 50%(0.54, 0.49) EC 50%	$^{235}U(d,n)$; $^{235}U(\alpha,p2n)$; $^{238}U(d,4n)$; $^{237}Np(n,2n)$
^{236}Np	1.1 X 10^5 y	EC 91% β^- 9%	$^{235}U(d,n)$; $^{238}U(d,4n)$
^{237}Np	2.14 X 10^6 y	α(4.787, 4.770, 4.765, plus others ranging from 4.873 to 4.514)	$^{237}U(\beta^-)$
^{238}Np	2.117 d	β^-(1.236, 0.28, 0.25)	$^{237}Np(n,\gamma)$; $^{237}U(d,2n)$
^{239}Np	2.35 d	β^-(0.713, 0.654, 0.437, 0.393, 0.332)	$^{239}U(\beta^-)$
^{240m}Np	7.5 m	β^- 99.89%(2.18, 1.60, 1.30, 0.7) IT 0.11%	$^{240}U(\beta^-)$
^{240}Np	67 m	β^-(0.89)	$^{238}U(\alpha,pn)$; $^{235}U(^3He,p)$
^{241}Np	16.0 m	β^-(1.3)	$^{238}U(\alpha,p)$

Table 6

Decay Properties of the Plutonium Isotopes

Isotope	Half-Life	Mode of Disintegration	Source
^{232}Pu	34 m	80%≤EC≤98% 2%≤α≤20%(6.60, 6.54)	$^{233}U(\alpha,5n)$; $^{235}U(\alpha,7n)$
^{233}Pu	20.9 m	EC 99.88% α 0.12%(6.30)	$^{233}U(\alpha,4n)$
^{234}Pu	8.8 h	EC 94% α 6%(6.202, 6.151, 6.031)	$^{233}U(\alpha,3n)$; $^{235}U(\alpha,5n)$; $^{235}Cm(\alpha)$
^{235}Pu	25.6 m	EC >99% α 0.003%(5.85)	$^{235}U(\alpha,4n)$; $^{233}U(\alpha,2n)$
^{236}Pu	2.85 y	α(5.768, 5.721, 5.615)	$^{235}U(d,n)$; $^{240}Cm(\alpha)$; Daughter ^{235}Np, $^{235}U(\alpha,3n)$
^{237m}Pu	0.18 s	IT	Daughter ^{241}Cm
^{237}Pu	45.4 d	EC >99% α 0.0033%(5.65, 5.36)	$^{235}U(\alpha,2n)$; $^{235}U(\alpha,5n)$; $^{237}Np(d,2n)$
^{238}Pu	87.74 y	α(5.4992, 5.4565, 5.359)	$^{238}U(d,2n)$; $^{242}Cm(\alpha)$ Daughter ^{235}Np
^{239}Pu	2.41×10^4 y	α(5.155, 5.143, 5.105)	$^{239}Np(\beta^-)$
^{240}Pu	6.57×10^3 y	α(5.1683, 5.1234, 5.02)	$^{239}Pu(n,\gamma)$
^{241}Pu	14.4 y	β^- >99%(0.0208) α 0.0024%(4.896, 4.853, plus others ranging from 5.055 to 4.69)	$^{240}Pu(n,\gamma)$
^{242}Pu	3.76×10^5 y	α(4.901, 4.857)	$^{241}Pu(n,\gamma)$; Daughter ^{242}Am
^{243}Pu	4.956 h	β^-(0.58, 0.48)	$^{242}Pu(n,\gamma)$
^{244}Pu	8.1×10^7 y	α(4.589, 4.546)	$^{243}Pu(n,\gamma)$
^{245}Pu	10.5 h	β^-(1.21, 0.93, ≈0.4)	$^{244}Pu(n,\gamma)$
^{246}Pu	10.85 d	β^-(0.33, 0.15)	$^{245}Pu(n,\gamma)$

Table 7

Decay Properties of the Americium Isotopes

Isotope	Half-Life	Mode of Disintegration	Source
^{237}Am	1.22 h	EC >99% α 0.025%(6.042)	$^{239}Pu(p,3n)$; $^{239}Pu(d,4n)$; $^{237}Np(\alpha,4n)$; $^{237}Np(^{3}He,3n)$
^{238}Am	1.63 h	EC >99% α 1.0×10^{-4}%(5.94)	$^{239}Pu(p,2n)$; $^{239}Pu(d,3n)$; $^{237}Np(\alpha,3n)$
^{239}Am	11.9 h	EC >99% α 0.010%(5.776, 5.734, 5.680)	$^{239}Pu(p,n)$; $^{239}Pu(d,2n)$; $^{237}Np(\alpha,2n)$
^{240}Am	50.8 h	EC >99% α 1.9×10^{-4}%(5.378, 5.337, 5.286)	$^{239}Pu(d,n)$; $^{239}Pu(\alpha,p2n)$; $^{237}Np(\alpha,n)$
^{241}Am	433 y	α(5.4857, 5.4430, plus others ranging from 5.545 to 4.800)	$^{241}Pu(\beta^-)$
^{242m}Am	152 y	IT 99.52% α 0.48%(5.205, 5.140, plus others ranging from 5.408 to 5.065)	$^{241}Am(n,\gamma)$
^{242}Am	16.01 h	β^- 82.7%(0.667, 0.625) EC 17.3%	$^{241}Am(n,\gamma)$
^{243}Am	7.37×10^3 y	α(5.275, 5.233, plus others ranging from 5.350 to 4.695)	$^{242}Am(n,\gamma)$; $^{243}Pu(\beta^-)$
^{244m}Am	26 m	β^- >99%(1.50) EC 0.036%	$^{243}Am(n,\gamma)$
^{244}Am	10.1 h	β^-(0.387)	$^{243}Am(n,\gamma)$
^{245}Am	2.05 h	β^-(0.950)	$^{245}Pu(\beta^-)$
^{246}Am	25.0 m	β^-(2.10, 1.60, 1.31)	$^{246}Pu(\beta^-)$
^{246}Am	39 m	β^-	$^{244}Pu(\alpha,d)$; $^{244}Pu(^{3}He,p)$
^{247}Am	24 m	β^-	$^{244}Pu(\alpha,p)$

Table 8

Decay Properties of the Curium Isotopes

Isotope	Half-Life	Mode of Disintegration	Source
^{238}Cm	2.3 h	EC <90% α >10%(6.52)	$^{239}Pu(\alpha,5n)$
^{239}Cm	2.9 h	EC	$^{239}Pu(\alpha,4n)$
^{240}Cm	27 d	α(6.291, 6.248)	$^{239}Pu(\alpha,3n)$
^{241}Cm	32.8 d	EC 99.0% α 1.0%(5.939, 5.884, plus others ranging from 6.082 to 5.687)	$^{239}Pu(\alpha,2n)$
^{242}Cm	162.8 d	α(6.1129, 6.0696 5.972, plus others) β stable	$^{239}Pu(\alpha,n)$; $^{242}Am(\beta^-)$
^{243}Cm	28.5 y	α 99.74%(6.065, 6.056, 6.009, 5.992, 5.785, 5.742, plus others) EC 0.26% β stable	$^{242}Cm(n,\gamma)$
^{244}Cm	18.11 y	α(5.80496, 5.76283, 5.667) β stable	$^{243}Cm(n,\gamma)$; $^{243}Am(n,\gamma)^{244}Am(\beta^-)$; Multiple n-capt from ^{239}Pu
^{245}Cm	8.5×10^3 y	α(5.362, 5.304, plus others ranging from 5.5292 to 5.235) β stable	Multiple n-capt from ^{239}Pu, ^{238}U; Daughter ^{245}Bk
^{246}Cm	4.7×10^3 y	α(5.386, 5.343) β stable	$^{245}Cm(n,\gamma)$; Multiple n-capt from ^{239}Pu, ^{238}U
^{247}Cm	1.6×10^7 y	α(5.266, 5.211, 5.146 4.984, 4.942, 4.869, 4.819)	Multiple n-capt from ^{239}Pu, ^{238}U; $^{246}Cm(n,\gamma)$
^{248}Cm	3.5×10^5 y	α 91.74%(5.078, 5.034) Spontaneous fission 8.26% β stable	Daughter ^{252}Cf; Multiple n-capt from ^{239}Pu, ^{238}U
^{249}Cm	65 m	β^-(0.9)	$^{248}Cm(n,\gamma)$; Multiple n-capt from ^{239}Pu, ^{238}U
^{250}Cm	$\leq 1.1 \times 10^4$ y	Spontaneous fission	Multiple n-capt from ^{239}Pu, ^{238}U
^{251}Cm	16.8 m	β^-(1.42)	$^{250}Cm(n,\gamma)$

Table 9

Decay Properties of the Berkelium Isotopes

Isotope	Half-Life	Mode of Disintegration	Source
^{242}Bk	7 m	EC	$^{235}U(^{11}B,5n)$; $^{232}Th(^{15}N,5n)$
^{243}Bk	4.5 h	EC 99.85% α 0.15%(6.758, 6.718, 6.574, 6.542, 6.502, 6.210, 6.182, plus others)	$^{241}Am(\alpha,2n)$; $^{242}Cm(d,n)$; $^{243}Am(\alpha,4n)$
^{244}Bk	4.4 h	EC >99% α 0.006%(6.667, 6.625)	$^{243}Am(\alpha,3n)$; $^{244}Cm(d,2n)$; $^{244}Cm(p,n)$; $^{241}Am(\alpha,n)$
^{245}Bk	4.90 d	EC 99.88% α 0.12%(6.349, 6.309, 6.145, 6.117, 6.081, 5.885, 5.853, plus others)	$^{243}Am(\alpha,2n)$; $^{244}Cm(d,n)$, $^{242}Cm(\alpha,p)$; $^{244}Cm(\alpha,p2n)$
^{246}Bk	1.80 d	EC	$^{244}Cm(\alpha,pn)$; $^{243}Am(\alpha,n)$
^{247}Bk	1.4×10^3 y	α(5.794, 5.754, 5.710, 5.688, 5.654, 5.610, 5.531, 5.501, 5.456)	Daughter ^{247}Cf; $^{244}Cm(\alpha,p)$; $^{245}Cm(\alpha,pn)$; $^{246}Cm(\alpha,p2n)$
^{248}Bk	23.5 h	β^- 70%(0.65) EC 30%	$^{247}Bk(n,\gamma)$; $^{245}Cm(\alpha,p)$
^{248}Bk	>9 y	decay not observed	$^{246}Cm(\alpha,pn)$
^{249}Bk	0.88 y	β >99%(0.125) α 0.0015%(5.437, 5.417, 5.390, 5.487, plus others)	Multiple n-capt from ^{238}U, ^{239}Pu
^{250}Bk	3.22 h	β^-(1.76, 0.73)	$^{249}Bk(n,\gamma)$; Daughter ^{234}Es
^{251}Bk	56 m	β^-($\approx$1.0, $\approx$0.5)	Daughter ^{255}Es; $^{251}Cm(\beta^-)$

Table 10

Decay Properties of the Californium Isotopes

Isotope	Half-Life	Mode of Disintegration	Source
^{239}Cf	39^{+37}_{-12} s	α 40% (7.630)	$^{243}Fm \xrightarrow{\alpha}$
^{240}Cf	1.1 m	α(7.59)	$^{233}U(^{12}C,5n)$
^{241}Cf	4 m	α 30% (7.335)	$^{233}U(^{12}C,4n)$
^{242}Cf	3.5 m	α 80% (7.385, 7.35)	$^{233}U(^{12}C,3n)$; $^{235}U(^{12}C,5n)$; $^{236}U(^{12}C,6n)$; $^{235}U(^{12}C,4n)$
^{243}Cf	11 m	EC ≈86%, est. α ≈14%, est.(7.17, 7.06)	$^{235}U(^{12}C,4n)$; $^{236}U(^{12}C,5n)$; $^{238}U(^{12}C,7n)$; $^{242}Cm(^{3}He,2n)$
^{244}Cf	19 m	α(7.218, 7.178)	$^{242}Cm(\alpha,2n)$; $^{244}Cm(\alpha,4n)$; $^{238}U(^{12}C,6n)$; $^{236}U(^{12}C,4n)$
^{245}Cf	44 m	EC ≈79% α ≈30%(7.137, 7.084, 7.036, 6.983, 6.886)	$^{242}Cm(\alpha,n)$; $^{244}Cm(\alpha,3n)$ $^{238}U(^{12}C,5n)$
^{246}Cf	35.7 h	α(6.758, 6.719, 6.626) β stable	$^{244}Cm(\alpha,2n)$; $^{238}U(^{12}C,4n)$; $^{238}U(^{14}N,p5n)$; $^{239}Pu(^{9}Be,2n)$
^{247}Cf	3.15 h	EC 99.96% α 0.04%(6.301)	$^{244}Cm(\alpha,n)$; $^{235}U(^{14}N,p4n)$; $^{245}Cm(\alpha,2n)$
^{248}Cf	333 d	α(6.26) β stable	$^{245}Cm(\alpha,n)$; $^{246}Cm(\alpha,2n)$; $^{238}U(^{14}N,p3n)$
^{249}Cf	351 y	α(6.194, 5.946, 5.903, 5.849, 5.812, 5.760, plus others) β stable	$^{249}Bk(\beta^-)$
^{250}Cf	13.1 y	α(6.031, 5.989, 5.892, 5.738) β stable	Multiple n-capt from ^{238}Pu; $^{249}Bk(n,\gamma)^{250}Bk(\beta^-)$; Daughter ^{254}Fm
^{251}Cf	900 y	α(6.014, 5.852, 5.677, plus others ranging from 6.074 to 5.501) β stable	Multiple n-capt from ^{239}Pu; Daughter ^{255}Fm
^{252}Cf	2.64 y	α 96.91%(6.1183, 6.0757, 5.977, 5.826, 5.616) Spontaneous Fission 3.09% β stable	Multiple n-capt from ^{238}U, ^{239}Pu
^{253}Cf	17.8 d	β^- 99.69%(0.27) α 0.31%(5.979, 5.921)	Multiple n-capt from ^{239}Pu

Table 10

Decay Properties of the Californium Isotopes

Isotope	Half-Life	Mode of Disintegration	Source
^{254}Cf	60.5 d	Spontaneous Fission 99.69% α 0.31%(5.834, 5.792) β stable	Multiple n-capt from ^{239}Pu; $^{254m}Es(EC)$
^{256}Cf	12 m	Spontaneous Fission	$^{254}Cf(t,p)$

Table 11

Decay Properties of the Einsteinium Isotopes

Isotope	Half-Life	Mode of Disintegration	Source
^{243}Es	21 s	α(7.89)	$^{233}U(^{15}N,5n)$
^{244}Es	37 s	EC+β^+ 96% α ≈4%(7.57)	$^{233}U(^{15}N,4n)$
^{245}Es	1.3 m	EC 60% α 40%(7.73)	$^{235}U(^{14}N,5n)$; $^{238}U(^{14}N,7n)$; $^{237}Np(^{12}C,4n)$; $^{240}Pu(^{10}B,5n)$
^{247}Es	4.7 m	EC ≈93% α ≈7%(7.31)	$^{238}U(^{14}N,5n)$; $^{241}Am(^{12}C,\alpha 2n)$
^{248}Es	28 m	EC ≈99.7% α ≈0.3%(6.87)	$^{249}Cf(d,3n)$; $^{249}Bk(\alpha,5n)$; $^{249}Bk(^{3}He,4n)$
^{249}Es	1.70 h	EC 99.4% α 0.6%(6.770)	$^{249}Bk(\alpha,4n)$; $^{249}Cf(d,2n)$; $^{249}Cf(\alpha,p3n)$
^{250}Es	2.1 h	EC	$^{249}Bk(\alpha,3n)$; $^{249}Bk(^{3}He,2n)$ $^{249}Cf(\alpha,t)$; $^{249}Bk(^{3}He,2n)$
^{251}Es	33 h	EC 99.5% α 0.5%(6.492, 6.462, 6.452, 6.422, 6.410)	$^{249}Bk(\alpha,2n)$
^{252}Es	472 d	α 78%(6.632, 6.562, plus others) EC 22%	$^{249}Bk(\alpha n)$; $^{252}Cf(d,2n)$
^{253}Es	20.47 d	α(6.63273, 6.592, 6.552, 6.540, plus others) β stable	Daughter ^{253}Cf; Multiple n-capt from ^{235}U. ^{239}Pu
^{254m}Es	39.3 h	β^- 99.9%(1.127, 0.475) α 0.33%(6.591, 6.382, 6.354, plus others) EC 0.08%	$^{253}Es(n,\gamma)$; Multiple n-capt from ^{239}Pu
^{254}ES	276 d	α(6.429, 6.416, plus others)	$^{253}Es(n,\gamma)$; Multiple n-capt from ^{239}Pu
^{255}Es	38.3 d	β^- 92.0% α 8.0%(6.299, 6.260, 6.212) Spontaneous Fission 0.004%	Multiple n-capt from ^{238}U
^{256}Es	7.6 h	β^-	$^{254}Es(t,p)$
^{256}Es	22 m	β^-	$^{255}(n,\gamma)$

Table 12

Decay Properties of the Fermium Isotopes

Isotope	Half-Life	Mode of Disintegration	Source
^{243}Fm	0.2 sec	α(8.546)	$^{206}Pb(^{40}Ar,3n)$
^{244}Fm	$3.27\ ^{+1.78}_{-0.55}$ ms	SF	$^{206}Pb(^{40}Ar,2n)$
^{245}Fm	4 s	α(8.15)	$^{233}U(^{16}O,4n)$
^{246}Fm	1.2 s	α 92%(8.24) Spontaneous Fission 8%	$^{235}U(^{16}O,5n)$; $^{239}Pu(^{12}C,5n)$ $^{223}U(^{18}O,5n)$
^{247}Fm	35 s	EC ≤50% α ≥50%(7.93, 7.87)	$^{239}Pu(^{12}C,4n)$
^{247}Fm	9 s	α(8.18)	$^{239}Pu(^{12}C,4n)$
^{248}Fm	36 s	α 99.9%(7.87, 7.83) Spontaneous Fission 0.1%	$^{240}Pu(^{12}C,4n)$; $^{238}U(^{16}O,6n)$
^{249}Fm	3 m	α(7.53)	$^{238}U(^{16}O,5n)$
^{250m}Fm	1.8 s	IT	$^{249}Cf(\alpha,3n)$
^{250}Fm	30 m	α(7.44)	$^{249}Cf(\alpha,3n)$; $^{238}U(^{16}O,4n)$
^{251}Fm	5.3 h	EC 98.2% α 1.8%(6.834, 6.783, plus others ranging from 7.306 to 6.580)	$^{249}Cf(\alpha,2n)$; $^{235}U(^{18}O,5n)$
^{252}Fm	25.4 h	α(7.04)	$^{249-252}Cf(\alpha,xn)$; $^{250}Cf(^{8}Be,\alpha 3n)$ $^{235}U(^{18}O,4n)$
^{253}Fm	3.0 d	EC 88% α 12%(6.943, 6.901, 6.847 from 7.085 to 6.542)	$^{249-252}Cf(\alpha,xn)$
^{254}Fm	3.240 h	α >99%(7.187, 7.145, 7.048) Spontaneous Fission 0.0590%	Multiple n-capt from ^{239}Pu; $^{254m}Es(\beta^-)$; $^{252}Cf(^{9}Be,\alpha 3n)$
^{255}Fm	20.1 h	α(7.022, 6.963, plus others ranging from 7.127 to 6.488)	Daughter ^{255}Es; $^{252}Cf(^{9}Be,\alpha 2n)$ Multiple n-capt from ^{239}Pu
^{256}Fm	2.63 h	Spontaneous Fission 91.9% α 8.1%(6.915)	$^{255}Es(n,\gamma)^{256}Es(\beta^-)$; $^{253}Es(\alpha,p)$ $^{252}Cf(^{9}Be,\alpha n)$; $^{253}Es(\alpha,n)^{256}Md$ $^{255}(n,\gamma)$
^{257}Fm	100.5 d	α 99.79%(6.756, 6.695, 6.520, 6.441, 6.346) Spontaneous Fission 0.21%	Multiple n-capt from ^{239}Pu; ^{11}B on ^{252}Cf; ^{12}C on ^{252}Cf

Table 12

Decay Properties of the Fermium Isotopes

Isotope	Half-Life	Mode of Disintegration	Source
^{258}Fm	0.4 ms	Spontaneous Fission	$^{257}Fm(d,p)$
^{259}Fm	1.5 s	Spontaneous Fission	$^{257}Fm(t,p)$

Table 13

Decay Properties of the Mendelevium Isotopes

Isotopes	Half-Life	Mode of Disintegration	Source
^{247}Md	$2.9^{+1.7}_{-1.2}$ s	α (8.428)	^{209}Bi(^{40}Ar, 2n)
^{248}Md	7 s	EC+β$^+$ 80% α 20%(8.36, 8.32)	^{241}Am(^{12}C,5n)
^{249}Md	24 s	EC+β$^+$ <80% α ≥20%(8.03)	^{241}Am(^{12}C,4n)
^{250}Md	0.9 m	EC+β$^+$ 94% α 6%(7.82, 7.75)	^{243}Am(^{13}C,6n); ^{245}Am(^{12}C,5n); ^{241}Am(^{16}O,α3n); ^{240}Pu(^{15}N,5n)
^{252}Md	2 m	EC+β$^+$	^{238}U(^{19}F,5n); ^{243}Am(^{13}C,4n)
^{254}Md	10 m	EC	^{253}Es(α,3n)
^{255}Md	27 m	EC 92% α 8%(7.333)	^{253}Es(α,2n); ^{254}Es(α,3n) ^{11}B on ^{252}Cf; ^{12}C on ^{252}Cf
^{256}Md	75 m	EC 90.1% α 9.9%(7.71, 7.66, 7.48, 7.45, 7.32, 7.22, 7.15)	^{253}Es(α,n); ^{11}B on ^{252}Cf; ^{12}C on ^{252}Cf
^{257}Md	5.0 h	EC 90% α 10%(7.068)	^{11}B on ^{252}Cf; ^{12}C on ^{252}Cf; ^{255}Es(α,2n); ^{254}Es(α,n)
^{258}Md	56 d	α(6.79, 6.716)	^{255}Es(α,n)
^{259}Md	1.6 h	Spontaneous Fission	^{257}Fm(t,p)

Table 14

Decay Properties of the Nobelium Isotopes

Isotope	Half-Life	Mode of Disintegration	Source
^{252}No	2.3 s	α 73%(8.42, 8.37) Spontaneous Fission 27%	^{244}Cm(^{12}C,4n); ^{244}Cm(^{13}C,5n); ^{241}Am(^{15}N,4n); ^{235}U(^{22}Ne,5n); ^{239}Pu(^{15}O,5n)
^{253}No	1.7 m	α(8.01)	^{244}Cm(^{13}C,5n); ^{246}Cm(^{12}C,5n); ^{242}Pu(^{16}O,5n); ^{239}Pu(^{18}O,4n)
^{254m}No	0.28 s	IT	^{249}Cf(^{12}C,α3n); ^{246}Cm(^{12}C,4n)
^{254}No	55 s	α(8.10)	^{246}Cm(^{12}C,4n); ^{242}Pu(^{16}O,4n); ^{243}Am(^{15}N,4n); ^{238}U(^{22}Ne,6n)
^{255}No	3.1 m	α 62%(8.12, 8.08, 8.01 7.93, 7.77, plus others ranging from 8.31 to 7.62) EC 38%	^{246}Cm(^{13}C,4n); ^{248}Cm(^{12}C,5n); ^{242}Pu(^{18}O,5n); ^{238}U(^{22}Ne,5n); ^{249}Cf(^{12}C,α2n)
^{256}No	3.2 s	α ≈99.7%(8.43) Spontaneous Fission ≈0.3%	^{245}Cm(^{12}C,4n); ^{245}Cm(^{13}C,3n); ^{242}Pu(^{18}O,4n); ^{238}U(^{22}Ne,4n)
^{257}No	26 s	α(8.32, 8.27, 8.22)	^{248}Cm(^{12}C,3n); ^{246}Cm(^{12}C,n)
^{259}No	58 m	α ≈78%(7.67, 7.59, 7.52, 7.49, 7.44) EC ≈22%	^{248}Cm(^{18}O,α3n)

Table 15

Decay Properties of the Lawrencium Isotopes

Isotopes	Half-life	Mode of Disintegration	Source
^{254}Lr	10^{+7}_{-5} s	α (8.446)	$^{258}_{105} \xrightarrow{\alpha}$
^{255}Lr	22 s	α(8.43, 8.37)	^{243}Am(^{16}O,4n); ^{249}Cf(^{10}B,4n); ^{249}Cf(^{11}B,5n)
^{256}Lr	27 s	α(8.64, 8.52, 8.47, 8.43, 8.39, 8.32)	^{243}Am(^{18}O,5n); ^{15}N on ^{246}Cm; ^{12}C on ^{249}Bk; ^{11}B on ^{249}Cf
^{257}Lr	0.65 s	α(8.86, 8.80)	^{249}Cf(^{11}B,3n); ^{249}Cf(^{15}N,α3n)
^{258}Lr	4.3 s	α(8.65, 8.61, 8.59, 8.54)	^{246}Cm(^{15}N,3n); ^{248}Cm(^{15}N,5n) ^{249}Cf(^{15}N,α2n); ^{244}Pu(^{19}F,5n) ^{249}Bk(^{12}C,3n)
^{259}Lr	5 s	α(8.46)	^{248}Cm(^{15}N,5n); ^{250}Cf(^{15}N,α2n)
^{260}Lr	3.0 m	α(8.04)	^{248}C(^{15}N,3n); ^{18}O on ^{249}Bk

Table 16

Decay Properties of the Isotopes of Rutherfordium

Isotope	Half-Life	Mode of Disintegration	Source
^{255}Rf	$1.38^{+0.60}_{-0.30}$ s	Spontaneous Fission (45%) α 55% (8.726)	$^{207}Pb(^{50}Ti,2n)$
^{256}Rf	$8.1^{+1.3}_{-0.8}$ ms	Spontaneous Fission	$^{208}Pb(^{50}Ti,2n)$
^{257}Rf	5 s	α(9.016, 8.951, 8.870, 8.824, 8.78, 8.720, 8.663, 8.615, 8.553)	$^{249}Cf(^{12}C,4n)$
^{259}Rf	3 s	α(8.86, 8.77)	$^{249}Cf(^{13}C,3n)$; $^{245}Cm(^{16}O,5n)$ $^{246}Cm(^{18}O,5n)$; $^{242}Pu(^{22}Ne,5n)$
^{261}Rf	1.1 m	α(8.29)	$^{245}Cm(^{18}O,5n)$

Table 17

Decay Properties of the Isotopes of Hahnium

Isotopes	Half-Life	Mode of Disintegration	Source
^{257}Ha	$2.5^{+8.2}_{-0.3}$ s	α(8.963)	^{209}Bi(^{50}Ti,2n)
^{258}Ha	$1.8^{+1.1}_{-0.7}$ s	α(9.181, 9.104)	^{262}107 $\xrightarrow{\alpha}$
^{260}Ha	1.5 s	α 90%(9.12, 9.07, 9.04)	^{249}Cf(^{15}N,4n); ^{243}Am(^{22}Ne,5n)
^{261}Ha	2 s	α ≈ 75%(8.93) Spontaneous Fission ≈25%?	^{250}Cf(^{15}N,4n); ^{249}Bk(^{16}O,4n); ^{243}Am(^{22}Ne,4n)
^{262}Ha	≈40 s	Spontaneous Fission or EC ? ≈60% α ≈40% (8.66, 8.45)	^{249}Bk(^{18}O,5n)

Table 18

Table of Ground State Spontaneous Fission Activities

Nuclide	(J,π)	$t_{\frac{1}{2}}(SF)$
^{230}Th	0 +	$\geq 1.5 \times 10^{17}$ y
^{231}Pa	$^{3}/_{2}-$	$\geq 1.1 \times 10^{16}$ y
^{232}Th	0 +	$\geq 1 \times 10^{21}$ y
^{232}U	0 +	8×10^{13} y
^{233}U	$^{5}/_{2}+$	1.2×10^{17} y
^{234}U	0 +	2×10^{16} y
^{235}U	$^{7}/_{2}-$	3.5×10^{17} y
^{236}U	0 +	2×10^{16} y
^{236}Pu	0 +	3.5×10^{9} y
^{237}Np	$^{5}/_{2}+$	$\geq 1 \times 10^{18}$ y
^{238}U	0 +	8.19×10^{15} y
^{238}Pu	0 +	4.77×10^{10} y
^{239}Pu	$^{1}/_{2}+$	5.5×10^{15} y
^{240}Pu	0 +	1.340×10^{11} y
^{240}Cm	0 +	1.9×10^{6} y
^{241}Am	$^{5}/_{2}-$	1.147×10^{14} y
^{242}Pu	0 +	6.75×10^{10} y
^{242}Cm	0 +	6.09×10^{6} y
^{243}Am	$^{5}/_{2}-$	2.0×10^{14} y
^{244}Pu	0 +	6.55×10^{10} y
^{244}Cm	0 +	1.345×10^{7} y
^{246}Cm	0 +	1.80×10^{7} y
^{246}Cf	0 +	2.0×10^{3} y
^{246}Fm	0 +	15 s
^{248}Cm	0 +	4.24×10^{6} y
^{248}Cf	0 +	3.2×10^{14} y
^{248}Fm	0 +	10 h
^{249}Bk	$^{7}/_{2}+$	1.87×10^{9} y
^{249}Cf	$^{9}/_{2}-$	6.87×10^{10} y
^{250}Cm	0 +	1.13×10^{4} y
^{250}Cf	0 +	1.66×10^{4} y
^{250}Fm	0 +	10 y
^{252}Cf	0 +	87.9 y
^{252}Fm	0 +	115 y
^{252}No	0 +	8.555 y

Table of Ground State Spontaneous

Fission Activities

(Continued)

Nuclide	(J,π)	$t_{\frac{1}{2}}(SF)$
^{253}Es	$^{7}/_{2}+$	6.3 X 10^{5} y
^{254}Cf	0 +	60.7 y
^{254}Es	(7)+	2.5 X 10^{7}
^{254}Fm	0 +	228.8 X d
^{255}Es	$(^{7}/_{2}+)$	2621 y
^{255}Fm	$^{7}/_{2}+$	1.0 X 10^{4}
^{256}Cf	0 +	12.3 m
^{256}Fm	0 +	2.86 h
^{256}No	0 +	1067 s
^{257}Fm	$(^{9}/_{2}+)$	131.01 y
^{258}Fm	0 +	380 μs
^{258}No	0 +	1.2 ms
^{259}Fm		∿1.5 s
^{259}Md		∿95 m
$^{259}_{104}$		48 ± 36 sec
$^{260}_{105}$		15.8 s
$^{261}_{105}$		7.2 s

Table 19

Availability of Transuranium Element Target Materials

Nuclide	$t_{1/2}$	Isotopic Composition(%)	Amounts Available	Specific Activity(dpm/μg)
^{237}Np	2.14×10^{6}y	100	kg	1.566×10^{3}
^{238}Pu	87.74y		10-100g	3.862×10^{7}
^{239}Pu	2.41×10^{4}y	99.7	kg	1.362×10^{5}
^{240}Pu	6.57×10^{3}y	98.3	10-50g	5.014×10^{5}
^{241}Pu	14.4y	93.4	1-10g	2.337×10^{8}
^{242}Pu	3.76×10^{5}y	99.9	100g	8.481×10^{3}
^{244}Pu	8.1×10^{7}y	88.6	10-100mg	39.312
^{241}Am	433y	100	kg	7.611×10^{6}
^{243}Am	7.37×10^{3}y		10-100g	4.435×10^{5}
^{242}Cm	162.8d	100	100g	7.304×10^{9}
^{243}Cm	28.5y		10-100mg	1.021×10^{8}
^{244}Cm	18.11y	> 95%	10-100g	1.798×10^{8}
^{248}Cm	3.5×10^{5}y	97	10-100mg	8.340×10^{3}
^{249}Bk	0.88y	100	10-50mg	3.708×10^{9}
^{249}Cf	351y	100	1-10mg	9.062×10^{6}
^{250}Cf	13.1y	100	10mg	2.429×10^{8}
^{252}Cf	2.64y		10-1000mg	1.198×10^{9}
^{254}Cf	60.5d		μg	4.135×10^{9}
^{253}Es	20.47d		1-10mg	5.598×10^{10}
^{254}Es	276d	100	1-5μg	4.135×10^{9}
^{257}Fm	100.5d		1pg	1.200×10^{10}

Table 20

Maximum Permissible Concentrations (MPC) of Some Heavy Elements

Nuclide	Critical Organ	MPC, Whole Body referred to critical organ (μg)	MPC, air 168 h week (μ Ci/ml)
^{226}Ra	Bone	0.1	10^{-11}
^{232}Th	Bone	3.6×10^{5}	7×10^{-13}
^{238}U	Kidney	1.5×10^{3}	3×10^{-11}
^{239}Pu	Bone	6.5×10^{-1}	6×10^{-13}
^{244}Pu	Bone	2.3×10^{3}	6×10^{-13}
^{241}Am	Bone	1.5×10^{-2}	2×10^{-12}
	Kidney	3.1×10^{-2}	
^{248}Cm	Bone	1.6	2×10^{-13}
^{249}Bk	Bone	4.2×10^{-4}	3×10^{-10}
^{252}Cf	Gastrointestinal Tract (GI)	1.8×10^{-5}	2×10^{-12}
	Lower large intestine (LLI)		
	Bone		
^{254}Es	GI, LLI, Bone	1.1×10^{-5}	6×10^{-12}

Figure Captions

Figure 1. The modern periodic table showing the places of elements through Element 118.

Figure 2. Spontaneous fission decay curves for products formed in the reactions of ^{249}Bk and 82 MeV ^{15}N as performed at: Dubna, (top) and Berkeley (bottom).

Figure 3. A schematic view of the fission barrier showing the barrier as calculated by: a) the liquid droplet model (dashed curve), and b) the shell corrected droplet model (solid curve).

Figure 4. Experimental measurements of fission barrier heights from Back and Britt (Br 81). The symbols E_A and E_B are defined in Figure 3.

Figure 5. left) Calculated and experimental (dots) first barrier heights.
middle) Calculated and experimental (dots) second minimum heights.
right) Calculated (with inclusions of mass asymmetry) and experimental (dots) second barrier heights.

Figure 6. Part of the nuclear chart giving the half-lives of all fission isomers known at present. Two values for the same nucleus indicate spin-isomeric states in the second minimum.

Figure 7. Simple phenomenological description of spontaneous fission half-lives including the effect of a magic neutron number and the odd-even effect. The solid curves are the predictions of the semi-empiric of formula with the best fit parameters. The points are experimental data. From Metag (Me 75).

Figure 8. Stability limits in the rotating liquid drop model. The figure shows, for nuclei along the β-stability line, the angular momentum

I for which the fission barrier vanishes ($B_f = 0$), and also the angular momentum for which B_f assumes the value 8 MeV. The latter value is chosen equal to the average neutron separation energy. From (Co 74).

Figure 9. The calculated heights of the first and second barrier of ^{214}Th as functions of angular momentum. The heights refer to the first minimum which remains lowest up to I = 80. From (Åb 80).

Figure 10. Contour diagram indicating at which spin value the calculated fission barrier is 8 MeV high. From (Åb 80).

Figure 11. Variation of α-decay energy with neutron number N for transuranium nuclei. The calculated values are estimated using the Moller-Nix mass formula (Mö 80).

Figure 12. Variation of the partial half-life for α-decay for e-e transuranium nuclei with the α-decay energy.

Figure 13. Variation of Q_β with mass number A for odd A transuranium nuclei. From (Wa 77).

Figure 14. Variation of Q_β with mass number A for even A transuranium nuclei.

Figure 15. The dependence of spontaneous fission half-lives for e-e transuranium nuclei upon neutron number N.

Figure 16. Theoretical predictions for SF half-lives of even-even nuclei in the transuranium region (Ra 76). The black squares at element 104 indicate possible assignments of experimental results.

Figure 17. Dependence of "corrected" spontaneous fission half-lives upon fissility parameter x. ● e-e, x odd A, ■ o-o.

Figure 18. Schematic variation of fission fragment mass distributions with the Z, A, E*, J of the fissioning system. From Hoffman and Hoffman (Ho 74).

Figure 19. Classification of techniques used to isolate transuranium reaction products by minimum detectable $t_{\frac{1}{2}}$ and production cross section. See text for a discussion of these techniques. From (Ni 77).

Figure 20. Schematic diagram of chemical procedures used by Schadel et al. (Sc 78) to isolate actinide elements from heavy ion irradiated U targets.

Figure 21. Schematic representation of a "gas-jet" recoil transport assembly. Thermalized product atoms are transported in the He gas stream and collected on the periphery of a wheel or other suitable collection device. Periodically, the wheel is moved to position the spot in front of the detectors. A "mother-daughter" detector assembly is illustrated in the lower portion of the figure and is used to establish a genetic link. From Bemis (Be 74).

Figure 22. Rotating and scanning drum system for the detection of short-lived spontaneously fissioning nuclei. From (Ni 80).

Figure 23. Details of a tape system for the collection and detection of short-lived spontaneously fissioning nuclei. From (Ni 80).

Figure 24. A schematic diagram of the velocity filter SHIP at GSI.

Figure 25. The $^{238}U + ^{238}U$ reaction at $\leq$ 7.5 MeV/u energy: (a) charge distribution for quasielastic transfer and sequential fission at low excitation energies (open circles), and for damped collisions with the associated sequential fission process (full circles), and the reconstructed primary fragment distribution (dashed curve); (b) independent cross section isopleths in a Z-A plane. From (Sc 78b).

Figure 26. Production cross sections of transuranium nuclei in the ^{238}U + ^{238}U and ^{136}Xe + ^{238}U reaction. From (Sc 78b).

Figure 27. Cross-section distribution of polonium and fermium isotopes representing the lightest and heaviest complementary reaction products observed in the damped collision of ^{238}U with ^{238}U. From (He 78).

Figure 28. (top) Cross-sections for the formation of heavy actinides in the reaction of 7.4 MeV/u ^{238}U projectiles with thick ^{248}Cm targets.

(bottom) Intercomparison of formation cross-sections for heavy actinides from the reaction of $\leq$ 7.4 MeV ^{238}U + ^{248}Cm (squares); $\leq$ 5.6 MeV/u ^{48}Ca + ^{248}Cm (Hu 77) (triangles); $\leq$ 6.4 MeV/u ^{136}Xe + ^{248}Cm (Mo 80) (circles) and $\leq$ 7.5 MeV/u ^{238}U + ^{238}U (Sc 79) (crosses).

Figure 29. Transuranium products distributions observed for the interaction of 98 MeV ^{16}O (open symbols) and 97 MeV ^{18}O (solid symbols) with ^{248}Cm. From (Le 81).

Figure 30. The (heavy ion, 4n) cross-sections as a function of the (Z,A) of the nuclei being synthesized. Data for several different heavy ions are shown. After (Og 81).

Figure 31. Dependence of the minimum excitation energy of the compound nucleus, E^*_{min}, on the projectile mass, for different target-projectile systems leading to the formation of the same compound nuclei ^{242}Fm, $^{252}104$, and $^{266}108$. From (Og 81).

Figure 32. Sequence of time correlated α-decay chains observed by Münzenberg et al. (Mü 81) to identify the production of ^{209}Bi (^{54}Cr,n) $^{262}107$.

1 H																	2 He
3 Li	4 Be											5 B	6 C	7 N	8 O	9 F	10 Ne
11 Na	12 Mg											13 Al	14 Si	15 P	16 S	17 Cl	18 Ar
19 K	20 Ca	21 Sc	22 Ti	23 V	24 Cr	25 Mn	26 Fe	27 Co	28 Ni	29 Cu	30 Zn	31 Ga	32 Ge	33 As	34 Se	35 Br	36 Kr
37 Rb	38 Sr	39 Y	40 Zr	41 Nb	42 Mo	43 Tc	44 Ru	45 Rh	46 Pd	47 Ag	48 Cd	49 In	50 Sn	51 Sb	52 Te	53 I	54 Xe
55 Cs	56 Ba	57 La	72 Hf	73 Ta	74 W	75 Re	76 Os	77 Ir	78 Pt	79 Au	80 Hg	81 Tl	82 Pb	83 Bi	84 Po	85 At	86 Rn
87 Fr	88 Ra	89 Ac	104 Rf	105 Ha	106	107	(108)	(109)	(110)	(111)	(112)	(113)	(114)	(115)	(116)	(117)	(118)

LANTHANIDES	58 Ce	59 Pr	60 Nd	61 Pm	62 Sm	63 Eu	64 Gd	65 Tb	66 Dy	67 Ho	68 Er	69 Tm	70 Yb	71 Lu
ACTINIDES	90 Th	91 Pa	92 U	93 Np	94 Pu	95 Am	96 Cm	97 Bk	98 Cf	99 Es	100 Fm	101 Md	102 No	103 Lr

XBL751-2037

Fig. 1

Fig 2

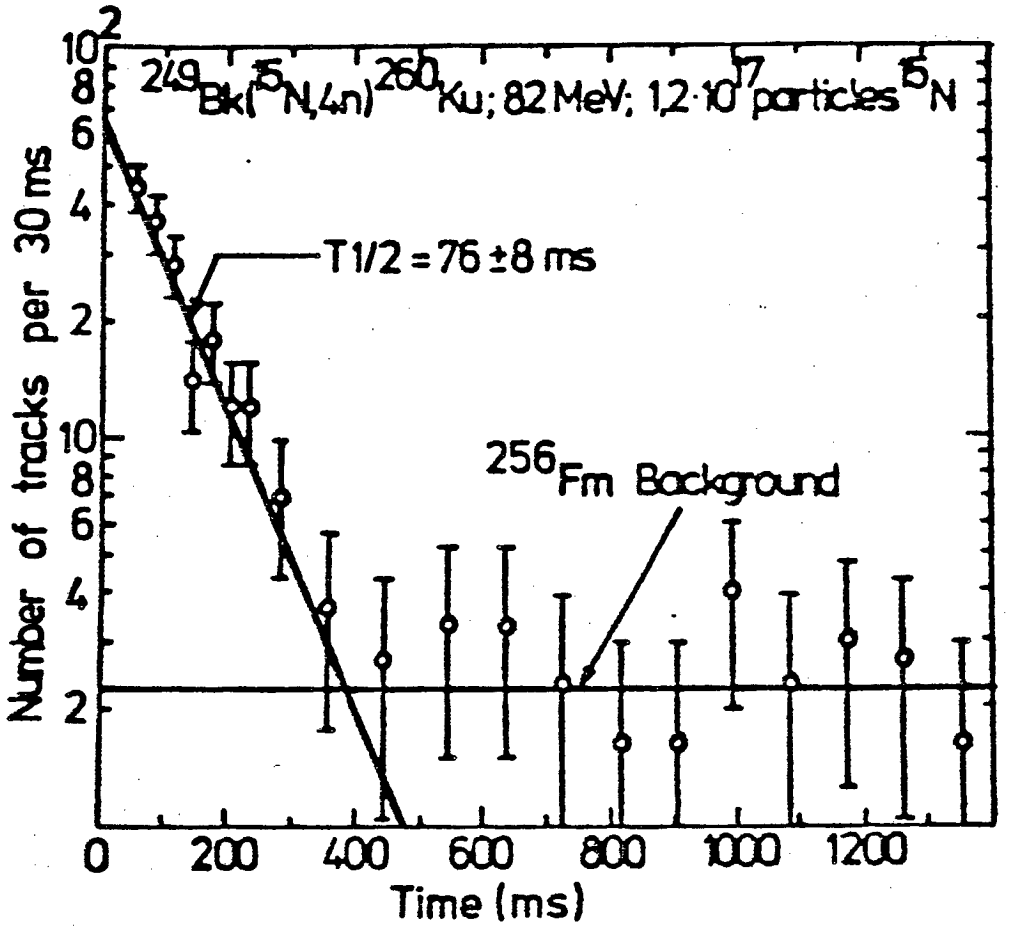

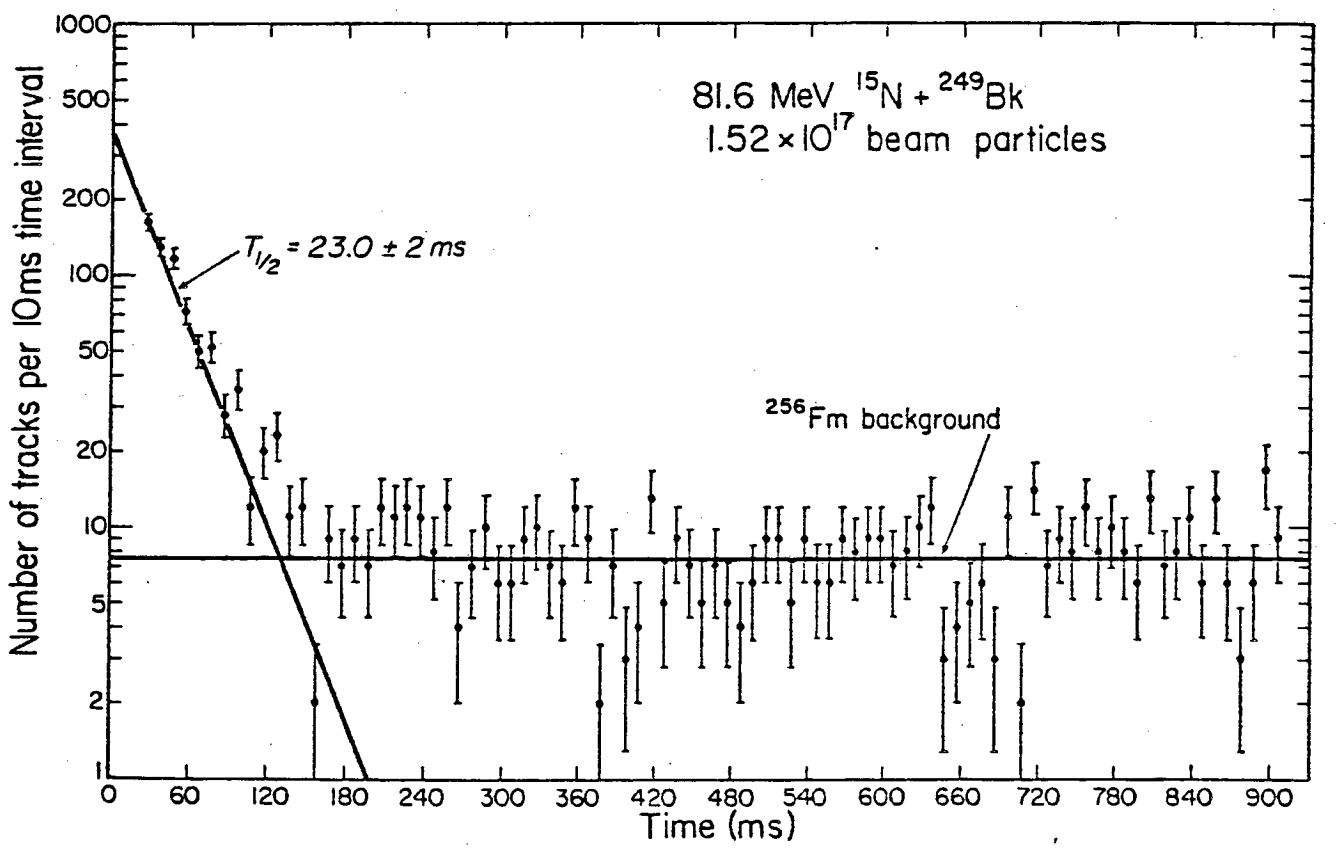

XBL 803-485

Fig 3

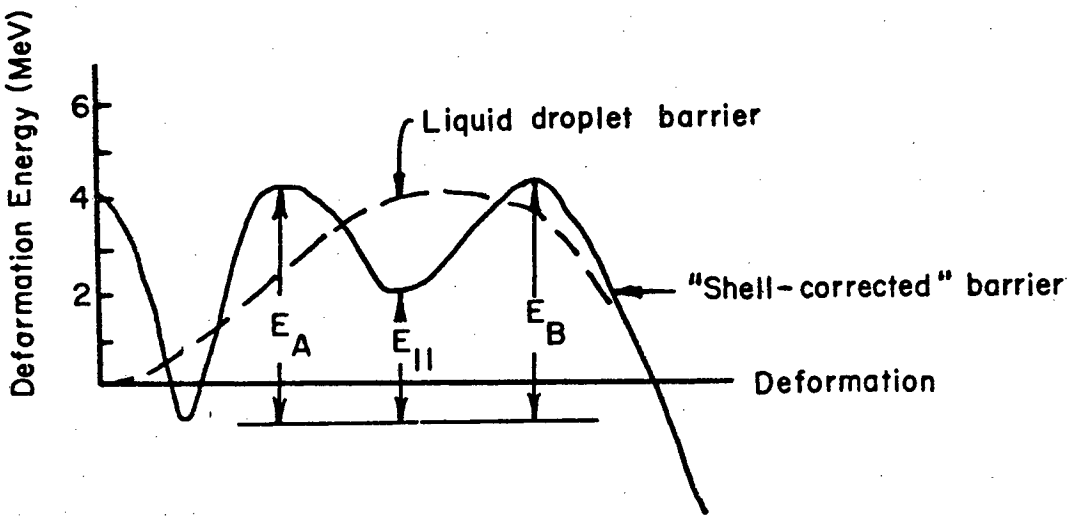
Deformation Energy (MeV)
6
4
2
Liquid droplet barrier
"Shell-corrected" barrier
E_A
E_{II}
E_B
Deformation

Fig 4

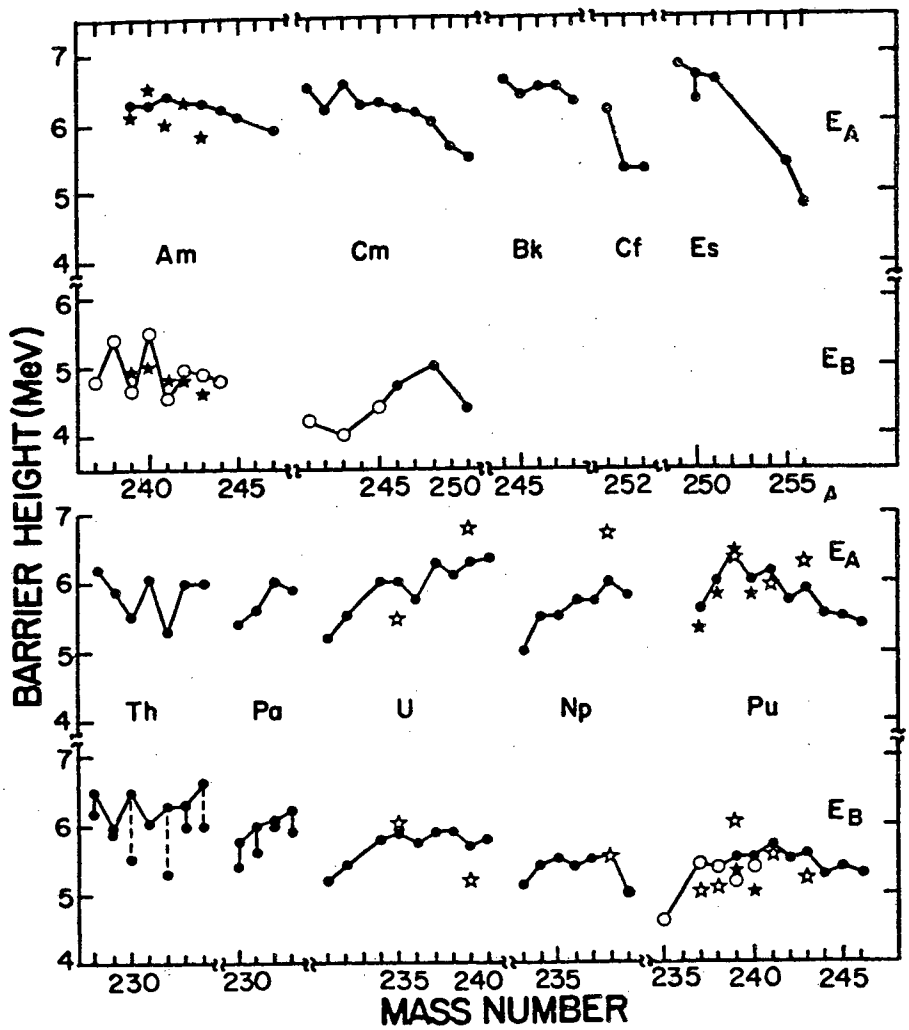
BARRIER HEIGHT (MeV)
MASS NUMBER
Am
Cm
Bk
Cf
Es
Th
Pa
U
Np
Pu
E_A
E_B
240
245
250
252
255
230
235
A

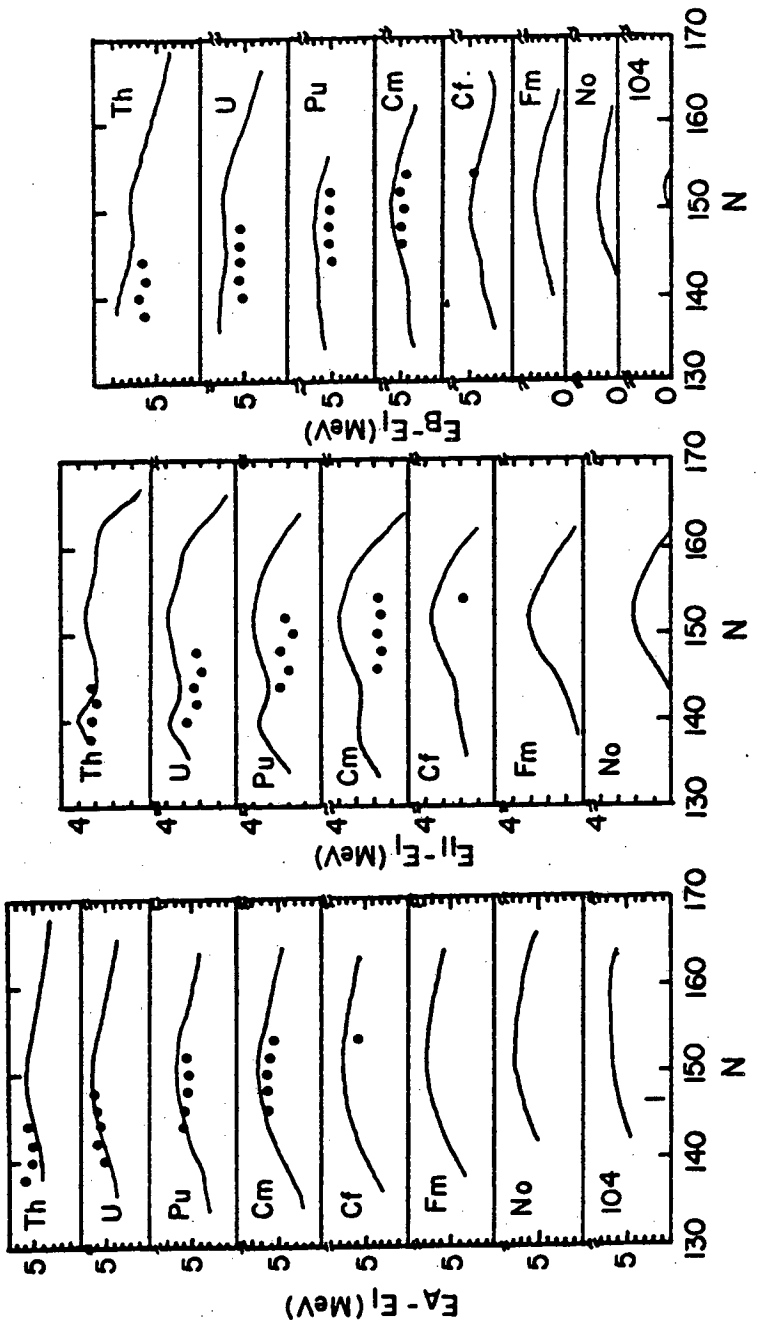
Th
U
Pu
Cm
Cf
Fm
No
104
$E_A - E_I$ (MeV)
$E_{II} - E_I$ (MeV)
$E_B - E_I$ (MeV)
N
130
140
150
160
170

Fig. 5

Fig 6

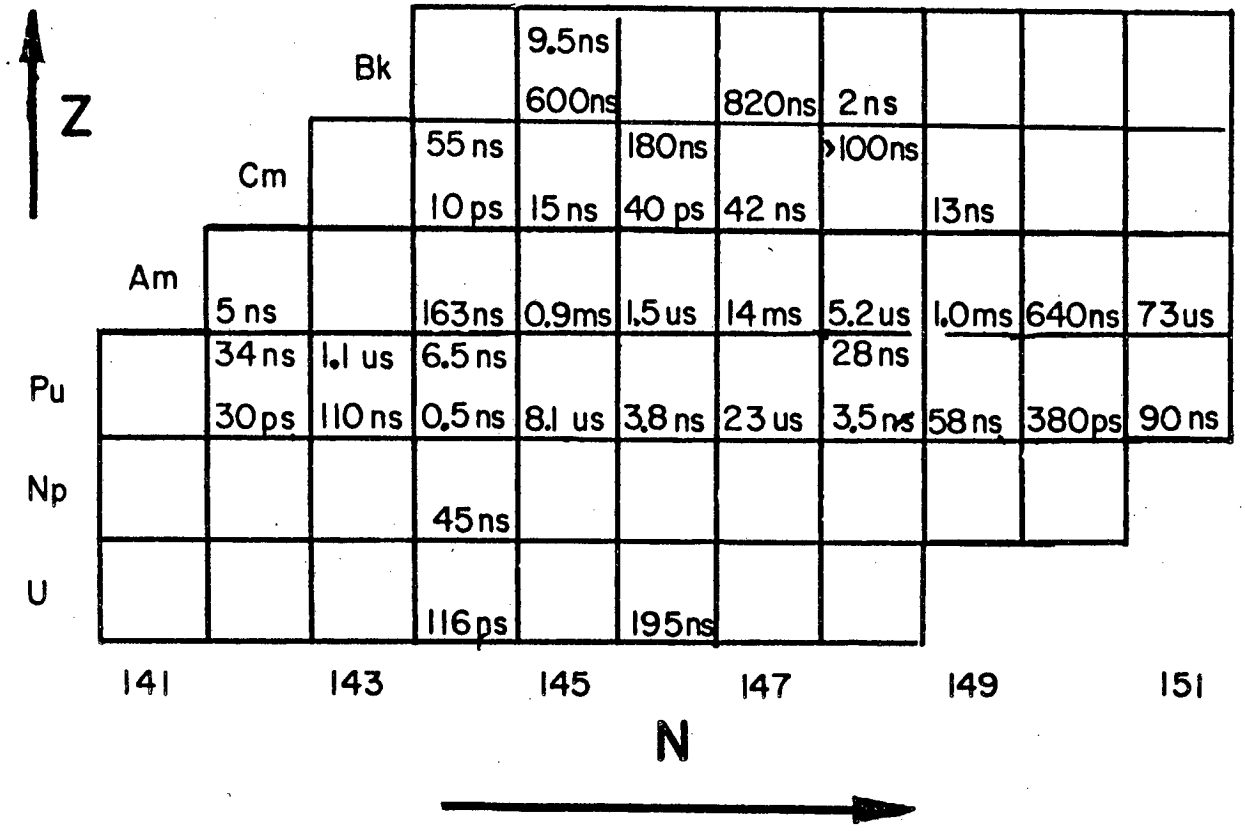
Z
Bk
Cm
Am
Pu
Np
U
9.5ns
600ns
820ns
2 ns
55 ns
10 ps
15 ns
180ns
40 ps
42 ns
>100ns
13ns
5 ns
163ns
0.9ms
1.5 us
14 ms
5.2 us
1.0ms
640ns
73us
34 ns
30 ps
1.1 us
110 ns
6.5 ns
0.5 ns
8.1 us
3.8 ns
23 us
28 ns
3.5 ns
58 ns
380ps
90 ns
45 ns
116 ps
195ns
141
143
145
147
149
151
N

Fig 7

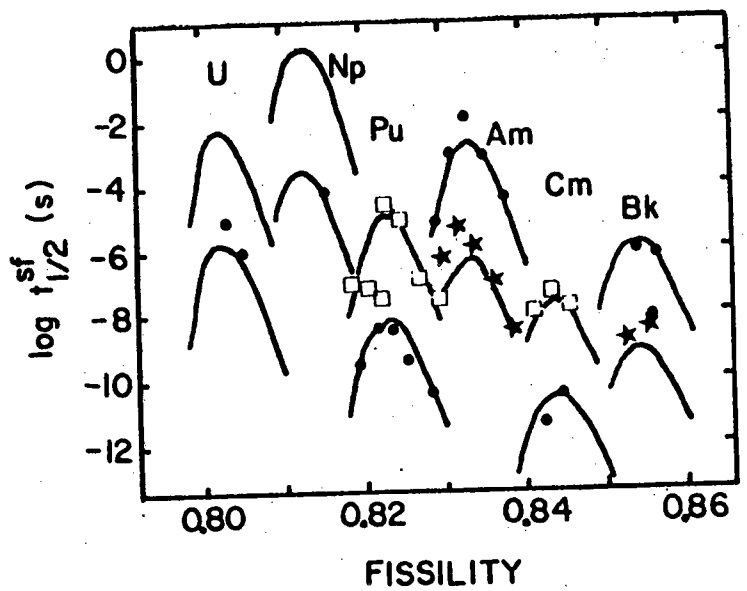
U
Np
Pu
Am
Cm
Bk
0
-2
-4
-6
-8
-10
-12
log $t^{sf}_{1/2}$ (s)
0.80
0.82
0.84
0.86
FISSILITY

Fig 8

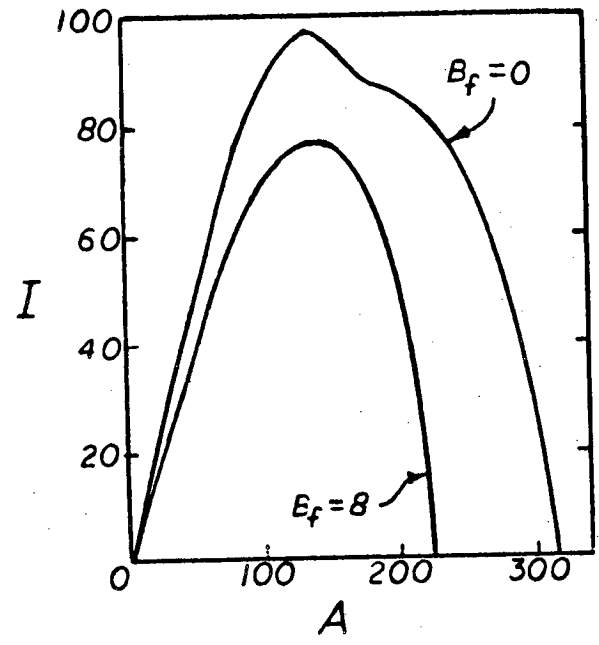

Fig 9

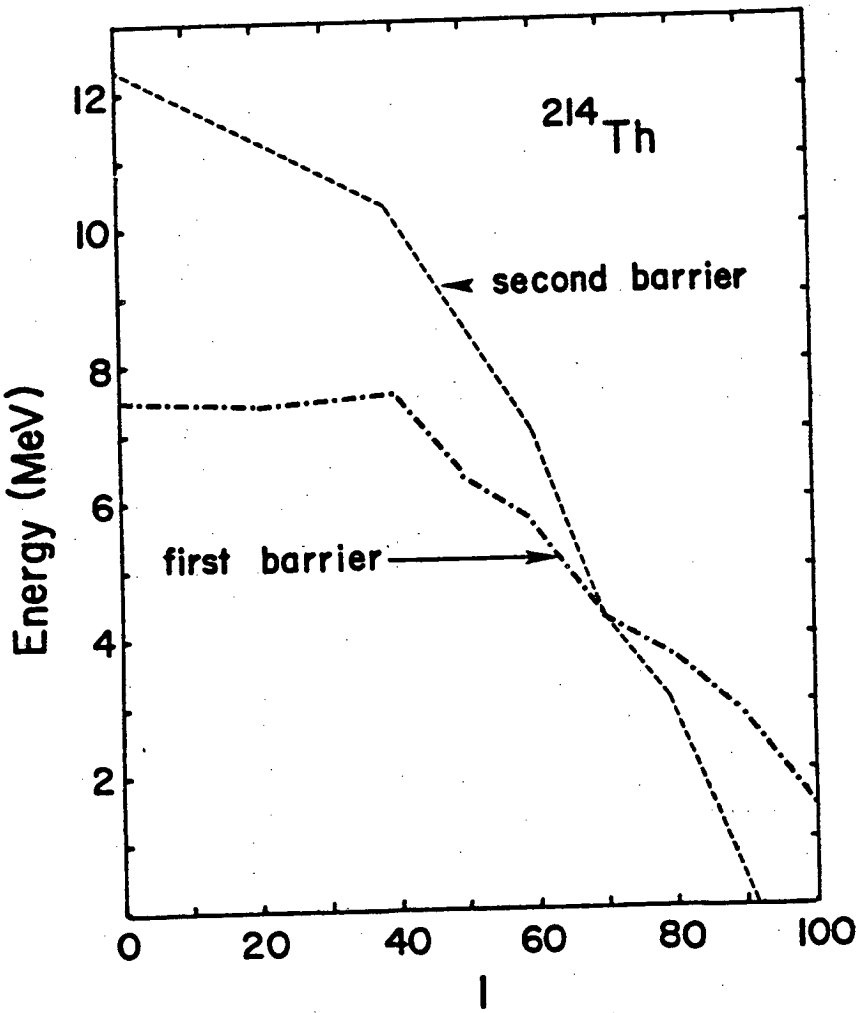
^{214}Th
second barrier
first barrier
Energy (MeV)
12
10
8
6
4
2
0
20
40
60
80
100
l

Fig 10

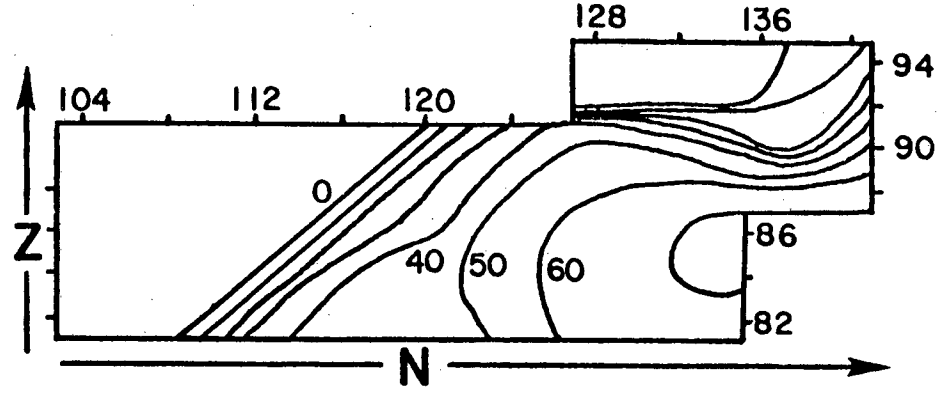

Fig 11

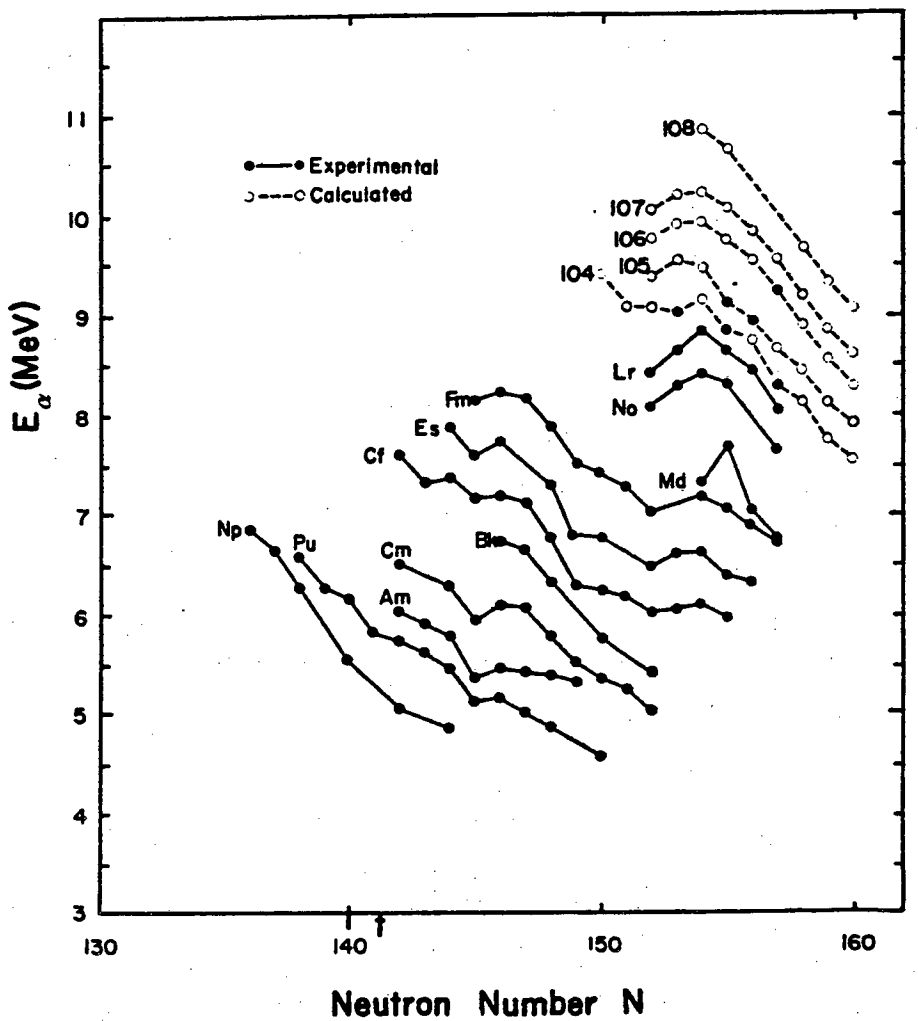
Experimental
Calculated
108
107
106
105
104
Lr
No
Md
Fm
Es
Cf
Np
Pu
Cm
Bk
Am
11
10
9
8
7
6
5
4
3
130
140
150
160
E_α (MeV)
Neutron Number N

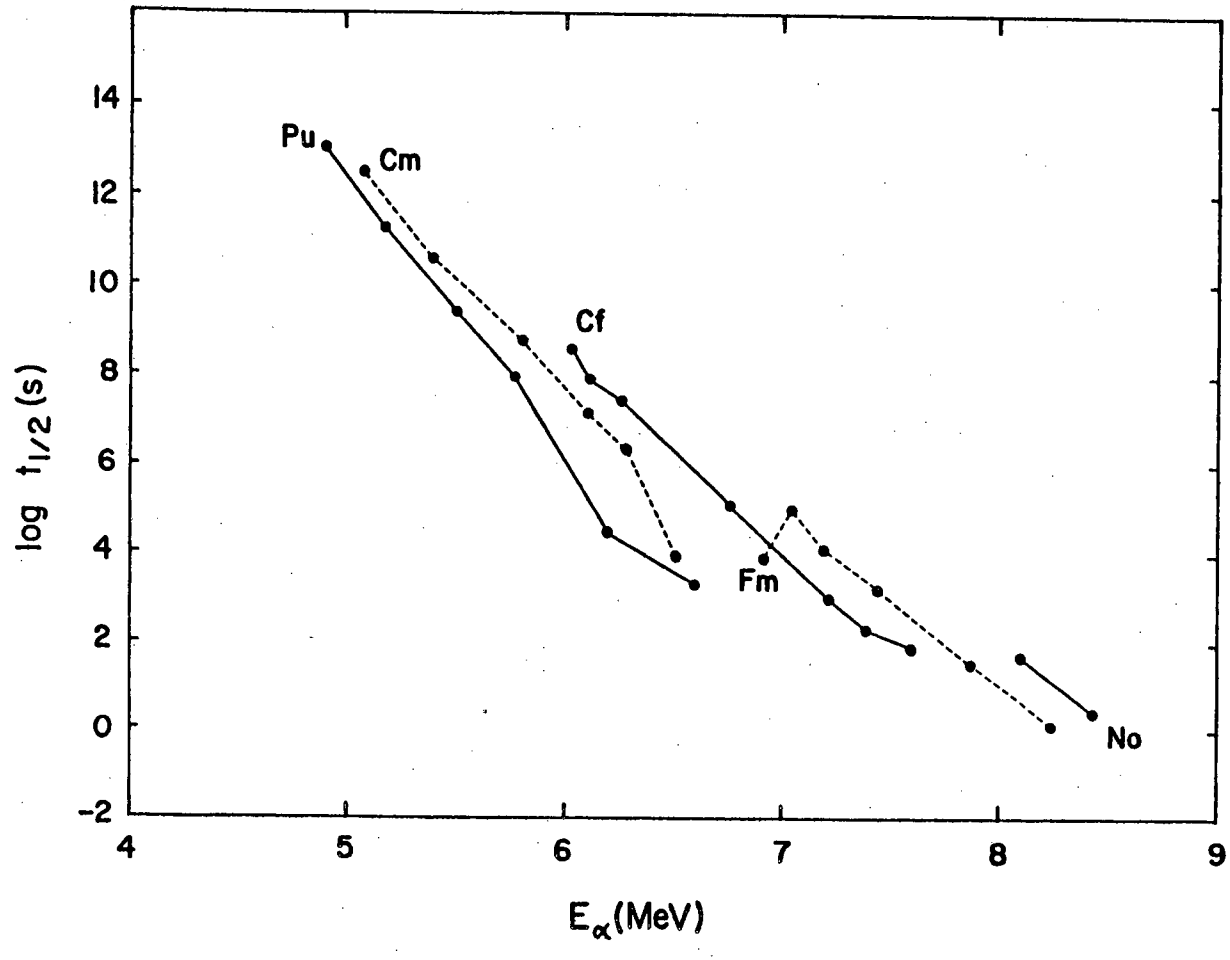

Fig. 12

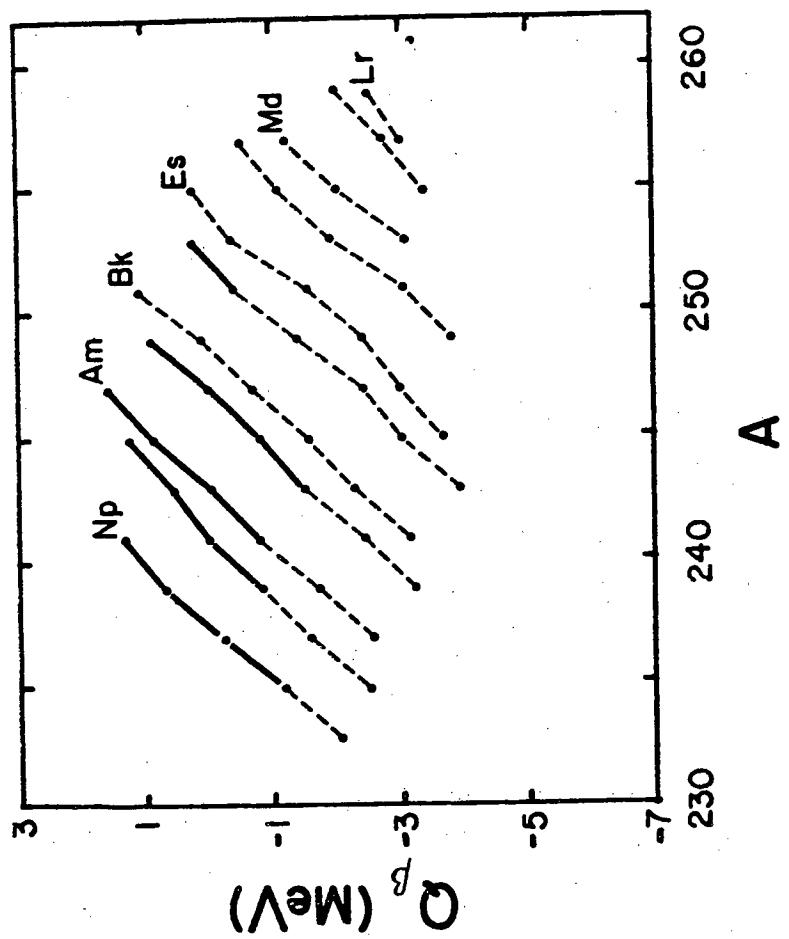

Fig. 13

Fig 14

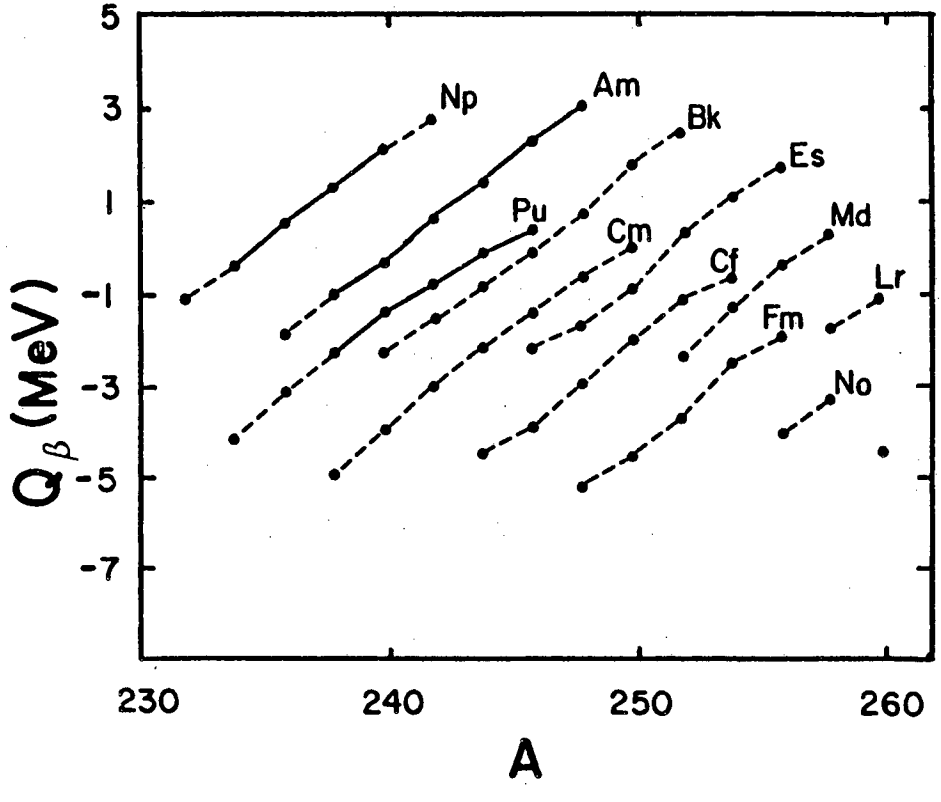
5
3
1
-1
-3
-5
-7
Q_β (MeV)
230
240
250
260
A
Np
Am
Pu
Bk
Cm
Es
Cf
Md
Fm
Lr
No

Fig 15

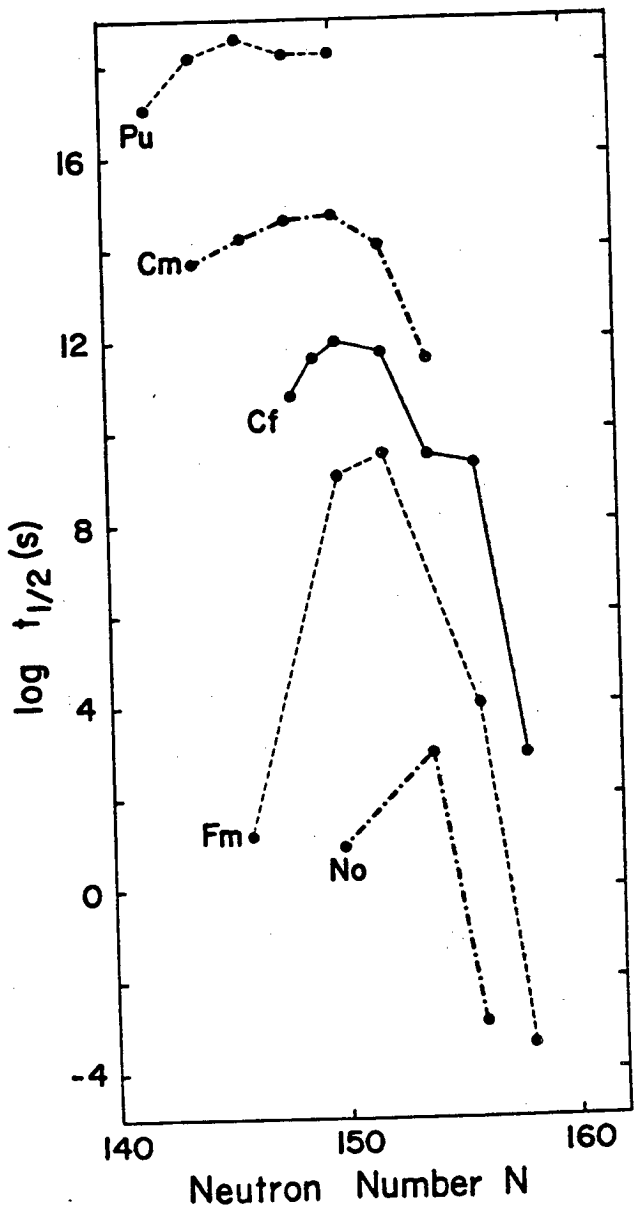

Fig 16

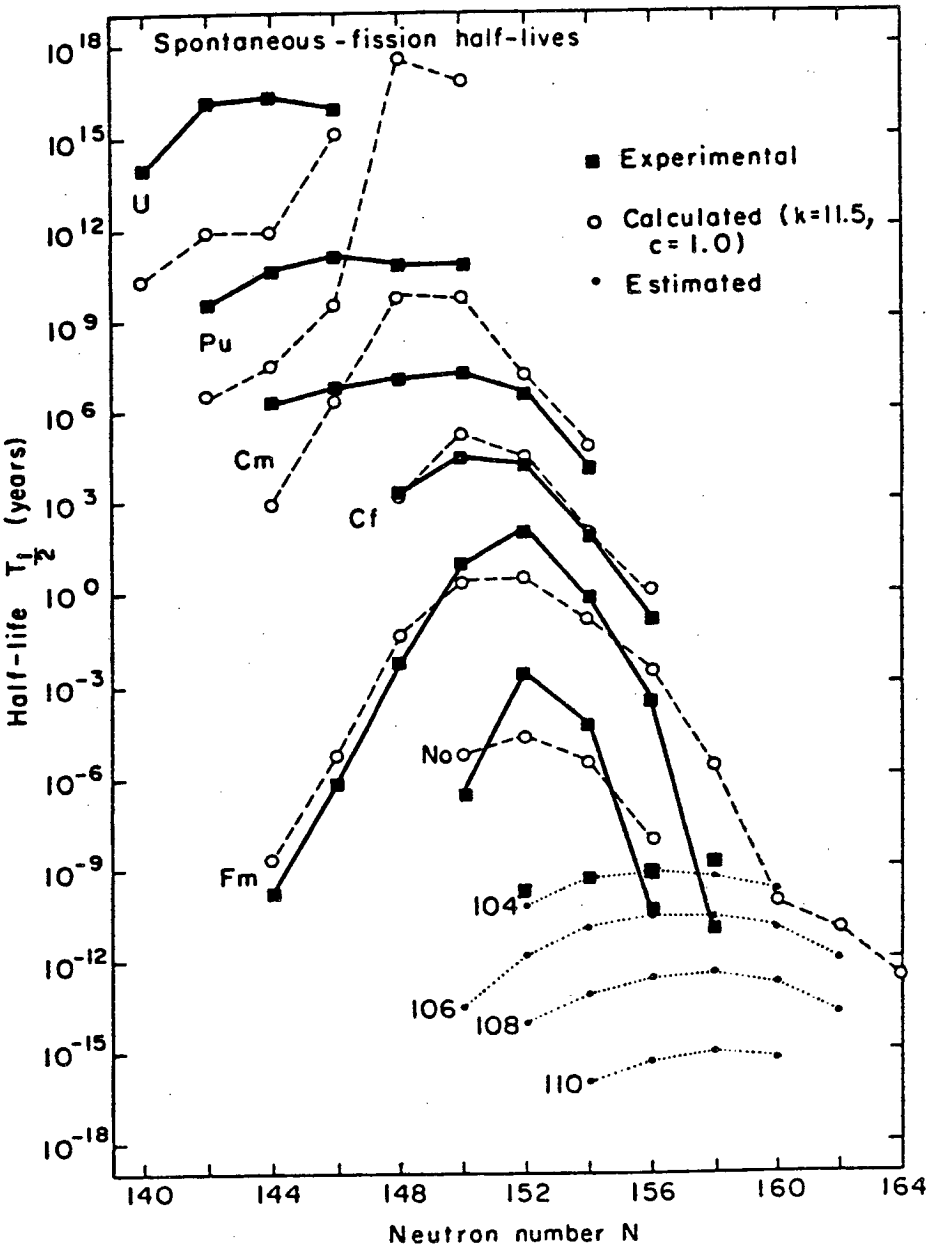
Spontaneous-fission half-lives
Experimental
Calculated (k=11.5, c=1.0)
Estimated
U
Pu
Cm
Cf
No
Fm
104
106
108
110
Half-life $T_{\frac{1}{2}}$ (years)
10^{18}
10^{15}
10^{12}
10^{9}
10^{6}
10^{3}
10^{0}
10^{-3}
10^{-6}
10^{-9}
10^{-12}
10^{-15}
10^{-18}
140
144
148
152
156
160
164
Neutron number N

Fig 17

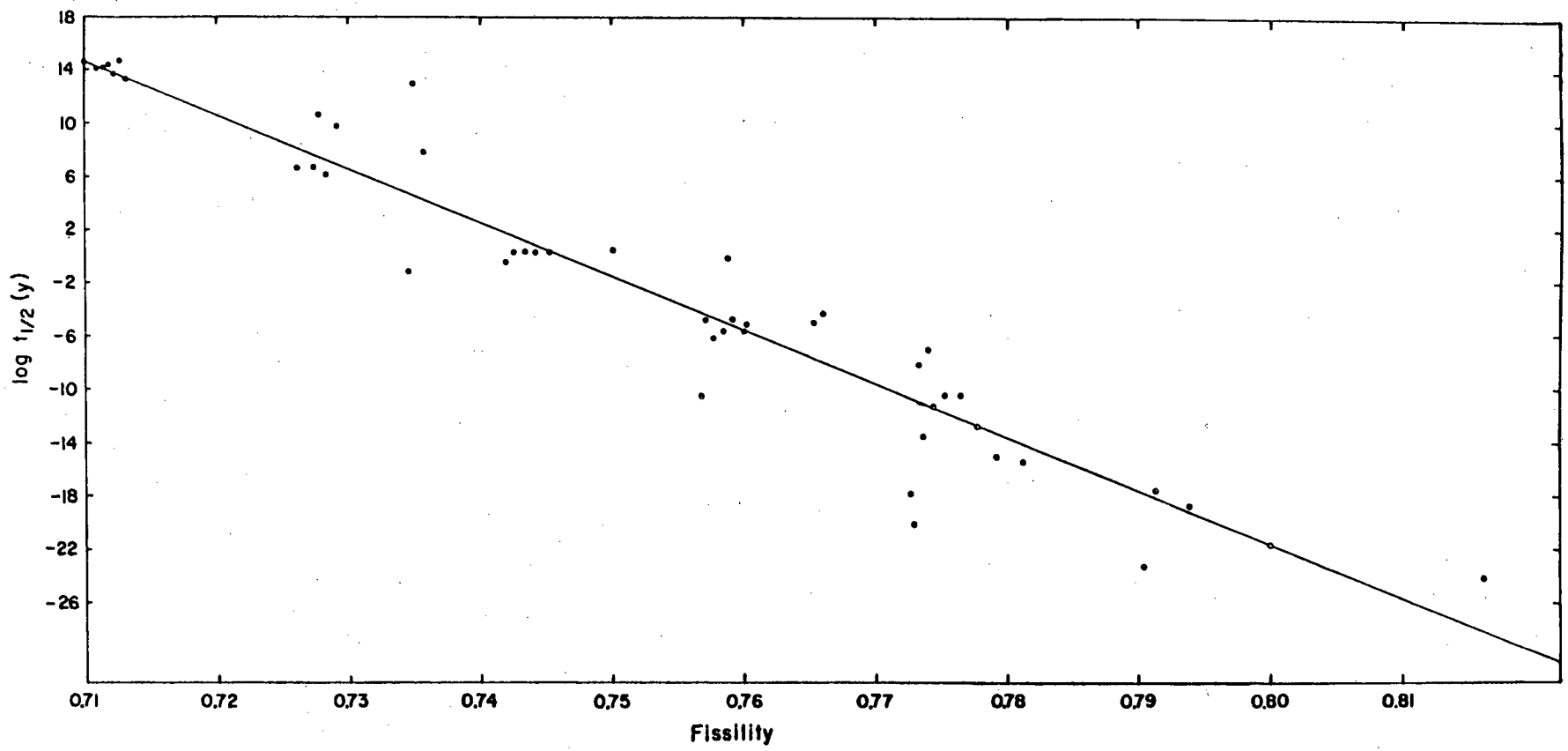
18
14
10
6
2
-2
-6
-10
-14
-18
-22
-26
log $t_{1/2}$ (y)
0.71
0.72
0.73
0.74
0.75
0.76
0.77
0.78
0.79
0.80
0.81
Fissility

Fig 18

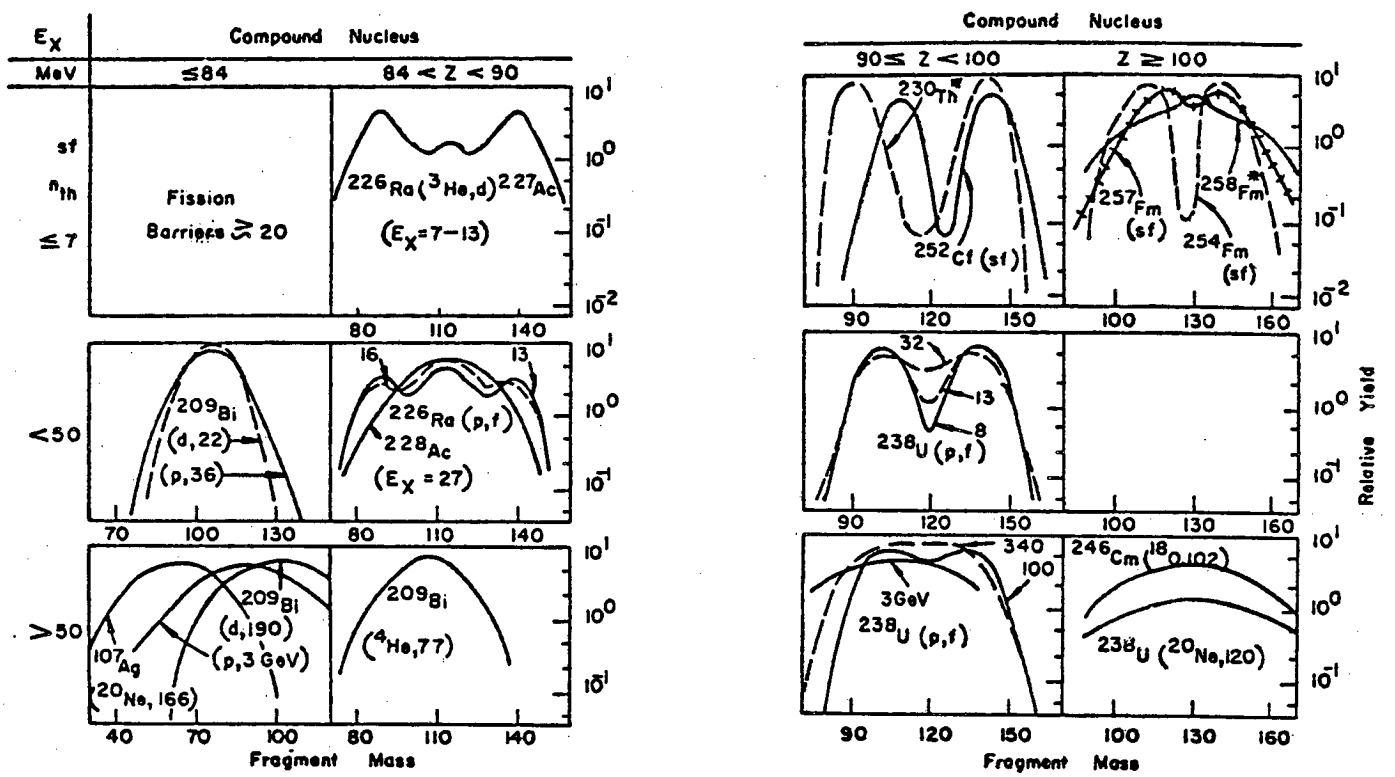
Compound Nucleus
E_X
MeV
≤84
84 < Z < 90
sf
n_{th}
≤7
Fission
Barriers ≳ 20
^{226}Ra(^{3}He,d)^{227}Ac
(E_X=7–13)
<50
^{209}Bi
(d,22)
(p,36)
16
13
^{226}Ra (p,f)
^{228}Ac
(E_X = 27)
>50
^{107}Ag
^{20}Ne, 166)
^{209}Bi
(d,190)
(p,3 GeV)
^{209}Bi
(^{4}He,77)
Fragment Mass
Compound Nucleus
90≤ Z < 100
Z ≥ 100
^{230}Th
^{252}Cf (sf)
^{257}Fm (sf)
^{258}Fm
^{254}Fm (sf)
32
13
8
^{238}U (p,f)
340
100
3GeV
^{238}U (p,f)
^{246}Cm(^{18}O,102)
^{238}U (^{20}Ne,120)
Relative Yield
Fragment Mass

Fig 19

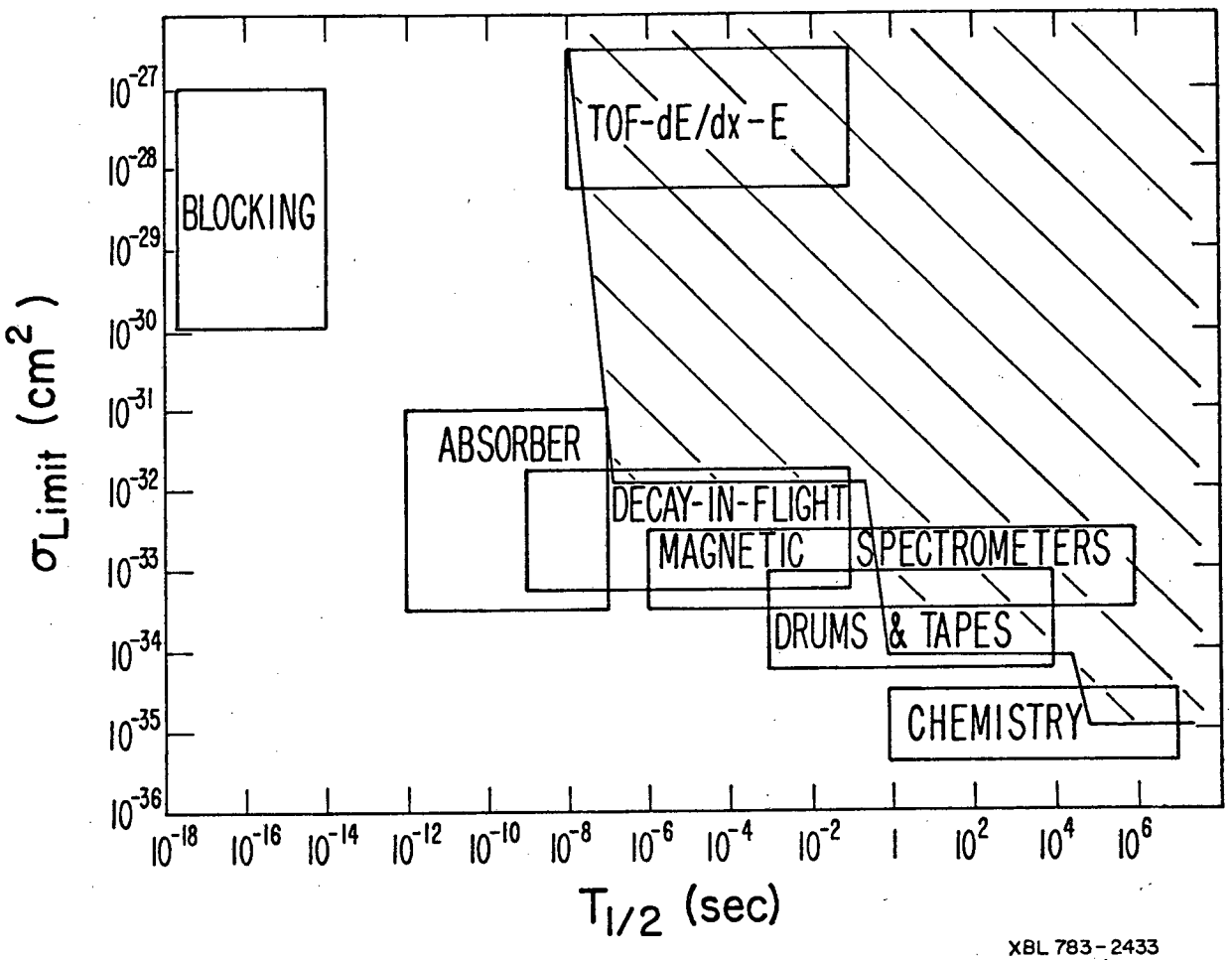

XBL 783-2433

Fig 20

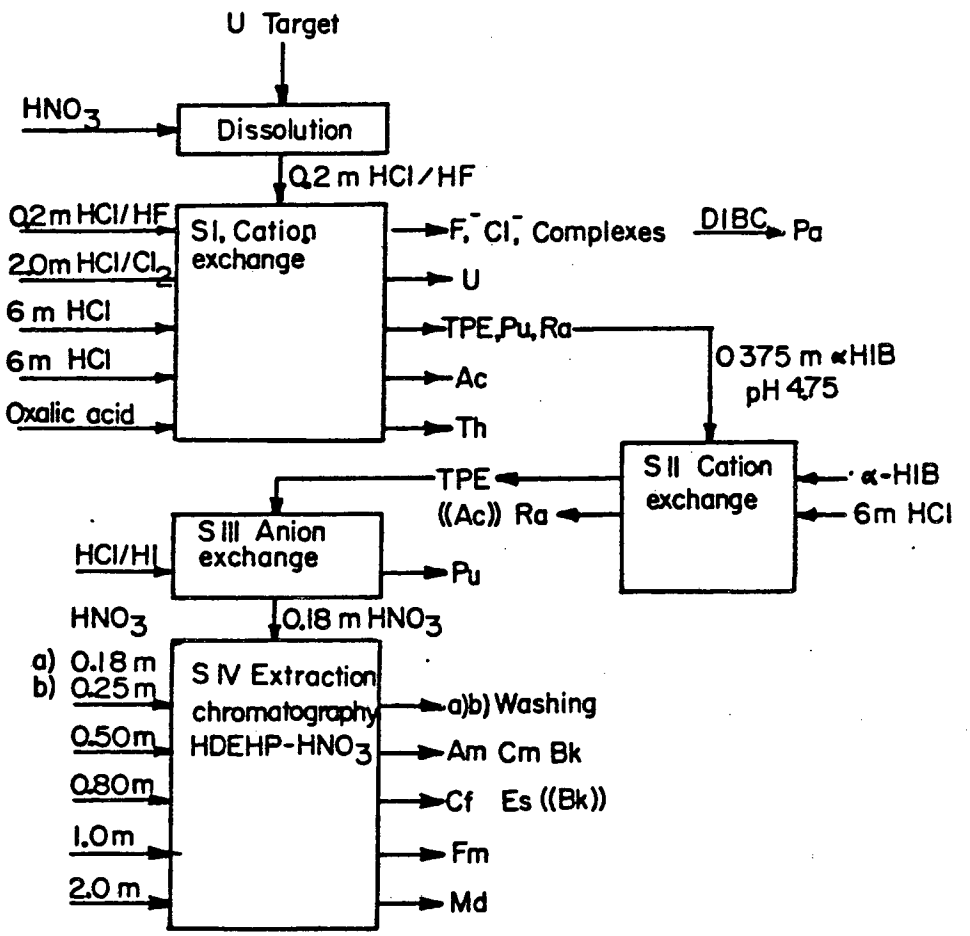
U Target
HNO3
Dissolution
0.2 m HCl/HF
0.2m HCl/HF
2.0m HCl/Cl2
6 m HCl
6m HCl
Oxalic acid
S I, Cation exchange
F⁻, Cl⁻, Complexes
DIBC
Pa
U
TPE, Pu, Ra
Ac
Th
0.375 m α-HIB
pH 4.75
S II Cation exchange
α-HIB
6m HCl
TPE
((Ac)) Ra
S III Anion exchange
HCl/HI
Pu
HNO3
0.18 m HNO3
a) 0.18 m
b) 0.25 m
0.50m
0.80m
1.0m
2.0 m
S IV Extraction chromatography HDEHP-HNO3
a)b) Washing
Am Cm Bk
Cf Es ((Bk))
Fm
Md

Fig 21

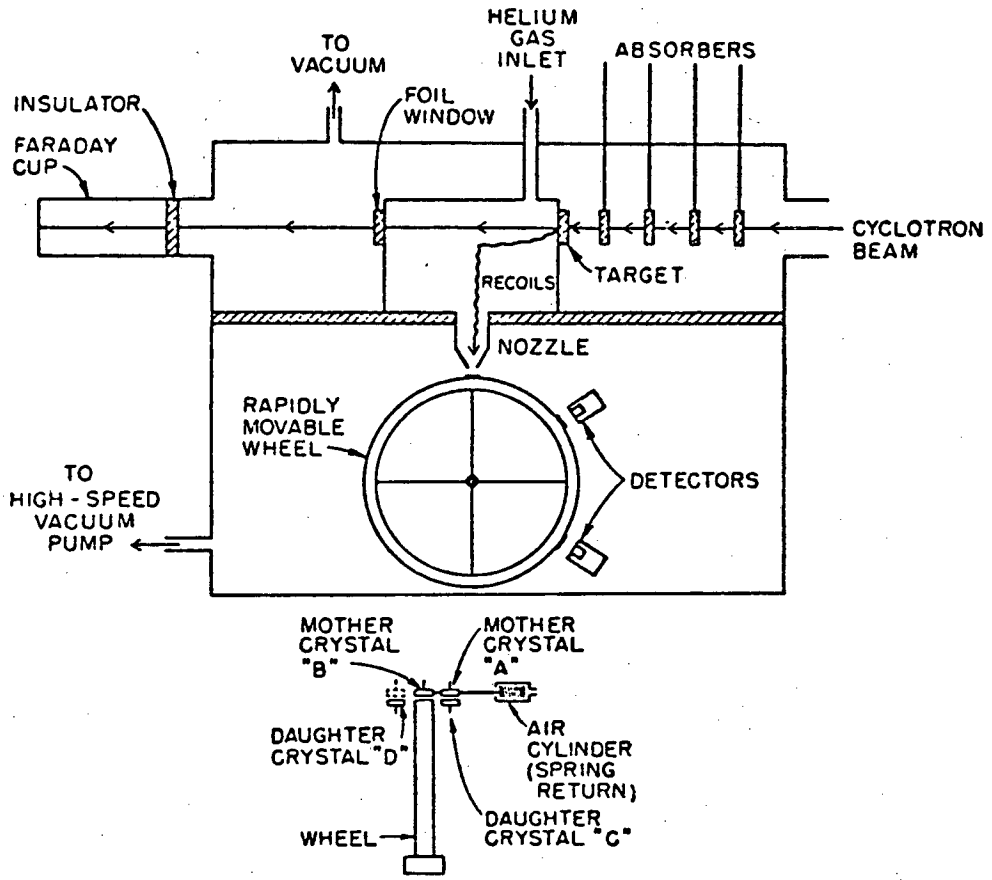

MULTIPLE DETECTOR UNIT

Fig 22

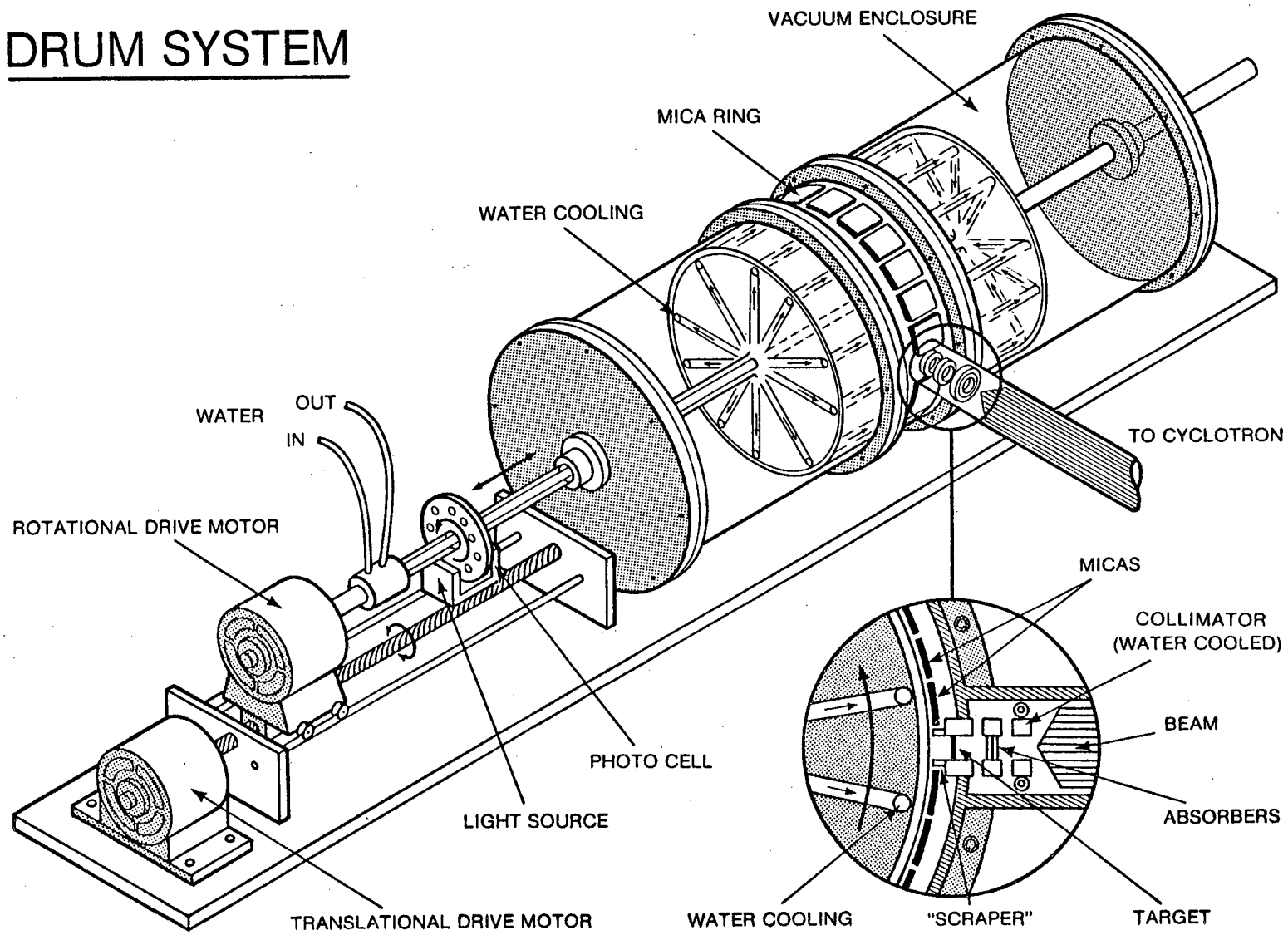

XBL 7912-13728

Fig 23

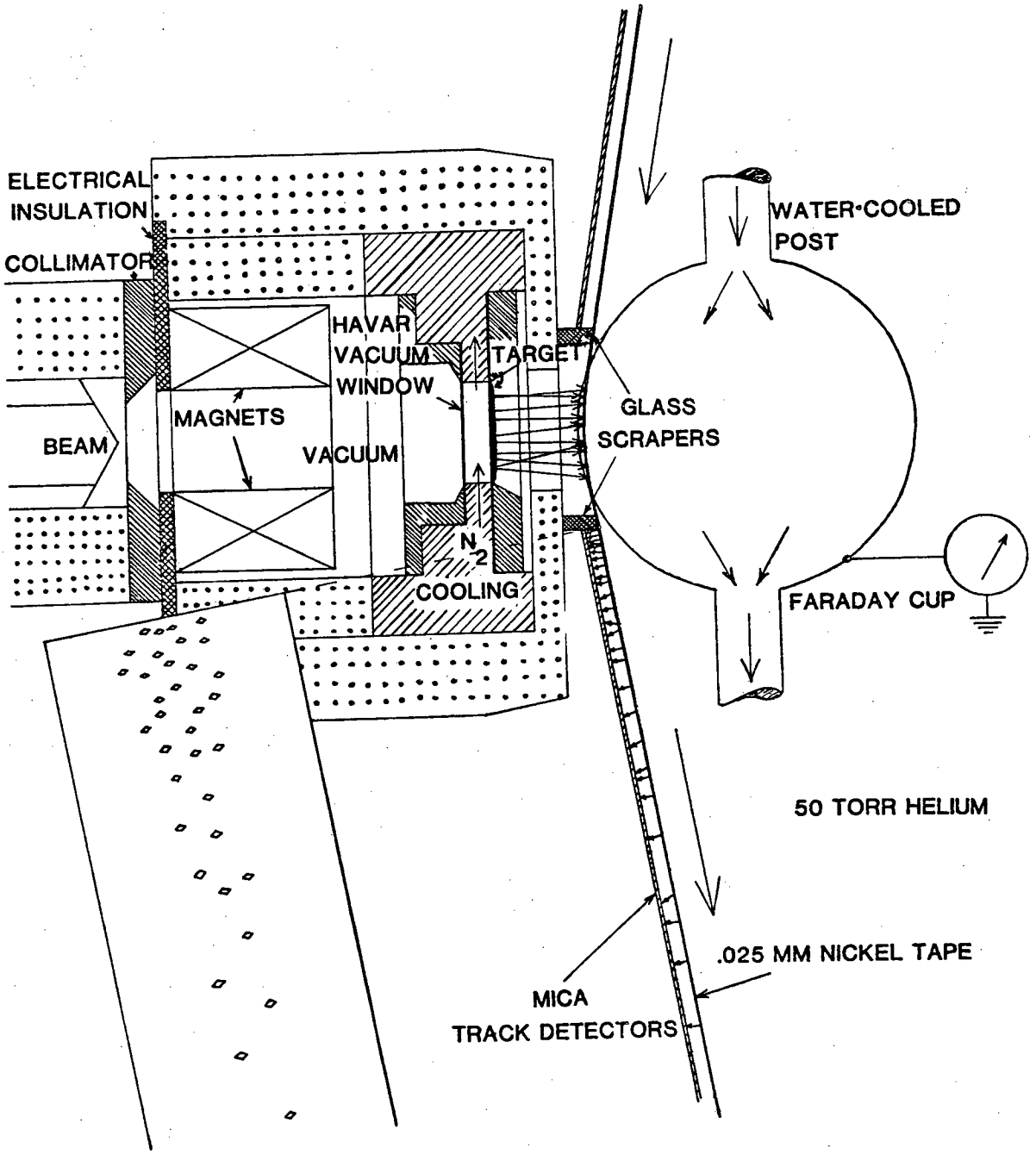

XBL 799-11395

Fig 24

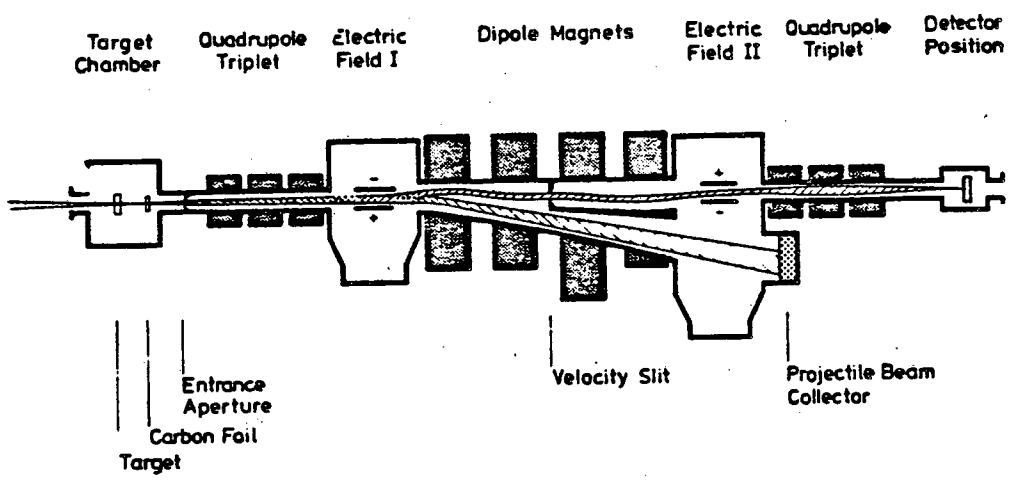
Target Chamber
Quadrupole Triplet
Electric Field I
Dipole Magnets
Electric Field II
Quadrupole Triplet
Detector Position
Entrance Aperture
Carbon Foil
Target
Velocity Slit
Projectile Beam Collector

Fig 25

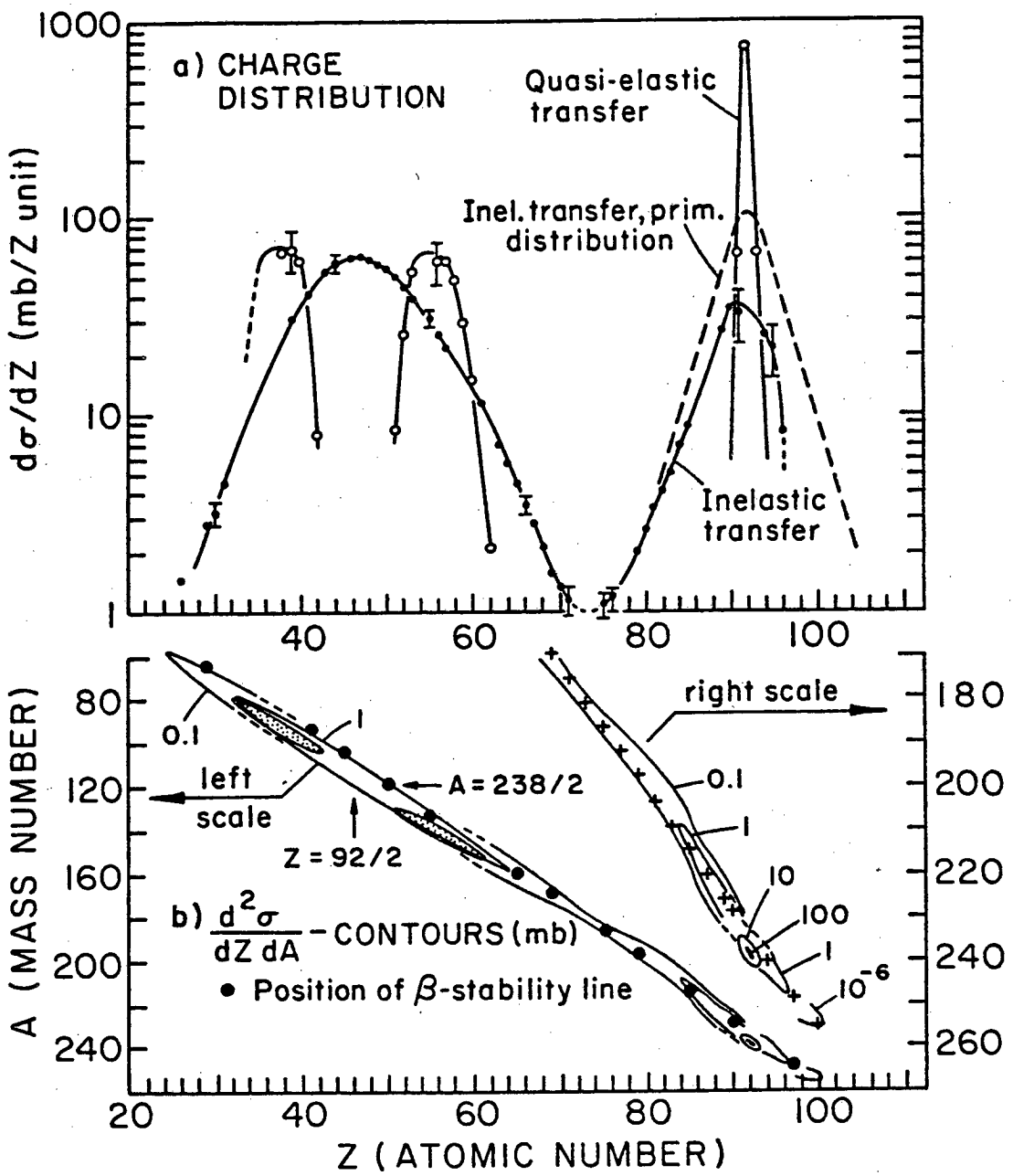

XBL 788-10627

Fig 26

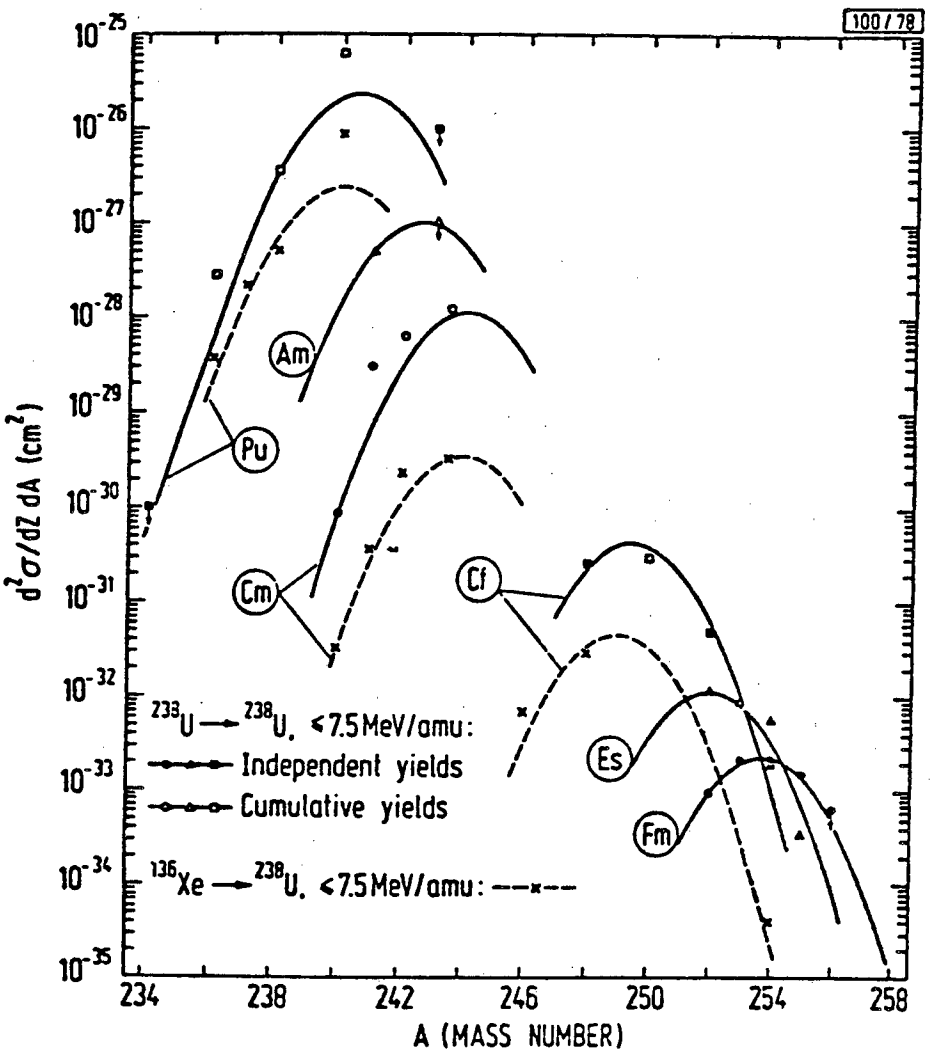
100/78
10^{-25}
10^{-26}
10^{-27}
10^{-28}
10^{-29}
10^{-30}
10^{-31}
10^{-32}
10^{-33}
10^{-34}
10^{-35}
$d^2\sigma/dZ\,dA$ (cm^2)
Am
Pu
Cm
Cf
Es
Fm
$^{233}U \rightarrow {}^{238}U$, <7.5 MeV/amu:
Independent yields
Cumulative yields
$^{136}Xe \rightarrow {}^{238}U$, <7.5 MeV/amu:
234
238
242
246
250
254
258
A (MASS NUMBER)

Fig 27

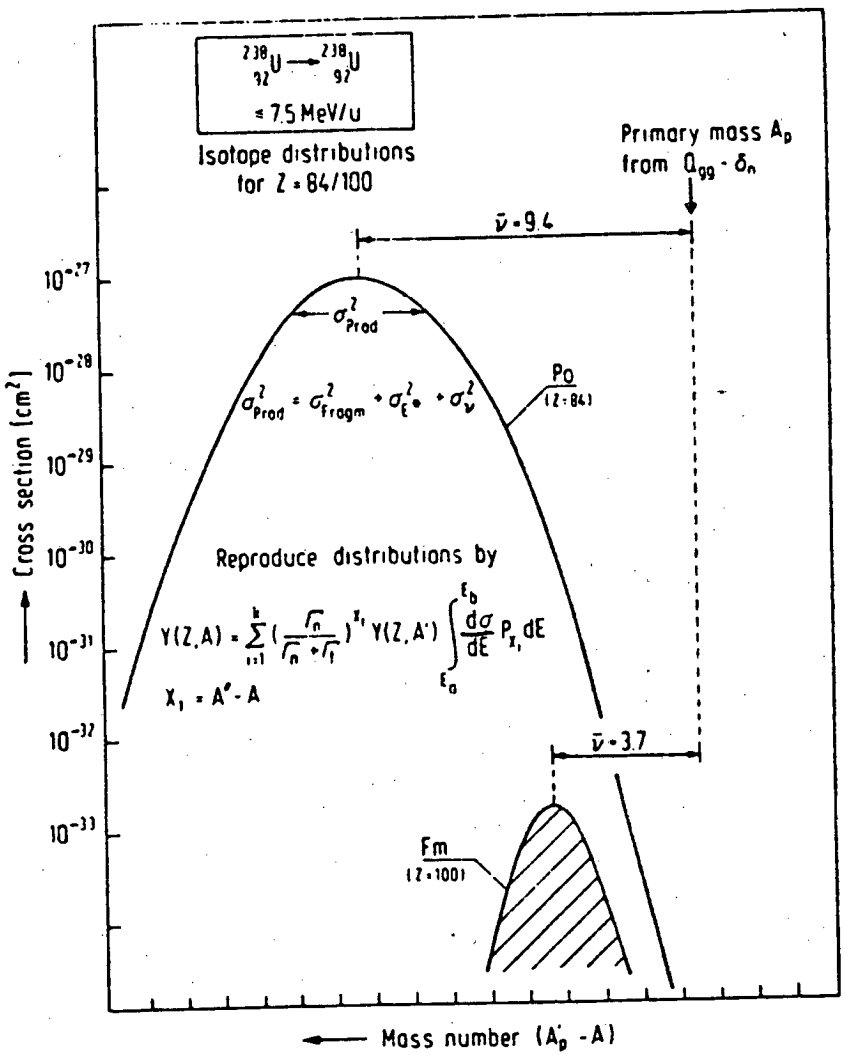
$^{238}_{92}U \rightarrow ^{238}_{92}U$
≤ 7.5 MeV/u
Isotope distributions for Z = 84/100
Primary mass A_p from $Q_{gg} - \delta_n$
$\bar{\nu} = 9.4$
σ^2_{Prod}
$\sigma^2_{Prod} = \sigma^2_{fragm} + \sigma^2_{E^*} + \sigma^2_{\nu}$
Po (Z = 84)
Reproduce distributions by
$Y(Z,A) = \sum_{i=1}^{k} \left(\frac{\Gamma_n}{\Gamma_n + \Gamma_f}\right)^{X_i} Y(Z,A') \int_{E_a}^{E_b} \frac{d\sigma}{dE} P_{X_i} dE$
$X_i = A' - A$
$\bar{\nu} = 3.7$
Fm (Z = 100)
Cross section [cm²]
10^{-27}
10^{-28}
10^{-29}
10^{-30}
10^{-31}
10^{-32}
10^{-33}
Mass number (A'_p - A)

Fig 28

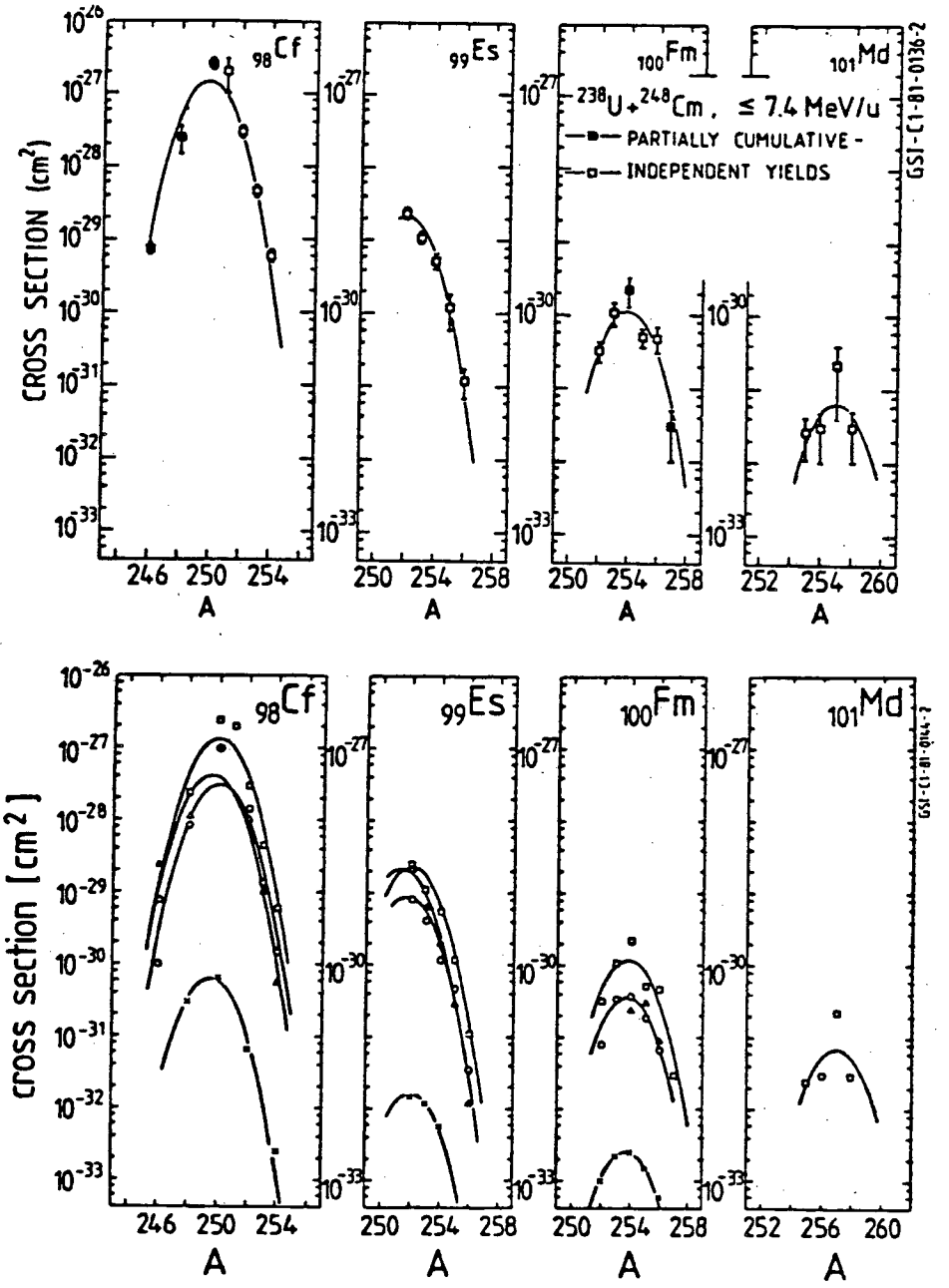
CROSS SECTION (cm²)
98Cf
99Es
100Fm
101Md
238U+248Cm, ≤ 7.4 MeV/u
PARTIALLY CUMULATIVE -
INDEPENDENT YIELDS
GSI-C1-81-0136-2
A
cross section [cm²]
GSI-C1-81-0144-2

Fig 29

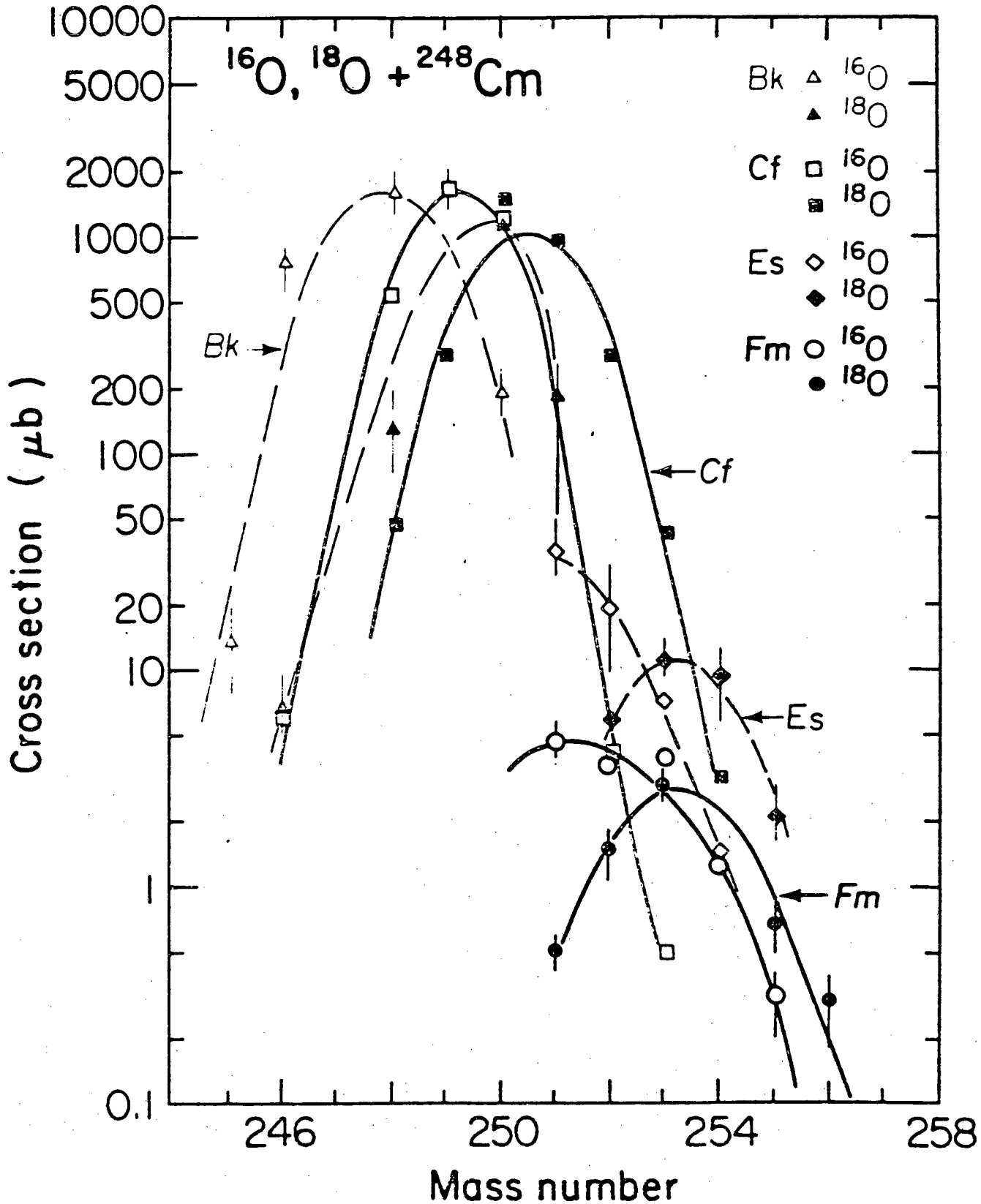

XBL 807-1716

Fig 30

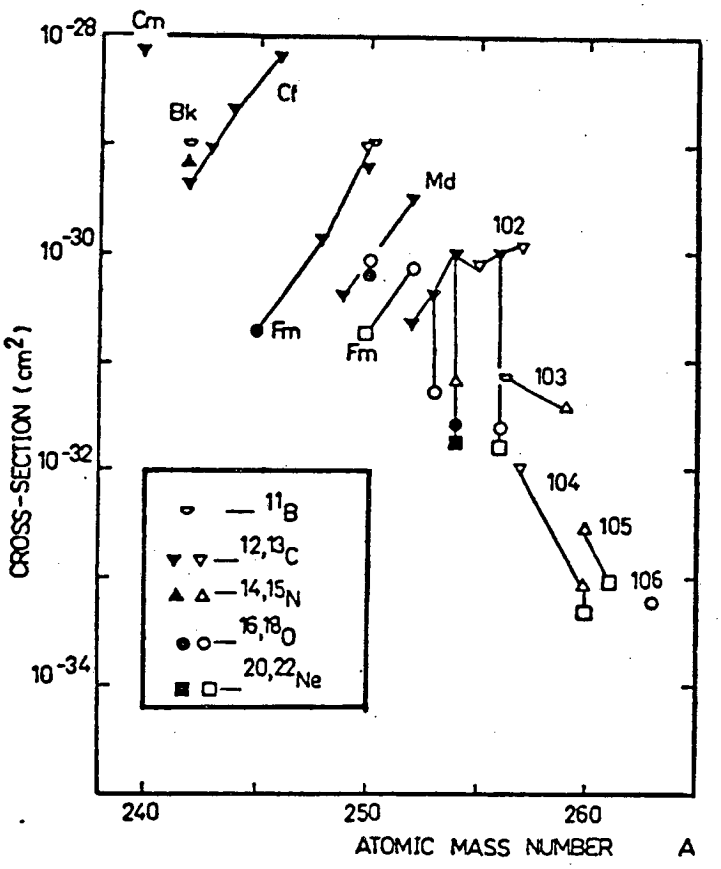
Cm
Cf
Bk
Md
102
Fm
Fm
103
104
105
106
10^{-28}
10^{-30}
10^{-32}
10^{-34}
CROSS-SECTION (cm^2)
— ^{11}B
— $^{12,13}C$
— $^{14,15}N$
— $^{16,18}O$
— $^{20,22}Ne$
240
250
260
ATOMIC MASS NUMBER
A

Fig 31

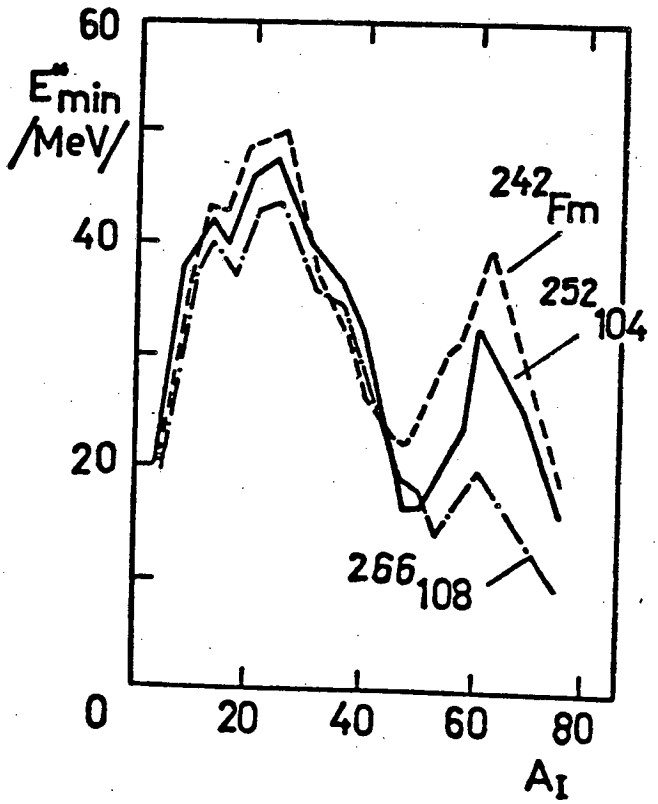

Fig 32

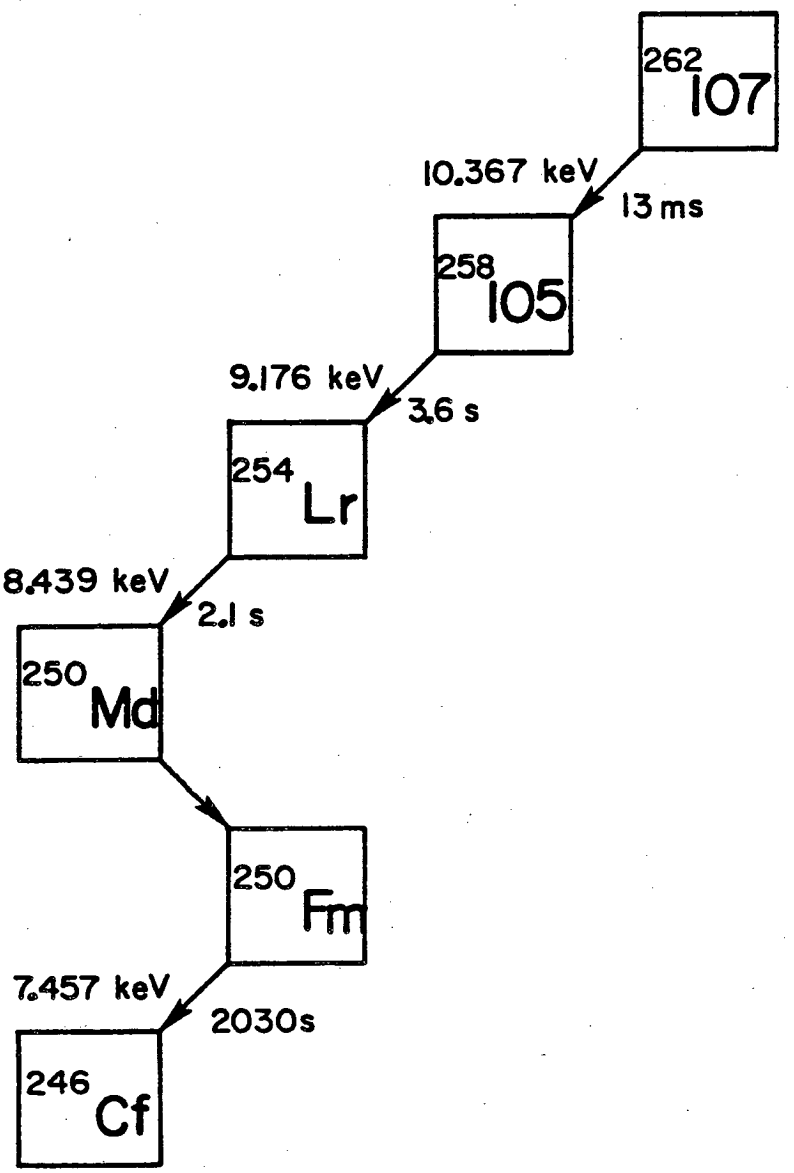
262 107
10.367 keV
13 ms
258 105
9.176 keV
3.6 s
254 Lr
8.439 keV
2.1 s
250 Md
250 Fm
7.457 keV
2030s
246 Cf

This report was done with support from the Department of Energy. Any conclusions or opinions expressed in this report represent solely those of the author(s) and not necessarily those of The Regents of the University of California, the Lawrence Berkeley Laboratory or the Department of Energy.

Reference to a company or product name does not imply approval or recommendation of the product by the University of California or the U.S. Department of Energy to the exclusion of others that may be suitable.

TECHNICAL INFORMATION DEPARTMENT
LAWRENCE BERKELEY LABORATORY
UNIVERSITY OF CALIFORNIA
BERKELEY, CALIFORNIA 94720